

Evaluation of Skid Resistance at Different Speeds in Idaho

A Thesis

Presented in Partial Fulfillment of the Requirements for the

Degree of Master of Science

with a

Major in Civil Engineering

in the

College of Graduate Studies

University of Idaho

by

Simpson Lamichhane

Major Professor: Emad Kassem, Ph.D., P.E.

Committee Members: Richard J. Nielsen, Ph.D., PE, Christopher Williams, Ph.D.

Department Chair: Patricia J. S. Colberg, Ph.D., P.E.

August 2019

Authorization to Submit Thesis

This thesis of Simpson Lamichhane, submitted for the degree of Master of Science with a Major in Civil Engineering and titled "Evaluation of Skid Resistance at Different Speeds in Idaho " has been reviewed in final form. Permission, as indicated by the signatures and dates below, is now granted to submit final copies to the College of Graduate Studies for approval.

Major Professor: _____ Date: _____

Emad Kassem, Ph.D., P.E.

Committee Members: _____ Date: _____

Richard J. Nielsen, Ph.D., PE.

_____ Date: _____

Christopher Williams, Ph.D.

Department Chair: _____ Date: _____

Patricia J. S. Colberg, Ph.D., P.E.

Abstract

Adequate skid resistance is essential for road safety. Many transportation agencies measure the skid number using a locked-wheel skid trailer at a reference speed (e.g., 40 mph in Idaho). Due to some limitations (e.g., speed limit, road geometry), the skid number is often measured at lower speeds. In addition, some interstate highways have a speed limit up to 80 mph, yet the skid numbers are collected at lower speeds that may impose hazard to motorists. This study developed a statistical model to describe the change in skid number with speed as a function of pavement macrotexture. This model can be used to predict the skid number at a reference speed based on measurement of skid numbers at any operation and safe speed between 20 mph and 60 mph and mean profile depth of pavement surface. The model results exhibited a good correlation between measured and predicted skid numbers. In addition, this study developed a simple software application to calculate skid numbers at any the desired speed. The software imports the texture and skid data collected using the pavement friction tester and then calculates the skid number at a reference speed specified by the user using the developed model. The outcome of this study will improve the safety of the skid crew and motorists; in addition, it will expedite skid data collection.

Keywords: Skid resistance, skid number, pavements, microtexture, macrotexture, skid truck, mean profile depth

Acknowledgements

I express my sincere gratitude to my supervisor Dr. Emad Kassem who guided me all along my research. He was always there to steer me out of troubles and direct me towards my objectives. He believed in me more than I believed in myself, and always encouraged to do better. It is his continuous support and supervision that helped me accomplish everything so far.

I would like to thank my committee members Dr. Richard Nielson and Dr. Christopher Williams for continuously reviewing my research work and providing me with feedback to improve. Without their input, I would not be able develop my model and validate my results.

I would like to acknowledge my friend and my colleague, Mohammad Al Assi, who helped me with my field work and provided feedback on my results. I am thankful to my colleagues Hamza, Robin, Niyi, Hasnat, Mohammad, Charles, Ebenezer, Sandarva and Sabreena for their support during my research.

Finally, I want to thank my parents for their support and encouragement throughout my graduate study. I am forever indebted to my wife, Roshna Siwakoti, who helped to manage my personal and social life while I was busy in my research study.

This research would not be possible without them.

This study is part of a research project (RP 266) funded by Idaho Transportation Department.

Dedication

In dedication to my parents, my wife, and my friends from Malekhu E6 who have supported me throughout and inspired to be a better person.

Table of Contents

Authorization to Submit Thesis.....	ii
Abstract.....	iii
Acknowledgements.....	iv
Dedication	v
Table of Contents.....	vi
List of Tables.....	x
List of Figures.....	xi
CHAPTER 1 INTRODUCTION	1
1.1 Background	1
1.2 Problem Statement	2
1.3 Research Objectives	2
1.4 Research Tasks	3
1.4.1 Task 1: Literature Review.....	3
1.4.2 Task 2: Identify and Select Pavement Sites for Evaluation.....	3
1.4.3 Task 3: Measure Skid Number at Different Speeds	4
1.4.4 Task 4: Measure the Surface Friction Characteristics	4
1.4.5 Task 5: Analyze Collected Data	4
1.4.6 Task 6: Establish Correlations at Different Speeds	4
1.5 Thesis Organization.....	5
CHAPTER 2 LITERATURE REVIEW	6
2.1 Introduction	6
2.2 Skid Resistance.....	6
2.3 Factors Affecting Skid Resistance of Pavements.....	7
2.3.1 Pavement Texture	8
2.3.2 Traffic	10
2.3.3 Slip Speed or Slip Ratio.....	10

2.3.4 Tire Properties.....	11
2.3.5 Temperature	12
2.3.6 Presence of Water	12
2.3.7 Speed.....	13
2.4 Characterization of Surface Frictional Characteristics.....	13
2.4.1 Locked-Wheel Devices.....	14
2.4.2 Side Force Devices	14
2.4.3 Fixed Slip Devices	15
2.4.4 Variable Slip Devices	15
2.4.5 British Pendulum Tester (BPT)	15
2.4.6 Dynamic Friction Tester (DFT).....	16
2.4.7 Circular Track Meter (CTM).....	16
2.4.8 Laser Profiler	17
2.4.9 Volumetric Method.....	18
2.5 Current Practices of Measurement of Skid Number by DOTs.....	18
2.6 Relation between Skid Resistance and Speed	20
2.6.1 Corsello (1993)	20
2.6.2 Rizenbergs et al. (1973).....	20
2.6.3 Penn State Model.....	21
2.6.4 Kulakowski (1991)	22
2.6.5 Jackson (2008).....	23
2.6.6 Flintsch et al. (2010).....	24
CHAPTER 3 SELECTION OF TEST SECTIONS AND FIELD TESTING	27
3.1 Introduction	27
3.2 Skid Number Measurements	32
3.3 Measurement of Surface Texture Characteristics.....	33
3.3.1 Measurement using Dynamic Friction Tester (DFT)	33

3.3.2 Measurement by Sand Patch Test.....	35
3.3.3 Measurement using Laser Profiler.....	35
CHAPTER 4 RESULTS AND DISCUSSION	38
4.1 Introduction	38
4.2 Distribution of Friction (SN) And Texture (MPD) for the Test Sites	38
4.3 Effect of Pavement Type on Friction Characteristics.....	41
4.4 Variation in Skid Number Measurements	43
4.5 Correlation between Friction, Speed and Texture.....	45
4.6 Development of Prediction Model	51
4.7 Model Validation.....	57
4.8 Individual Prediction Models	58
4.8.1 Model for Seal Coat Surface.....	59
4.8.2 Model for HMA Pavements.....	60
4.8.3 Concrete Skid Prediction Model.....	61
4.9 Comparison between Models	62
4.10 Sensitivity Analysis of the Model	63
CHAPTER 5 DEVELOPMENT OF THE SKID PREDICTION SOFTWARE	67
5.1 Overview	67
5.2 Single Test Site.....	68
5.2.1 Command Buttons	69
5.2.2 Software Outputs	69
5.3 Multiple Test Site	70
CHAPTER 6 CONCLUSIONS AND RECOMMENDATIONS	74
6.1 Summary	74
6.2 Findings	75
6.2.1 Skid and Texture Data Analysis	75
6.2.2 Development of Skid Prediction Model	76

6.2.3 Development of a Skid Prediction Software.....	76
6.3 Recommendations for Future Research	77
References	78
APPENDIX A TEST DATA	86
APPENDIX B DATA FOR MODEL DEVELOPMENT AND VALIDATION	92
APPENDIX C RELATION BETWEEN SN AND MPD.....	99
HMA SECTIONS	99
SEAL COAT SECTIONS.....	102
APPENDIX D RELATION BETWEEN SKID NUMBER (SN) AND DFT20	105
APPENDIX E SKID SOFTWARE EXAMPLES	108
APPENDIX F COPYRIGHT PERMISSSION	130

List of Tables

Table 2.1. Factors affecting skid resistance of pavements (Fuentes 2009).....	7
Table 2.2. Skid number adjustment factors constants at various test speeds (Cybernetics 2000)	19
Table 3.1. List of test sections in State of Idaho	28
Table 4.1. Statistical Parameters for Model	52
Table 4.2. VIF values for the independent variables in the model	55
Table 4.3. Statistical Parameters for Individual and General Model	62
Table 5.1. Command buttons and their function.....	69
Table 5.2. Single test site mode outputs.....	70

List of Figures

Figure 2.1. Diagrammatic representation of friction force on a moving body. Figure reproduced with permission from Hall <i>et al.</i> (2008).....	6
Figure 2.2. Friction values on a dense graded plant-mix asphaltic surface. Figure reproduced with permission from Shahin (1994).	7
Figure 2.3. Classification of pavement surface texture. Figure reproduced with permission from Bitelli <i>et al.</i> (2012).	8
Figure 2.4. Components of tire pavement friction. Figure reproduced with permission from Flintsch <i>et al.</i> (2012).	9
Figure 2.5. Variation of adhesion and hysteresis friction with the speed. Figure reproduced with permission from Shahin (1994).	9
Figure 2.6. Variation of pavement friction with tire slip. Figure reproduced with permission from Hall <i>et al.</i> (2009).	11
Figure 2.7. Effect of water film on pavement friction. Figure reproduced with permission from Hall <i>et al.</i> (2009).	13
Figure 2.8. (a) DFT device; (b) Bottom of the DFT with three rubber sliders.	16
Figure 2.9. Relationship between CTM and sand patch from NCAT test track. Reproduced with permission from Hanson & Prowell (2004).	17
Figure 2.10. Sample skid testing results for two sections of the Virginia smart road. Figure reproduced with permission from Flintsch <i>et al.</i> 2010.	25
Figure 3.1. Locations of the selected test sections in the state of Idaho.	30
Figure 3.2. Test section distribution by pavement surface type.....	30
Figure 3.3. Test section distribution by ITD district.....	31
Figure 3.4. Test section distribution by highway type.	31

Figure 3.5. ITD locked wheel skid trailer.	32
Figure 3.6. Location of DFT and sand patch measurements.	33
Figure 3.7. Measurement of microtexture using the DFT device.	34
Figure 3.8. Coefficient of friction measurements by DFT software.	34
Figure 3.9. Sand patch test measurements.	35
Figure 3.10. Measurement of MPD using laser profiler.	36
Figure 3.11. Examples of field testing.	37
Figure 4.1. Skid number values at 40 mph for all test sections and road types examined in this study.	39
Figure 4.2. Distribution of skid number at 40 mph (SN40) for all test sections measured in this study.	39
Figure 4.3. Mean Profile Depth (MPD expressed in mm) of the test sites and pavement types examined in this study.	40
Figure 4.4. Distribution of MPD measurements for all test sections examined in this study. ..	40
Figure 4.5. Average skid number measured at 40 mph for three pavement surfaces obtained from Tukey's HSD test. Categories with the different lettering (A, B , C) represents statistically significant difference.	42
Figure 4.6. Average MPD for three pavement surfaces obtained from Tukey's HSD test. Categories with the different lettering (A, B , C) represents statistically significant difference.	42
Figure 4.7. Average DFT20 values for three pavement surfaces obtained from Tukey's HSD test. Categories with the different lettering (A, B , C) represents statistically significant difference.	43
Figure 4.8. Standard deviation of measured skid number at 40 mph vs. speed and MPD.	44

Figure 4.9. Relationship between skid number and speed on HMA test sections examined in this study.	46
Figure 4.10. Relationship between skid number and speed on seal coat test sections examined in this study.	47
Figure 4.11. Relationship between skid number and speed on concrete test sections examined in this study.	48
Figure 4.12. Correlation of skid number speed gradient (G_v) with macrotexture for all the pavement surface types examined in this study.	49
Figure 4.13. Correlation between mean texture depth and mean profile depth for all the pavement surface types examined in this study.	49
Figure 4.14. Skid number measured at 60 mph expressed as a logarithm of mean profile depth for HMA sections.	50
Figure 4.15. Skid numbers measured at 20 mph versus DFT20 values for the test sections examined in this study.	50
Figure 4.16. Predicted Versus Measured Skid Number (SN).	52
Figure 4.17. Residuals of the model plotted against the fitted values/predicted values of skid number from the model.	54
Figure 4.18. Plot of standardized residuals of the model versus theoretical quartiles also knows as normal probability plot.	54
Figure 4.19. Plot of standardized residual of the model against the fitted values of the model (also knows as scale location plot).	56
Figure 4.20. Plot of residuals versus leverage for the prediction model.	56
Figure 4.21. Distribution of SN for test sections selected for validation.	57
Figure 4.22. Predicted versus measured SN (Model Validation).	58

Figure 4.23. Predicted versus measured skid numbers for model development and validation of seal coat skid model.	59
Figure 4.24. Predicted versus measured skid numbers for model development and validation of HMA skid model.	60
Figure 4.25. Predicted versus measured skid numbers for model development and validation of concrete skid model.	61
Figure 4.26. Change in predicted skid number with velocity ratio and mean profile depth....	64
Figure 4.27. Change in predicted skid number with velocity ratio and measured skid number.	65
Figure 4.28. Change in predicted skid number with measured skid number and mean profile depth. Note: the velocity ratio is constant at 1.5.	66
Figure 5.1. Skid prediction software interface	67
Figure 5.2. Interface of the single test site mode	68
Figure 5.3. Interface of the multiple test sites mode	71
Figure 5.4. Typical input file (SN) for the software obtained from skid truck	72
Figure 5.5. Output of the multiple test site mode.....	73

CHAPTER 1 INTRODUCTION

1.1 Background

Skid resistance is a major component in road safety (Noyce *et al.* 2005). Skid resistance is defined as the traction force generated between pavement surface and tires as they slide or roll on a pavement surface (Hall *et al.* 2008). The presence of water or other contaminants on a pavement surface reduces skid resistance significantly since water acts as a lubricant (Flintsch *et al.* 2012). The term ‘skid resistance of pavement’ is often used interchangeably with pavement friction and is expressed in terms of coefficient of friction, skid number (SN), or friction number. The coefficient of friction is the ratio of tangential force developed between the tire and pavement surface and the normal force acting on the tire (Åström & Wallman 2001). The SN is a dimensionless value obtained by multiplying the coefficient of friction by 100 (Corsello 1993).

Various factors influence skid resistance of pavements including pavement texture, vehicle speed, slip ratio, tire properties, and environmental (e.g., temperature and presence of water) (Fuentes 2009). Of these parameters, speed, texture and presence of water are the most dominant factors controlling the friction between the tire and pavement surface (Noyce *et al.* 2005; Åström & Wallman 2001; Kulakowski 1991). Friction decreases with increasing speed due to the reduction in the true contact area between two surfaces and the time duration over which the two surfaces remain in contact (Chowdhury *et al.* 2011). Reduced contact area and duration of contact decrease the molecular bonding between the asperities and rubber tires leading to reduced adhesion and consequently lower friction (Schallamach 1971; Bowden & Tabor 2001). This is why satisfactory skid resistance measured at one speed may not be adequate at a higher speed.

Pavement friction is affected by both surface microtexture and macrotexture (Bitelli *et al.* 2012). Microtexture is a function of the roughness of aggregate particles, and it changes during the life of the pavement due to polishing and abrasion under traffic loading. Changes in microtexture depend on aggregate quality and its resistance to polishing and abrasion (Kassem *et al.* 2013). The macrotexture is a function of the overall irregularities of the pavement surface and depends on aggregate gradation.

Skid resistance at lower speeds and dry conditions is affected mostly by the microtexture, whereas the macrotexture is the governing factor at higher speeds and wet conditions.

There are two main components of friction -- adhesion and hysteresis (Flintsch *et al.* 2012). Adhesion friction is a result of the formation of molecular bonds between the pavement surface and the tire rubber. The hysteresis friction is developed due to energy dissipation caused by the deformation of tire rubber around bulges and depressions in the pavement surface. The tire is in compression when sliding over the irregularities of the pavement surface and decompresses when leaving it. The hysteresis component of pavement friction is dominant at higher speeds and wet pavement condition, while the adhesion component is dominant at lower speeds and dry contact conditions (Hall *et al.* 2008).

1.2 Problem Statement

Pavement engineers use the skid number to determine if a treatment should be applied to improve surface friction of pavements. The current practice in the state of Idaho and at other transportation agencies in other states is to measure the skid number using a locked wheel friction testing trailer; the left wheel is locked and dragged on the surface to measure the skid number at a reference speed (e.g., 40 or 50 mph) depending on state specifications. In many cases, the skid number is measured at lower speeds due to state speed limits, the geometry of the roads and the size of skid truck. Although data collection at lower speeds is needed for safe operation, the data cannot be used in confidence for roadways with higher speed limits. In addition, several interstates in Idaho have speed limits of up to 80 mph. Yet the skid numbers are still measured at 40 mph, which is potentially unsafe for both operators and motorists. Therefore, there is a need to investigate and develop a correlation between skid numbers at lower speeds and skid numbers higher speeds. In principle, such a correlation could be used to predict skid numbers at a reference speed.

1.3 Research Objectives

This study had the following four objectives:

- Examine the correlation between skid number and speed (e.g., 20, 30, 40, 50, and 60 mph) for various pavement surfaces in Idaho including flexible pavements, rigid pavements, and seal coat or chip seal surfaces.

- Investigate the effect of pavement characteristics (e.g., microtexture and macrotexture) on the measured skid number and how it changes with speed.
- Develop a statistical model that describes the change in skid number with speed and is able to predict skid number at a reference speed using measured skid numbers at other testing speeds and pavement texture information.
- Develop a software application that can be used by operators to easily convert skid number measurements made at different speeds to a reference speed.

1.4 Research Tasks

Several tasks were performed to achieve the above-mentioned research objectives. All of the tasks performed in this study are listed and described below:

1.4.1 Task 1: Literature Review

The objective of this task was to conduct a comprehensive literature review on various aspects of skid resistance measurements and prediction. The main topics of the literature review were as follows:

- Factors that affect the skid number of flexible and rigid pavements.
- Test methods used to measure the surface frictional characteristics of pavements including macrotexture and microtexture.
- Relationships between skid number and skid trailer speed.
- Correlation of skid number at different speeds (e.g., 20 mph to 60 mph) to a reference speed (e.g., 40mph).
- Current practice followed by transportation agencies in measuring skid numbers at different speeds (e.g., 50 mph).

1.4.2 Task 2: Identify and Select Pavement Sites for Evaluation

Under this task, several test sections were identified and selected across Idaho. The objective of this task was to select sections with different characteristics to represent various pavement types and conditions. The test sections were distributed across the six districts in Idaho and included different pavement surfaces (i.e., seal coat, HMA, and concrete). The pavement sections had different mix designs, aggregate types, skid numbers, traffic levels, and ages.

1.4.3 Task 3: Measure Skid Number at Different Speeds

Under this task, the ITD crew, in coordination with UI research team, measured the skid numbers of the selected test sections at different speeds (e.g., 20 mph, 30 mph, 40 mph, 50 mph, and 60 mph). The ITD crew used the Dynatest 1295 Locked Wheel Friction Testing Trailer with a smooth tire. During this test, the left wheel of the friction testing trailer is locked to measure the skid number at the wheel path of the outside lane. The test was conducted according to the ASTM E274 “Standard Test Method for Skid Resistance of Paved Surfaces Using a Full-Scale Tire”. The common practice in Idaho is to measure the skid number at a reference speed of 40 mph.

1.4.4 Task 4: Measure the Surface Friction Characteristics

The researchers used the Dynamic Friction Tester (DFT) to measure the coefficient of friction of the pavement surface. The coefficient of friction measured using the DFT at 20 km/hr. (DFT20) is often used as an indirect measure of surface microtexture. The Sand Patch Test was performed to measure the surface macrotexture in terms of mean texture depth. In addition, the skid trailer was equipped with a laser sensor that measures the mean profile depth. A high mean profile depth indicates a coarse surface while a low mean profile depth indicates a fine surface.

1.4.5 Task 5: Analyze Collected Data

The data obtained during Task 4 include skid numbers at different speeds, microtexture (measured using the DFT), and macrotexture (measured using the sand patch test and laser profiler) of pavement surface. The main objective of this task was to investigate and establish a correlation between skid number and speed. In addition, statistical analyses were conducted to examine the effect of macrotexture and microtexture on the change in skid number with speed.

1.4.6 Task 6: Establish Correlations at Different Speeds

In this task, statistical data analyses were performed to develop a statistical model to estimate the skid number at a reference speed (e.g., 40 mph) using skid number measurements at other speeds and pavement textures. In addition, the researcher developed an Excel-based application that can import the friction and texture data collected by a pavement friction tester

and calculate the skid number at a reference speed specified by the user. This utility summarizes the mathematical correlations developed in this study and makes the calculations easier for the users.

1.5 Thesis Organization

This thesis consists of six chapters and six appendices.

Chapter 1 includes an introduction, problem statement, goal and objectives, research tasks, and thesis organization. Chapter 2 provides the main findings of the literature review on factors that affect skid resistance, devices used to measure skid resistance in the field and laboratory, the relationships between skid resistance and speed, and previous models used to predict skid number at different speeds.

Chapter 3 provides information about the test sections examined in this study. It also discusses the parameters considered when selecting the test sites, the distribution and type of the test sections. It presents the data collected in this study, including skid numbers at various speeds using the ITD locked-wheel skid trailer, coefficients of friction using DFT, mean texture depths using the sand patch test, and mean profile depths using the laser profiler.

Chapter 4 discusses the results of the various tests and the correlate skid number with speed. It presents the development of a statistical model to estimate the skid number at a reference speed using skid number measurements at other speeds and pavement textures. It also includes sensitivity analyses of the model parameters.

Chapter 5 discusses the development of an Excel-based application that can be used to easily convert skid number measurements at different speeds as a function of pavement texture.

Chapter 6 summarizes the main findings and conclusions of this study and provides recommendations for future research. The appendices provide additional information and figures that were cited and discussed in the thesis. They provide a summary of data collected during field testing including skid numbers and texture data.

CHAPTER 2 LITERATURE REVIEW

2.1 Introduction

This chapter reviews some of the major works that have been done in the area of skid resistance analysis, modeling and prediction. It provides an introduction to skid resistance, talks about the factors affecting skid resistance and the practices by various department of transportation in the United States for the measurement and standardization of skid resistance. It describes in detail the relationship between skid resistance and speed and various statistical models that attempt to predict the skid number for pavements.

2.2 Skid Resistance

Skid resistance is defined as the traction force generated between pavement surface and tires as they slide or roll on pavement surface (Figure 2.1; Hall *et al.* 2008). The presence of water or other contaminants on pavement surface reduces skid resistance as water acts as lubricant reducing the friction significantly (Flintsch *et al.* 2012; Cairney 1997). Water not only reduces the skid resistance but it also affects the change of skid resistance with speed. Moyer (1959) demonstrated that the change in skid with speed is significant in wet conditions compared to dry conditions as shown in Figure 2.2.

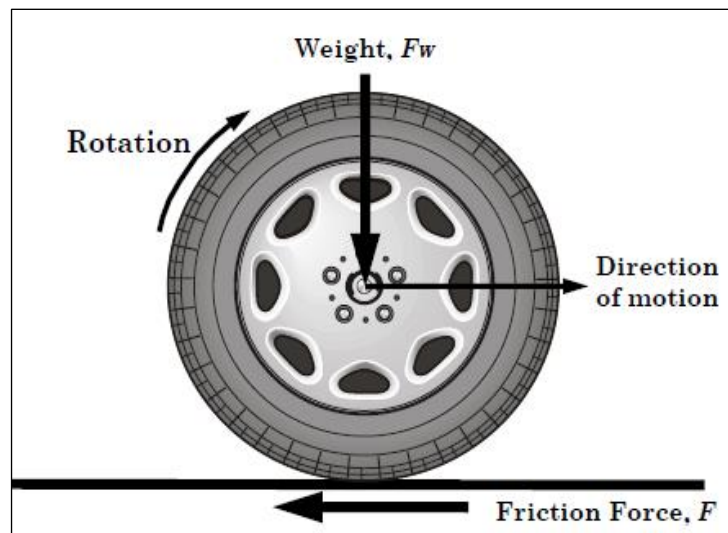


Figure 2.1. Diagrammatic representation of friction force on a moving body. Figure reproduced with permission from Hall *et al.* (2008).

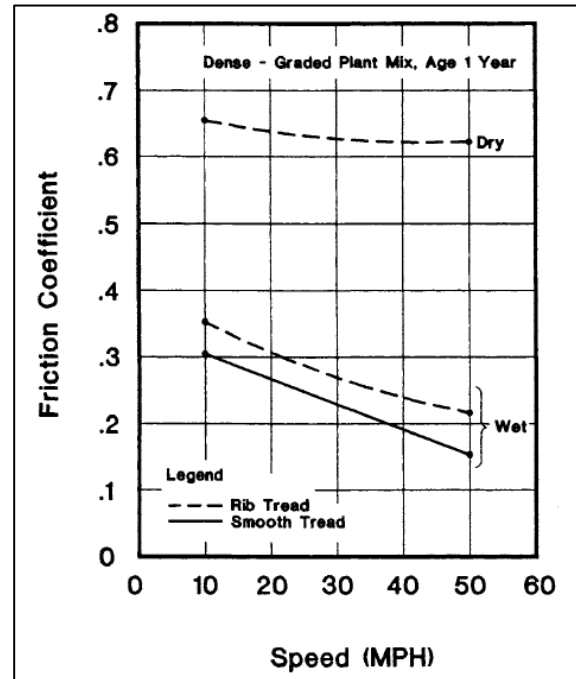


Figure 2.2. Friction values on a dense graded plant-mix asphaltic surface. Figure reproduced with permission from Shahin (1994).

2.3 Factors Affecting Skid Resistance of Pavements

There are several factors that affect the skid resistance of pavements. These factors include pavement texture, traffic level, slip speed, tire properties, temperature, presence of water and speed. Several studies have been conducted to investigate these factors. Fuentes (2009) categorized these factors into four groups as summarized in Table 2.1.

Table 2.1. Factors affecting skid resistance of pavements (Fuentes 2009)

Pavement Factors (Texture)	Vehicle Factors	Tire Factors	Environmental Factors
Microtexture	Vehicle slip ratio	Tire tread	Temperature
Macrotexture	Vehicle Speed	Tire pressure	Rainfall /Moisture

2.3.1 Pavement Texture

The properties of pavement texture are directly related to its frictional properties (Li 2005). Pavement texture is expressed as surface deviations from a true planar surface. It is classified by the World Road Association (PIARC 1987) based on the wavelength of the surface irregularities (Figure 2.3). Pavement texture is categorized as microtexture with wavelengths < 0.5 mm, macrotexture with wavelengths between 0.5mm to 50mm, and megatexture with wavelengths ranging from 50 mm to 500 mm. Pavement friction is affected mainly by the microtexture and macrotexture (Bitelli *et al.* 2012). Microtexture refers to the roughness of the individual particles forming the pavement; it is dependent on the characteristics of the aggregates or stones in the mixture. Pavement microtexture decreases over time due to polishing and abrasion caused by traffic. The rate of change in pavement microtexture depends on resistance of the aggregates to abrasion and polishing (Kassem *et al.* 2013). Macrotexture is due to the overall irregularities in the pavement surface due to size, spacing or voids between the aggregates particles. Macrotexture of the pavement surface is dependent on the aggregate gradation. Skid resistance at lower speed and under dry conditions is affected mostly by the microtexture, whereas macrotexture is the governing factor at higher speed and under wet conditions. (Cairney 1997)

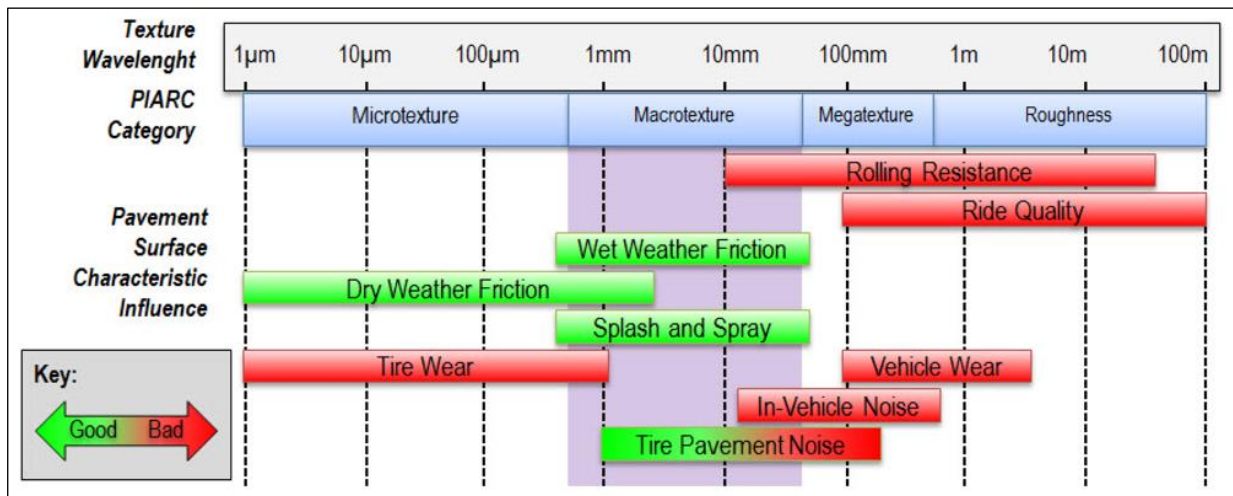


Figure 2.3. Classification of pavement surface texture. Figure reproduced with permission from Bitelli *et al.* (2012).

Adhesion and hysteresis friction are the two main components of pavement surface friction (Figure 2.4; Flintsch *et al.*, 2012). Adhesion friction is the result of the formation of molecular

bonds between the pavement surface and the tire, while hysteresis friction is the result of energy dissipation caused by the deformation of the tire around bulges and depressions in the pavement surface (Cairney 1997). Figure 2.5 illustrates that the hysteresis friction is dominant at higher speeds and under wet pavement conditions, while the adhesion friction is dominant at lower speeds and under dry contact conditions (Figure 2.5; Hall *et al.* 2008).

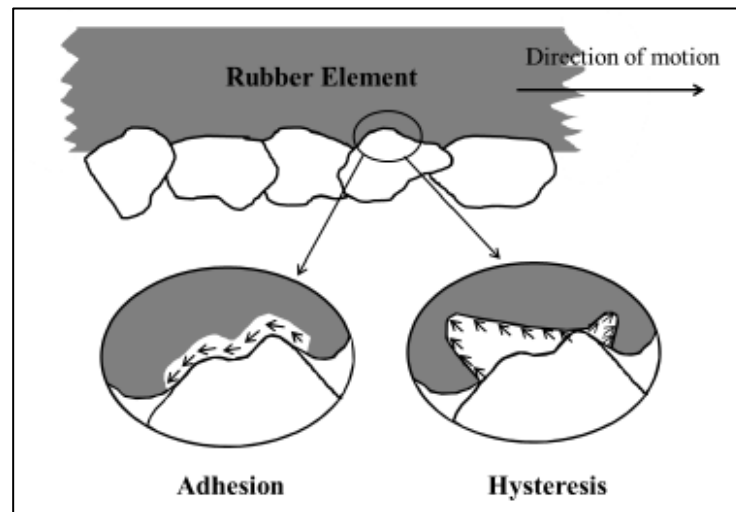


Figure 2.4. Components of tire pavement friction. Figure reproduced with permission from Flintsch *et al.* (2012).

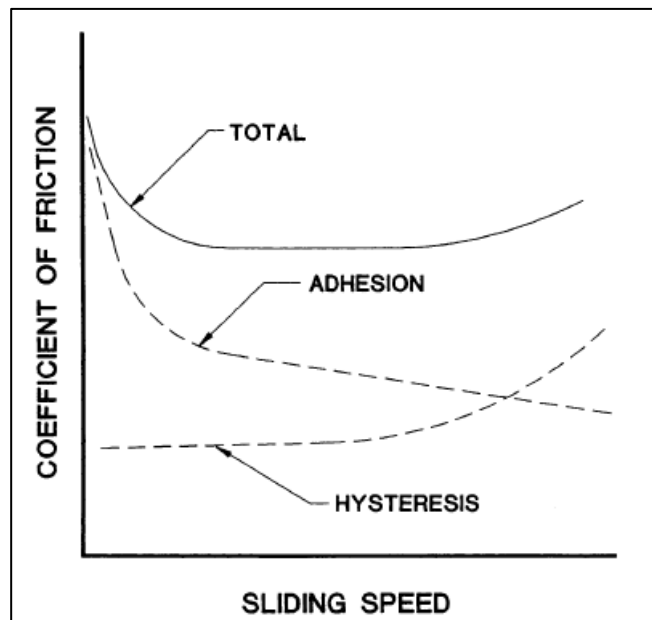


Figure 2.5. Variation of adhesion and hysteresis friction with the speed. Figure reproduced with permission from Shahin (1994).

2.3.2 Traffic

Over time, skid resistance is modified by traffic volume. Previous studies have shown that the pavement surfaces are polished under traffic, which reduces the microtexture and leads to reduced friction (Federal Aviation Administration 1971; Kassem *et al.* 2013). Oh *et al.* (2010) conducted a study that involved examining the effects of traffic and environment on skid resistance. They used a data set containing more than 50,000 observations along five freeway routes in seven districts of California and used the skid number at 40 mph (SN40) as a reference measure of skid resistance. The results suggested that seasonal conditions and temperatures have significant influences on skid resistance and that skid resistance decreased considerably with increases in average daily traffic. The National Cooperative Highway Research Program (NCHRP) synthesis of practices documented the effect of traffic volume on skid resistance. The daily volume of truck and passenger car volume was found to affect the side friction factor (Oh *et al.* 2010).

Trucks were found to have a significantly greater effect on skid resistance compared to passenger cars (Shahin 1994). Skid resistance decreased with traffic until it reached a terminal value. This terminal or minimum value depends on the properties and gradation of the aggregates (Kassem *et al.* 2013). The terminal value is higher for coarse graded mixes such as PFC and SMA compared to fine graded mixes such as Type F and Type C. Asphalt mixtures prepared with aggregates with rough texture and higher resistance to abrasion and polishing (e.g., sandstone) have better skid resistance compared to aggregates with smooth textures and less resistance to abrasion and polishing (e.g., limestone).

2.3.3 Slip Speed or Slip Ratio

Slip speed is defined as the difference between the vehicle speed and actual tire speed and slip ratio is obtained by dividing the slip speed by vehicle speed (Meyer 1982). Slip speed is equal to the vehicle speed; the slip ratio is 100 % at fully locked conditions. The slip speed and slip ratio equal zero at free rolling conditions. The tire pavement friction varies with the variation in slip speed or slip ratio. There is a critical slip ratio at which the coefficient of friction is at its maximum value. The friction increases with slip ratio until it reaches the critical value, then it decreases to an approximate constant value at 100 % of slip as shown in Figure 2.6. This constant value for the friction is called the coefficient of sliding friction. In general, the

friction is highest at slip ratios between 10 and 20 % (Hall *et al.* 2008; Hall *et al.* 2009). The reduction in coefficient of friction in the range from critical slip to fully locked conditions is about 50% and increases if the pavement surface is wet (Hall *et al.* 2009). A decrease in friction is mostly affected by pavement texture characteristics (microtexture and macrotexture) and the amount of water present on surface. It is important to note that the friction value before reaching critical slip is affected most by tire properties, whereas pavement texture affects friction after the critical slip is achieved (Flintsch *et al.* 2012).

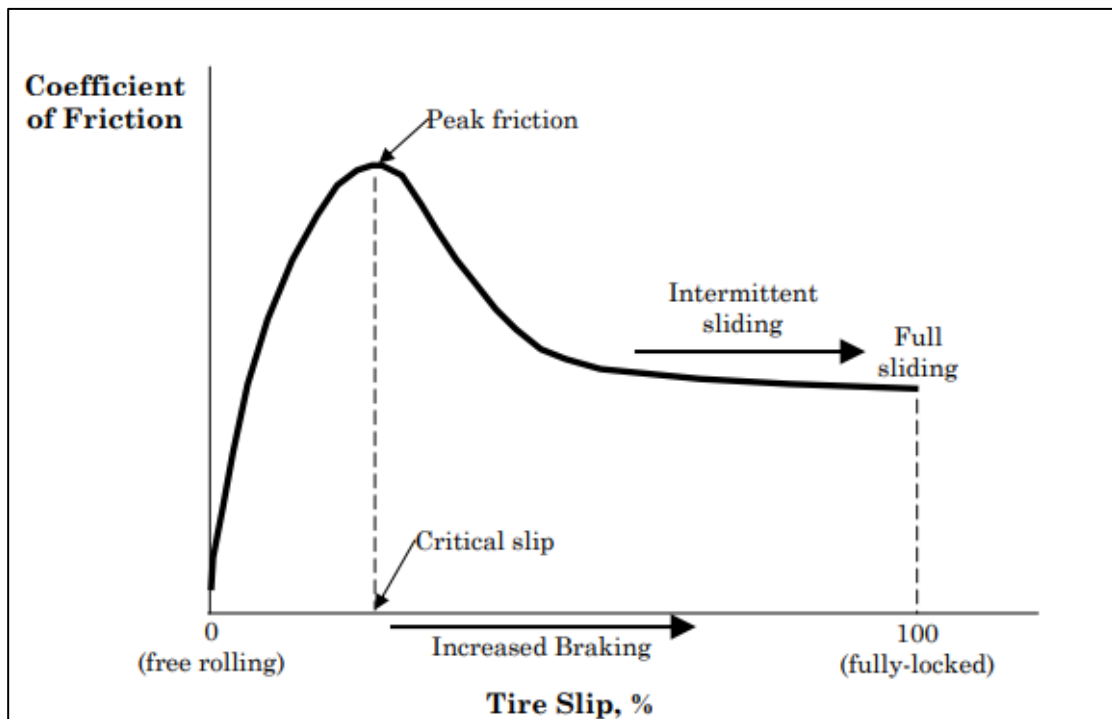


Figure 2.6. Variation of pavement friction with tire slip. Figure reproduced with permission from Hall *et al.* (2009).

2.3.4 Tire Properties

Properties of the tire such as tread, inflation pressure and wheel load also affect the skid resistance of pavements. The tire tread provides a path for water trapped between the pavement surface and tire to escape, leading to higher friction (Fuentes 2009). Tire pressure is another factor that affects skid resistance. The contact area between the tire and pavement surface decreases with an increase in inflation pressure. The heat generated during skidding is dissipated over a large area, which reduces tire temperature but increases the friction (Shahin

1994). Reduced contact area also reduces the adhesion friction (Dunford 2013). An increase in wheel load decreases the friction due to a decrease in contact area per unit load of wheel (Shahin 1994). Al-Assi & Kassem (2017) found a fair correlation between adhesion between tire rubber and aggregate and pavement friction. They obtained a strong correlation between rubber properties (i.e., elastic properties) and friction. Rubber with lower dynamic modulus provided higher friction.

2.3.5 Temperature

Tire rubber is a viscoelastic material, and its properties are affected by temperature. Previous studies have demonstrated that tire pavement friction decreases with the increases in temperature which explains the seasonal fluctuations of the skid resistance (Fuentes 2009; Shahin 1994). A study by Jayawickrama & Thomas (1998) documented that the skid resistance measured at 40 mph (SN40) decreased with an increase in air temperature. Another study by Oh *et al.* (2010) showed seasonal conditions and temperature were major factors influencing skid resistance; values were higher in fall and winter compared to summer and spring when temperatures were higher.

Luo (2003) also investigated the effect of pavement temperature on frictional properties and concluded that pavement temperature has a considerable effect on the frictional properties of pavements. It is also influenced by the test speed. There was a slight decrease in friction with increased temperature at low speeds when compared to the decreases measured at higher speeds.

2.3.6 Presence of Water

Water acts as a lubricant between tires and the pavement surfaces leading to reduced skid resistance (Moore 1975). There may be little to no contact between tires and the pavement surfaces based on water film thickness (Dunford 2013). In addition, water fills up the asperities present on the pavement surface, which prevents molecular bonds from forming between the pavement surface and tires and leads to reduced adhesion friction. Beautru *et al.* (2011) demonstrated that there is a considerable decrease in skid resistance with even small amounts of moisture on the pavement surface. Hall *et al.* (2009) demonstrated the effect of water film thickness on skid resistance for different tires (e.g., smooth tire, new ribbed tire,

and worn ribbed tire). The reductions in skid resistance were significant for smooth tires when compared to ribbed tires (Figure 2.7).

Harwood (1998) found that a water film thickness of 0.002 inches on the pavement surface reduced pavement friction by 20-30 % of dry friction. Additional increases in water film thickness at higher speeds can lead to hydroplaning. Hydroplaning occurs when there is no contact between the tires and pavement surface leading to a complete traction loss (Horne and Buhlmann, 1983).

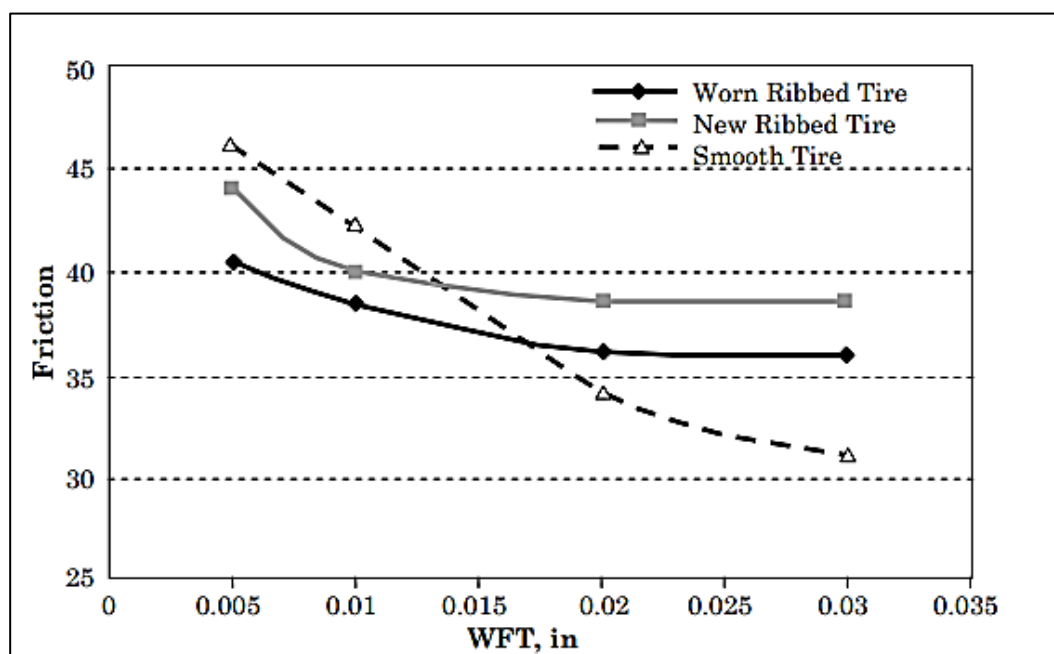


Figure 2.7. Effect of water film on pavement friction. Figure reproduced with permission from Hall *et al.* (2009).

2.3.7 Speed

Pavement friction decreases with speed. Several studies have shown that this decrease is not significant under dry conditions compared to wet conditions (Shahin 1994). The relationship between skid resistance and speed under wet conditions is explained in detail in Section 2.6.

2.4 Characterization of Surface Frictional Characteristics

Various devices are used to measure skid resistance based on different principles, such as locked wheel devices, side force devices, fixed slip ratio devices, and variable slip devices.

The Dynamic Friction Tester (DFT) and British Pendulum Tester (BPT), also measure pavement friction but the measurements are more related to the pavement microtexture. The Sand Patch Test (aka Volumetric Method) is a technique used to measure mean texture depth, while mean profile depth is most often measured using a laser-based technique.

2.4.1 Locked-Wheel Devices

The locked-wheel devices operate at a slip speed equal to the vehicle speed (i.e., slip ratio is 100 %; Henry 2000). These devices are typically installed on a trailer that is towed by a vehicle that operates at a standard reference speed. The testing wheel is equipped with either smooth or ribbed tires and the test is conducted in accordance with ASTM E274. The standards for smooth and ribbed tires used in the test are provided in ASTM E524 and ASTM E501, respectively. A water spraying system is attached to the towing truck and applies water on the pavement surface in front of the locked wheel. A layer of water of about 0.5 mm thickness is sprayed to achieve wet conditions (Henry 2000; Hall *et al.* 2008; Hall *et al.* 2009). When the towing truck reaches the desired speed, the brakes are applied, and the wheels are fully locked and dragged along the pavement surface. The force required to drag the wheel on the pavement surface is measured using torque transducers (ASTM E274 2011). The coefficient of friction is calculated by dividing the drag force by wheel load. It takes approximately 2.5 seconds to complete one friction test. The test wheels are unlocked, and the process is repeated for additional measurements.

2.4.2 Side Force Devices

Side force devices measure the sideways friction coefficient (SFC). The testing wheel has an angle to the direction of travel which is called the yaw angle. The test is conducted in accordance with ASTM E670. The British Mu-Meter and British Sideway Force Coefficient Routine Investigation Machine (SCRIM) are two common side force friction devices. The Mu Meter device measures the friction at a yaw angle of 7.5 degrees while the SCRIM measures the friction at a yaw angle of 20 degrees. These devices can be used to measure the friction on straight portions of roadways as well as at corners and curves. The friction measurements of these side force devices are influenced by pavement distresses such as potholes and cracks. Water is sprayed on the surface at a rate of 1.2 liter per minute before the friction testing. These devices operate at a low slip speed since they are sensitive to pavement macrotexture.

Separate devices are used to measure pavement macrotexture during friction testing (Henry 2000; Hall *et al.* 2008; Hall *et al.* 2009).

2.4.3 Fixed Slip Devices

These devices operate at a fixed slip ratio which is usually between 10 and 20 %. To maintain a fixed slip ratio, the angular velocity of the wheel is reduced by means of gear reduction, chains, belts or hydraulic braking . Like other friction testing equipment, water is sprayed in front of the testing tire. The trailer is towed by a truck that moves at 40 mph (Henry 2000; Hall *et al.* 2008). Both the drag force and wheel load are measured to calculate the coefficient of friction. Some of the typical fixed slip devices are Grip Tester, Slab Friction Tester, Road Analyzer and Recorder, Airport Surface Friction Tester (ASFT), and Roadway and Runway Friction Tester. The standards for the tires that are used in fixed slip devices are provided in ASTM E1551 (Hall *et al.* 2009).

2.4.4 Variable Slip Devices

Variable slip devices measure friction at various slip ratios in accordance with ASTM E1859. The slip ratio varies between zero (free rolling conditions) to 100 % (fully locked conditions). Like other devices, a 0.5 mm of water is sprayed on the surface before friction measurements are made. Test speed, wheel load, drag force on the wheel, and rotational speed of the tire are measured during the test and used to calculate the coefficient of friction at various slip ratios.

From the relationship between slip skid number and slip speed, other parameters including peak slip friction, critical slip ratio, longitudinal slip friction, and Rado shape factor can be calculated (Henry 2000; Hall *et al.* 2009).

2.4.5 British Pendulum Tester (BPT)

The British Pendulum Tester (BPT) is a portable device that is used to measure friction in the field as well as in the laboratory in accordance with ASTM E303. It consists of a rubber slider attached to a pendulum that is released from a certain height for the rubber slider to just touch the pavement surface. The amount of energy lost when the rubber slider passes over the pavement surface is used as a measure of skid resistance of the test surface. The results from the BPT are reported in terms of British Pendulum Number (BPN) (Martino & Weissmann 2008; Lu *et al.* 1971). The speed at which the rubber slider strikes the surface is about 10

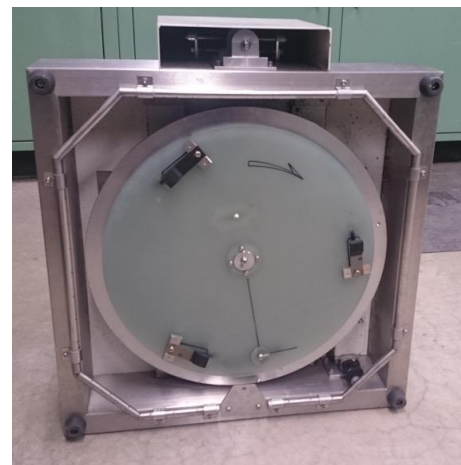
km/hr. Since the BPT measurements are performed at low speeds, it correlates well with pavement microtexture. The BPT is used to measure the skid at selected locations since it cannot be used for continuous measurements. The results of the BPT can be affected by the wind and operator performance (Lu *et al.* 1971; Hall *et al.* 2009).

2.4.6 Dynamic Friction Tester (DFT)

The Dynamic Friction Tester (DFT) is a portable device which can be used both in the field and the laboratory. The friction test can be measured under both dry and wet conditions. The test is conducted in accordance with ASTM E1911. The DFT consists of three rubber sliders attached to a rotating circular disk as shown in Figure 2.8. The circular disk rotates at a desired test speed (up to 100 km/h); the disk is then dropped so that the rubber sliders are in contact with the pavement surface. The coefficient of friction is measured as the speed of the rotating disk gradually decreases (Saito *et al.* 1996; Beautru *et al.* 2011; Aldagari *et al.* 2018). The coefficient of friction at 20 km/hr (DFT20) has been correlated with pavement microtexture; and is often used as an indirect method to measure pavement microtexture (Beautru *et al.* 2011; Kane *et al.* 2011).



(a)



(b)

Figure 2.8. (a) DFT device; (b) Bottom of the DFT with three rubber sliders.

2.4.7 Circular Track Meter (CTM)

The Circular Texture Meter (CTMeter) device is one of the more modern pieces of equipment used to measure pavement macrotexture. It can be used in the field as well as in the

laboratory. The test is conducted in accordance with ASTM E2157. The CTMeter has a charge-coupled device (CCD) laser displacement sensor attached to an arm mounted to the device. The arm rotates in a circle with a diameter of 28.4 cm. The laser sensor can collect about 1024 data points per round. The average mean profile depth (MPD) is calculated and reported according to ASTM E2157 (Abe *et al.* 2001; Masad *et al.* 2010) and has been found to correlate well with MTD measured using the Sand Patch Test (Hanson & Prowell 2005). Figure 2.9 shows the sand patch measurements against the CTMeter values based on data collected at the National Center for Asphalt Technology (NCAT) test tracks. The use of CTMeter in the field requires traffic control, which limit its use in field testing.

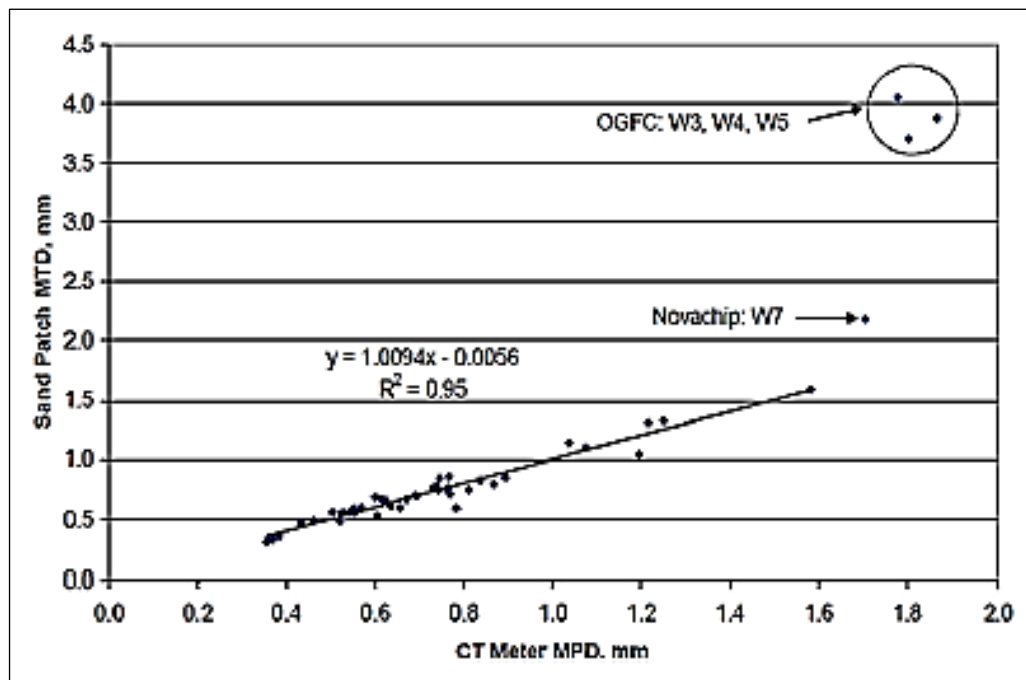


Figure 2.9. Relationship between CTM and sand patch from NCAT test track. Reproduced with permission from Hanson & Prowell (2004).

2.4.8 Laser Profiler

With advancements in laser-based technology, more accurate methods such as laser profiler are now available to measure pavement texture (Mataei *et al.* 2016). These devices use triangulation techniques for measurement of distance. They project a laser spot or line on the pavement surface and the reflection is recorded in an optical detector (Dunford 2013). Several parameters can be determined to represent the texture. The most common and widely used is

the mean profile depth (MPD) defined by ASTM E1845 Standard. The MPD represents the average value of the profile depth over certain segments of surface profile (Flintsch *et al.* 2012). The MPD measured by the laser profiler is correlated with the MTD calculated by the Sand Patch method.

2.4.9 Volumetric Method

The Volumetric Method or Sand Patch Test is a simple method to measure the macrotexture of pavement surface (Hall *et al.* 2008). The sand patch test is conducted in accordance with ASTM E965. In this test, a known volume of glass spheres is spread over a pavement surface and levelled using a spreader.

Before the use of glass spheres, Ottawa sand passing sieve No. 50 and retained on sieve No. 100 was used as a material for the test. Glass beads are recommended over sand since they are more uniform and can be manufactured commercially (Lu *et al.* 1971; Noyce *et al.* 2005). The pavement surface should be cleaned using a brush to remove any loose materials. Also, the surface should be free of any cracks or other irregularities before applying and spreading the glass spheres. The spheres are applied and levelled in a circular pattern. The average diameter of the circular patch is then calculated. The volume of the sand and the area of the patch are used to calculate the average depth of the circular patch which is referred to the Mean Texture Depth (MTD) of the pavement (Martino & Weissmann 2008).

2.5 Current Practices of Measurement of Skid Number by DOTs

Several highway agencies measure the skid resistance periodically (often every two years) to ensure an adequate level of friction. The Minnesota Department of Transportation (MnDOT) utilizes the Dynatest 1295 skid truck trailer in accordance with ASTM E274. MnDOT uses both ribbed and smooth standard test tires to measure skid resistance at a standard test speed of 40 mph under wet conditions. A skid number above 25 measured using a smooth tire is considered adequate, while a skid number below 15 indicates that the pavement requires surface treatment (Lebens & Troyer 2012) .

The Pennsylvania Department of Transportation (PennDOT) uses a skid friction tester (SFT) to measure skid number. The test is conducted using standard smooth or ribbed test tires according to ASTM E524 and ASTM E501, respectively. Using both smooth and ribbed tires

gives more data, but it is suggested to use only smooth tires if testing is to be performed using only one tire (Cybernetics 2000). At least five skid number measurements are collected for each test segment to ensure accuracy. PennDOT performs the friction testing at speeds between 25 to 50 mph; measured skid numbers are adjusted to an equivalent speed of 40 mph. The adjustments are made solely based on previous practice or experience. Table 2.2 summarizes the adjustment factors at various speeds. If the speed is greater than 45 mph, constant values are added to the measured skid number while constant values are subtracted from the skid number if the speed is lower than 40 mph. PennDOT policy is to take remedial actions and apply surface treatments if the skid number is less than 35 for the ribbed test tire or 20 for the smooth test tire.

Table 2.2. Skid number adjustment factors constants at various test speeds (Cybernetics 2000)

Test speed (mph)	Skid number adjustment constants
25	Subtract 7
30	Subtract 5
35	Subtract 2
40	No adjustment.
45	Add 2
50	Add 5

The Texas Department of Transportation (TxDOT) performs annual skid resistance measurements using the locked-wheel skid trailer. The test is performed at 50 mph using a smooth tire in accordance with ASTM E274. No standard practice has been established yet to conduct friction testing at various speeds (Zimmer & Fernando 2013; Aldagari *et al.* 2018).

The Idaho Transportation Department (ITD) manages about 12,000 lane miles of roadways. ITD pavement engineers use the measured skid numbers to determine the need for surface treatments to improve skid resistance. The current practice at ITD is to measure the skid number using a Dynatest 1295 Locked Wheel Friction Testing Trailer according to ASTM E274 using a smooth tire. The standard practice by ITD is to measure the skid number at 40 mph every tenth of a mile (Poorbaugh 2017).

2.6 Relation between Skid Resistance and Speed

Speed is one of the most important factors affecting the friction between two surfaces. If an object moves increasingly faster over a surface, there will be an increase in its momentum in the normal direction resulting in an upward force on the upper surface. This upward force creates a separation between the two surfaces, which decreases the true area of the contact between them. Further, as the speed increases, the time duration over which the two surfaces remain in contact decreases (Chowdhury *et al.* 2011). Reduced area and duration of contact decrease the molecular bonding between the asperities and rubber tires leading to reduced adhesion and consequently lower friction (Bowden & Tabor 1950; Schallamach 1971). Therefore, skid resistance found to be satisfactory at one speed may not be adequate at a higher speed.

A number of studies have examined the relationship between skid resistance and speed. The findings of some of these efforts are summarized in the following section.

2.6.1 Corsello (1993)

Moyer (1943) demonstrated that the coefficient of friction of rubber tires on a slippery surface is higher at low speeds and it decreases rapidly with speed which is consistent with the findings of Byrd. In addition, the driver demand for friction increases as vehicle speed increases (Byrd 1981). The dependency of frictional force on speed under wet conditions is influenced by the net contact area between the tire and pavement surface. This contact area is affected by how fast the water is removed from the pavement surface through the tire treads. Water presence on the pavement surface causes a degradation in the ability of tires to form a bond with the pavement surface at higher speeds and so minimizes contact area (Corsello 1993).

2.6.2 Rizenberg *et al.* (1973)

Using a skid trailer, Rizenberg *et al.* (1972) examined the correlation between skid resistance and various pavement surfaces, including flexible and rigid pavements. As expected, the skid number of pavements decreased with increase in speed. The speed gradient (i.e., the change in skid number with speed) had an average value of about 0.4 per mph between the speeds of 40 mph and 60 mph (i.e., if the speed increases from 40 mph to 60 mph, the skid number will

decrease by 8 points). They also found that the relationship between skid number and speed is not always linear (Rizenbergs *et al.* 1973).

Rizenbergs *et al.* (1973) found a strong linear relationship between the skid number at 70 mph (SN70) and the skid number at 40 mph (SN40) for asphalt pavements and Portland cement concrete (PCC) pavements. The R^2 values were 0.934 and 0.954 for asphalt and PCC pavements, respectively. The regression equations showed, as expected, that the skid number at 40 mph is higher than the skid number at 70 mph.

2.6.3 Penn State Model

Leu and Henry (1978) proposed a model for prediction of skid resistance as a function of speed and pavement texture measurements as given in Equation 2.1.

$$SN = C_0 \exp (C_1 V) \quad 2.1$$

where:

SN = skid number

C_0 = zero speed intercept

C_1 = change in slope gradient

V = speed (km/h)

They modified Equation 2.1 to obtain the Pennsylvania State University model for skid resistance speed behavior as given in Equation 2.2.

$$SN = (-31 + 1.38 \text{ BPN}) \exp [-0.041 V (\text{MTD})^{-0.47}] \quad 2.2$$

where:

BPN = British pendulum number

MTD = Mean texture depth

Equation 2.2 can be used to predict the skid number at any speed (V) based on BPN and MTD values. The result showed a good correlation ($R^2 = 0.85$) between the predicted skid number obtained from Equation 2.2 and measured value of skid number.

They proposed an alternative model, (shown in Equation 2.3) that can be used to predict the skid number based on the skid number at 40 mph and the MTD of the surface.

$$SN = SN_{40} \exp [-0.041 (V-40) MTD^{-0.47}] \quad 2.3$$

Equation 2.3 was used to predict skid number at 60 mph using the measured skid number at 40 mph and MTD and the result showed a very strong correlation ($R^2 = 0.99$) between the predicted skid numbers at 60 mph versus the measured ones.

2.6.4 Kulakowski (1991)

Kulakowski (1991) modified the Pennsylvania State University model by replacing the percent normalized gradient (PNG) with a speed constant (V_0) as shown in Equation 2.4 and Equation 2.5. PNG is a normalized gradient of skid number and speed in percentage (Kulakowski 1991).

$$SN_V = SN_0 \exp [-(V/V_0)] \quad 2.4$$

$$V_0 = 100 / PNG \quad 2.5$$

The speed constant (V_0) is a measure of the rate of change of the skid number with speed which was found to be related to the pavement macrotexture. The model requires two parameters (SN_0 and V_0) for the prediction of the skid number. Kulakowski (1991) proposed two methods for the calculation of these parameters: a direct method and an indirect method as discussed in this section.

In the direct method, the skid number is measured in accordance with ASTM E274 at two speeds (V_1 and V_2); therefore, two values for skid number (SN_{v1} and SN_{v2}) are obtained at two different speeds. Equations 2.6 and 2.7 are proposed to calculate the values of V_0 and SN_0 , respectively.

$$V_0 = (V_2 - V_1) / \ln (SN_{v1} / SN_{v2}) \quad 2.6$$

$$SN_0 = SN_{v1} e^{v1/v0} \quad 2.7$$

In the indirect method, the skid number is measured using ribbed and smooth tires at 40 mph. Equation 2.8 determines SN_0 , while Equation 2.9 determines PNG.

$$SN_0 = 35.4 - 0.682 SN^B + 2.894 SN^R - 12.75 (SN^R)^{1/2} + 24.7 / (SN^B)^{1/2} \quad \mathbf{2.8}$$

$$PNG = -0.49 - 0.01996 SN^B + 0.0106 SN^R + 0.113 (SN^R)^{1/2} + 3.48 / (SN^B)^{1/2} \quad \mathbf{2.9}$$

where

SN^R = Skid resistance measurement obtained using ribbed tire

SN^B = Skid resistance measurement obtained using smooth (blank) tire

V_0 was obtained from PNG using Equation 2.5.

The predicted skid number at 50 mph demonstrated a good correlation with the measured skid number obtained from both indirect method and direct method.

2.6.5 Jackson (2008)

Jackson (2008) conducted a study to harmonize the skid resistance measurements with speed using the concept of International Friction Index (IFI) as described in ASTM E1960. The objective of the study was to implement the IFI in Florida so that friction tests could be performed at variable speeds. Ten different roadway sections were selected, and DFT and CTMeter tests were performed on each location. Full-scale friction tests were conducted using the locked wheel friction test unit of the Florida DOT with both ribbed and smooth tires per ASTM E274.

While the study reported a good correlation between the DFT data and the full-scale locked wheel friction data, the correlation between the speed gradient from the DFT data and the MPD from the CTMeter was significant only for smooth tires. As such, the IFI index could not be used for harmonization of friction testing performed with ribbed tires. The IFI method was recommended for use with smooth tires only with the reservation that the test surfaces should have high difference in macrotexture as is the case for the open-graded and dense-graded surface.

Jackson proposed a second method to relate the pavement friction with test speed for ribbed tires. He examined the speed gradient of the locked wheel friction unit and found that the

slopes were similar for most ribbed tires. He suggested using the average speed gradient, for the tested pavements, to convert the locked wheel ribbed tire friction data at 30 mph and 50 mph to the standard 40 mph value. He proposed this method as a practical procedure for transforming friction test at various speeds measured using the Florida DOT locked wheel friction unit with ribbed tires.

2.6.6 *Flintsch et al. (2010)*

Flintsch et al. (2010) described a methodology to compute an adjustment factor to convert a skid number measured at one speed into a skid number at a different speed. They used friction data measured on Virginia Smart Roads from 2007 to 2009. A skid trailer was used to measure the skid number, and a CTMeter was used to measure the mean profile depth. The test sites included flexible pavements [Superpave mixes, Stone Matrix Asphalt (SMA), and Open Graded Friction Coarse (OGFC) as well as rigid pavements [Continuously Reinforced Concrete Pavement (CRCP)]. They measured the skid number at different speeds using both smooth and ribbed tires. They found an inverse linear relationship between measured skid number and speed for both smooth and ribbed tires. Figure 2.10 shows the relationships for OGFC and CRCP. Figure 2.10a shows that the trendlines for OGFC and CRCP have different slopes. They appear to cross each other at a speed of 30 mph for smooth tires, while they are almost parallel to one another for ribbed tires (Figure 2.10b). These results suggest that the smooth tires are more sensitive to the macrotexture than ribbed tires.

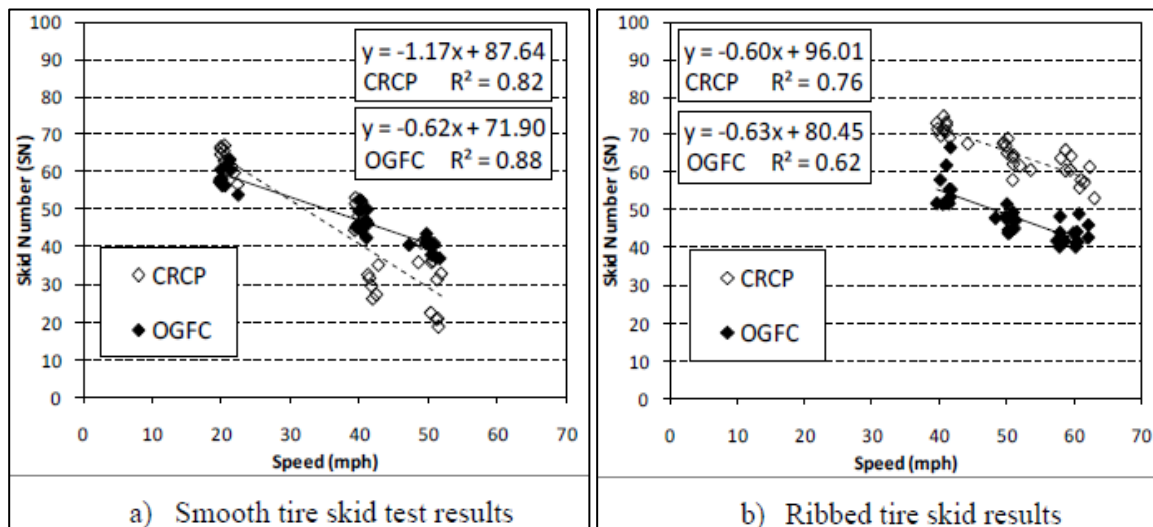


Figure 2.10. Sample skid testing results for two sections of the Virginia smart road. Figure reproduced with permission from Flintsch *et al.* 2010.

They also developed adjustment factors for estimating skid resistance at different speeds based upon one skid measurement conducted at a given speed. They grouped the surfaces into three categories according to their frictional behavior: SM and SMA, OGFC, and CRCP using the Principal Component Analysis Method. They established linear regressions between skid number and speed and computed the slope of the regression lines. The variations in skid number for smooth tires were greater than those for ribbed tires. The adjustment factor was found to have a good correlation with the mean profile depth for smooth tires ($R^2 = 0.76$). The correlation between the adjustment factor and the ribbed tire was very poor ($R^2 = 0.05$).

Based on the correlations for smooth tires, a relationship for the speed adjustment factor as a function of mean profile depth (MPD) was developed as given in Equation 2.10.

$$C = 0.85 \text{ MPD} - 1.64$$

2.10

where:

C = speed adjustment factor for all smooth tire units

MPD = Mean Profile Depth (mm)

Equation 2.10 calculates the change in skid number in increments of change in speed of one mile per hour. Equation 2.11 is a generalized form to convert skid number at one speed to skid number at another speed based upon the above adjustment factor which is as follows:

$$F_{v_2} = F_{v_1} + \Delta F \quad 2.11$$

where:

F_{V_2} = skid number at desired speed (V2)

F_{V_1} = skid number at measured speed (V1)

$\Delta F = C \Delta V = (0.85 * MPD - 1.64) * \Delta V$

$\Delta V = V_2 - V_1$

CHAPTER 3 SELECTION OF TEST SECTIONS AND FIELD TESTING

3.1 Introduction

Several candidate pavement sites were identified and selected across Idaho for field testing and evaluation. These sections were selected to cover different pavement types in the state. A total number of 34 test sites were selected in this study. Several criteria were considered when selecting the test sections including:

- Pavement type: flexible and rigid pavement test sections as well as seal coat surfaces were selected.
- Skid number: test sections with different levels of skid resistance were selected and evaluated.
- Environmental conditions: the test sections were distributed across the state and sites from all six districts were included in this study.
- Traffic level: interstate highways, US highways, and state highways subjected to different traffic levels were considered.
- Service life: pavement sites with different age were included. Old pavements are expected to provide lower skid numbers compared to newer pavement due to abrasion and polishing under traffic.

Of the total 34 pavement sections that were evaluated in this study, 12 sites were hot mix asphalt (HMA), 17 were seal coat and five sections were concrete pavements. Table 3.1 provides the list of test sections along with their type and location. Several criteria were considered when selecting the location of the test sections including:

- Each test section should be at least one mile long.
- The test section should be a straight segment (i.e., no curves or sharp turns).
- Test sections should have a low grade.
- Test sections should have a minimum number of exits/entrances.

The above criteria were considered to ensure that the skid truck was able to collect the skid numbers safely at various speeds and minimize traffic interruptions.

Figure 3.1 shows the location of test sections distributed across the state of Idaho. Figure 3.2 illustrates the distribution of the test sites by pavement type. About 53% of the test sections were flexible pavement surfaced with seal coat, 32% were HMA, and 15% were concrete,. The relatively low number of concrete sections is due to fact that about 95 % of pavements in Idaho are flexible pavements. The current practice in Idaho is to seal flexible pavement surface with chip seal early after the construction, which also explains the relatively large number of seal coat sections.

Figure 3.3 shows that the test sections were distributed across the six districts of Idaho. Figure 3.4 shows that most of test sections (i.e., 76%) were U.S. highways and Interstate highways. These highways have relatively high traffic volumes and speed limits, which are two major factors affecting skid resistance of pavements.

Table 3.1. List of test sections in State of Idaho

District	Highway	Milepost	Surface Type
District 1	SH-60	MP 003	Seal coat
	US-95	MP 440	HMA
	US-95	MP 405	HMA
District 2	US-95	MP 325	Seal coat
	US-95	MP 247	Seal coat
	US-95	MP 259	Concrete
	US-95	MP 289	HMA
District 3	I-84	MP 36	Concrete
	I-84	MP 55	HMA
	I-84	MP 72	Concrete
	I-84	MP 84	HMA
	SH-44	MP 08	Seal coat
	SH-45	MP 26	Seal coat
	SH-78	MP 56	Seal coat
	US-20	MP 38	HMA
District 4	I-84	MP 236	Seal coat
	SH-24	MP 039	Seal coat
	SH-81	MP 006	HMA

District 5	I-15	MP 078	HMA
	I-86	MP 047	HMA
	US-30	MP 365	Seal coat
	US-30	MP 382	Seal coat
	I-15	MP 031	Concrete
	I-15	MP 022	Seal coat
	I-15	MP 007	Seal coat
	I-15	MP 037	Seal coat
	I-15	MP 096	HMA
	I-86	MP 016	Concrete
	SH-34	MP 048	Seal coat
	SH-38	MP 023	Seal coat
	District 6	I-15	MP 165
US-20		MP 326	HMA
US-20		MP 315	HMA
US-26		MP 355	Seal coat

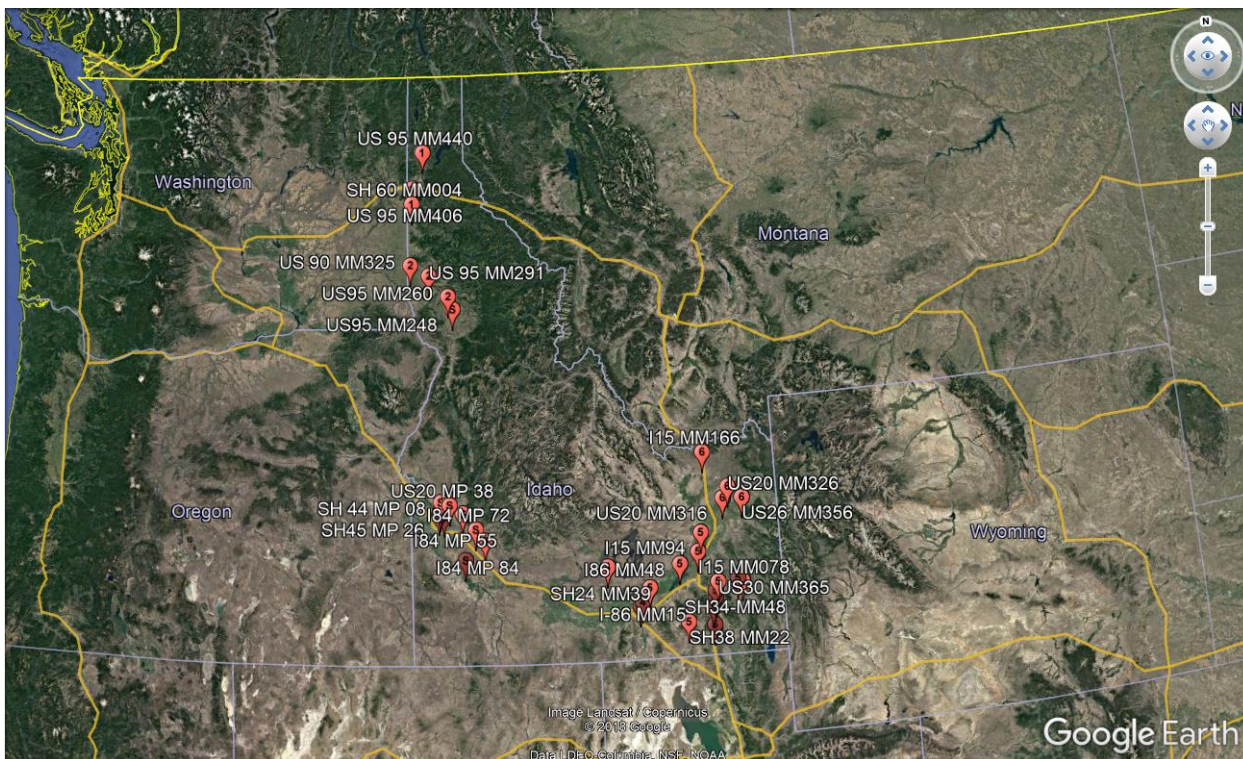


Figure 3.1. Locations of the selected test sections in the state of Idaho.

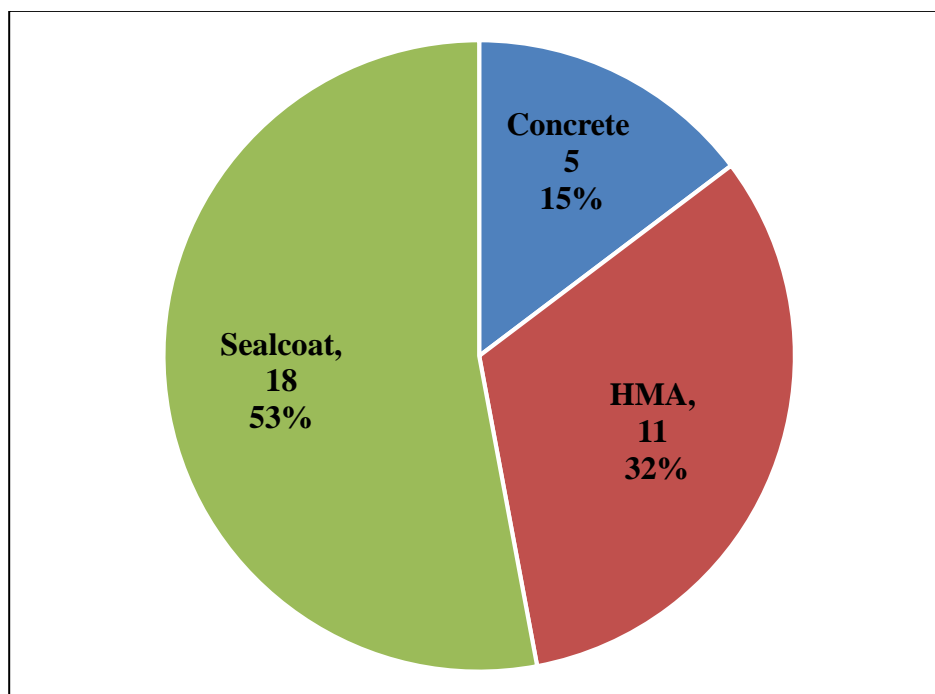


Figure 3.2. Test section distribution by pavement surface type.

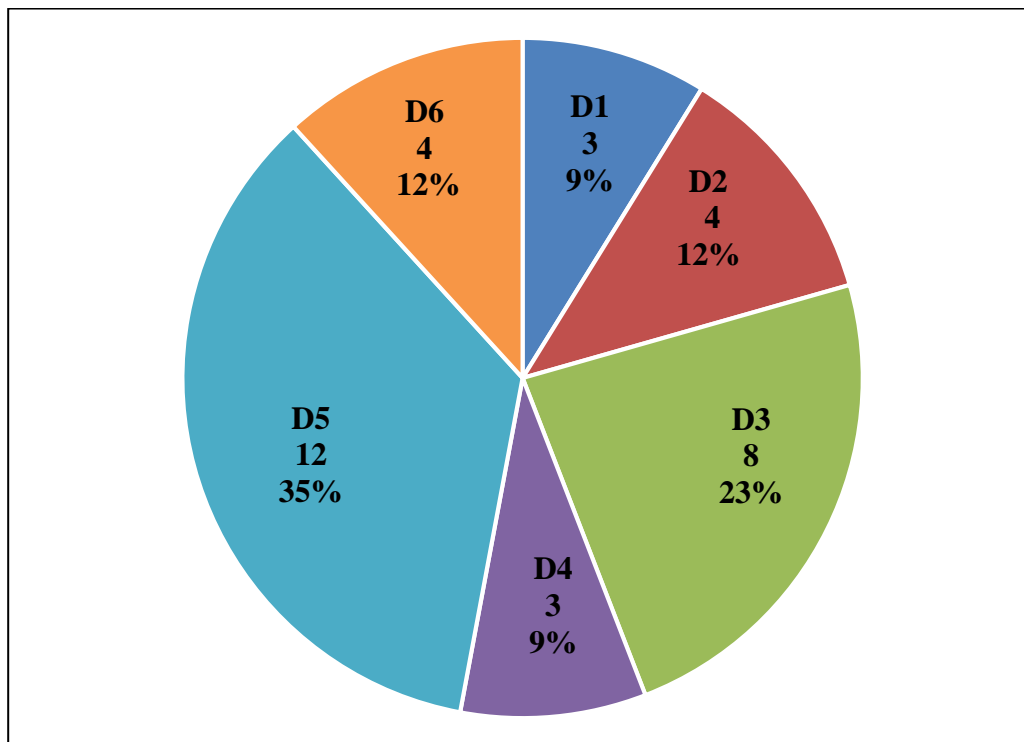


Figure 3.3. Test section distribution by ITD district.

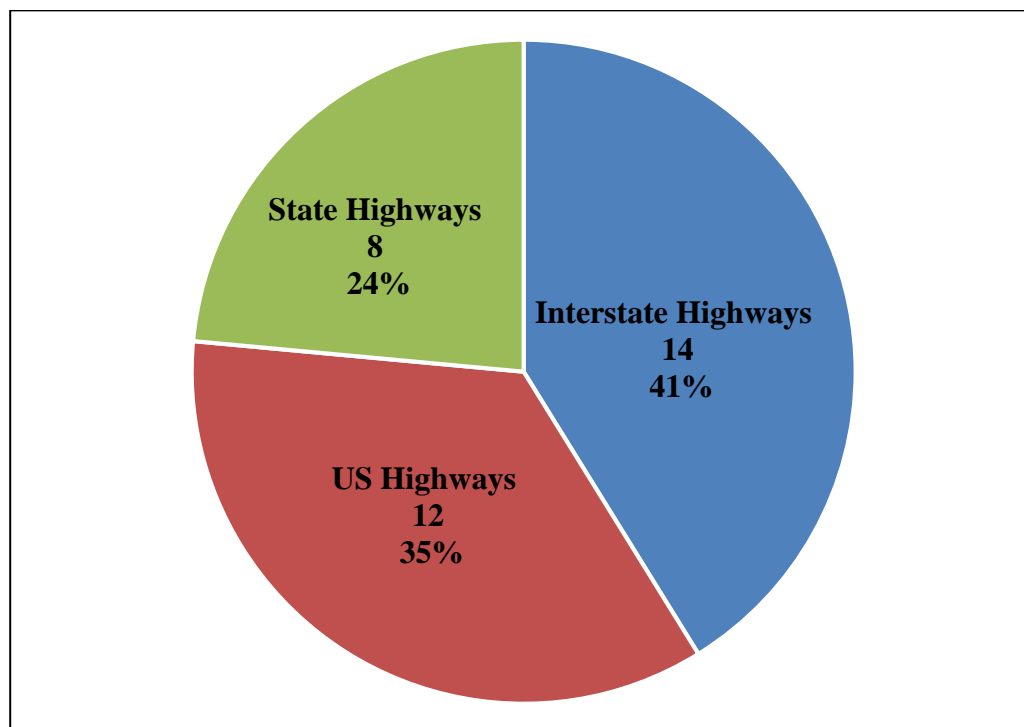


Figure 3.4. Test section distribution by highway type.

3.2 Skid Number Measurements

Skid number measurements were collected using the ITD locked-wheel skid trailer (Figure 3.5). ITD uses the 1295 Locked Wheel Friction Testing Trailer manufactured by Dynatest to measure the skid number at a standard speed of 40 mph in accordance with ASTM E274. The tests is performed using a smooth tire in accordance with ASTM E524.

A stretch of one mile of the outer lane of each test sites was selected for skid measurements at different speeds (i.e., 20, 30, 40, 50, and 60 mph). At least seven skid number measurements were recorded at each speed and the average skid number was calculated.

It should be noted that skid testing could not be conducted at all five test speeds (i.e., 20, 30, 40, 50, and 60 mph) for all test sections. In District 3, for example, due to high speed limits and traffic levels, friction testing was not conducted at lower speeds (i.e., 20 and 30 mph); instead, the skid number was measured at three speeds (i.e., 40, 50, and 60 mph). Similarly, it was not possible to measure skid numbers at 60 mph for two other sections since it was not safe to drive the skid truck at this higher speed at these two sections due to speed limit restrictions.



Figure 3.5. ITD locked wheel skid trailer.

3.3 Measurement of Surface Texture Characteristics

The surface texture characteristics of the test sections were measured using a Dynamic Friction Tester (DFT), Sand Patch Test and the laser sensor installed on the ITD skid trailer. The researcher measured the microtexture and macrotexture at the wheel path of the outer lane. Figure 3.6 shows the locations of test spots in a typical test section. For each test section, DFT and the Sand Patch Test were conducted at three locations separated by a distance of 200 ft. At each location, measurements were re-recorded at two spots 20 ft apart from each other. At least two DFT measurements were recorded at each location to ensure data reproducibility. The selected test spots were free of cracks, potholes, loose materials and other irregularities to avoid misleading texture results.

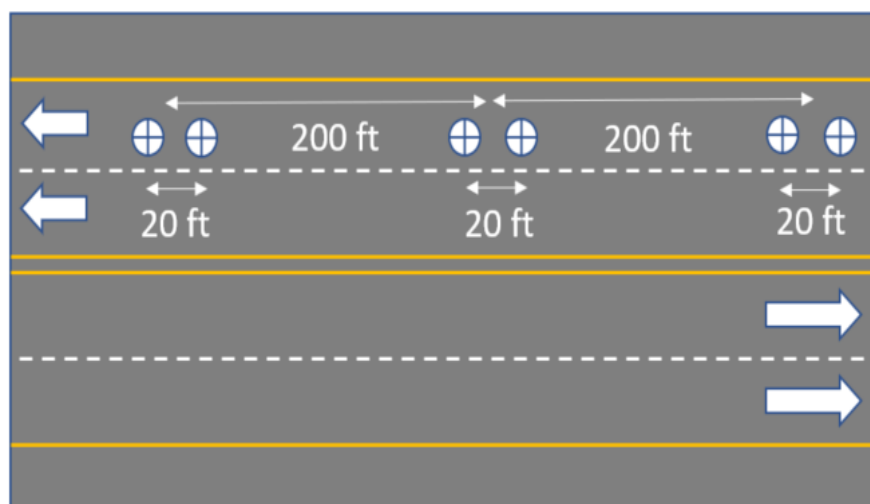


Figure 3.6. Location of DFT and sand patch measurements.

3.3.1 Measurement using Dynamic Friction Tester (DFT)

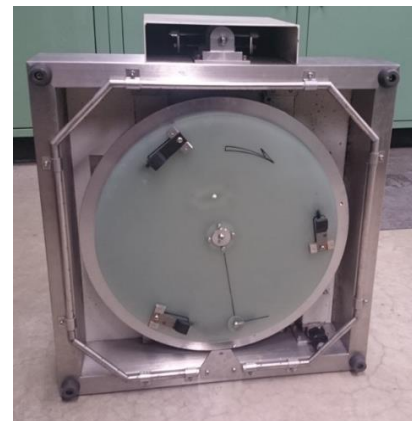
The surface microtexture was measured using the DFT device (Figure 3.7). Figure 3.6 shows typical field-testing using the DFT. Traffic control was provided during field testing. The DFT accompanied software was used to operate the device and record the coefficient friction during the test. Figure 3.8 shows the interface of the DFT software. After a number of friction tests and depending on the level of surface friction, the rubber sliders are replaced periodically. The coefficient of friction at 20 km/h (DFT20) was found to correlate well with pavement microtexture; thus it is used as an indirect method to measure pavement microtexture (Henry & Wambold 1992) in this study.



(a) DFT Measurements



(b) DFT Device



(c) Bottom of DFT Device

Figure 3.7. Measurement of microtexture using the DFT device.

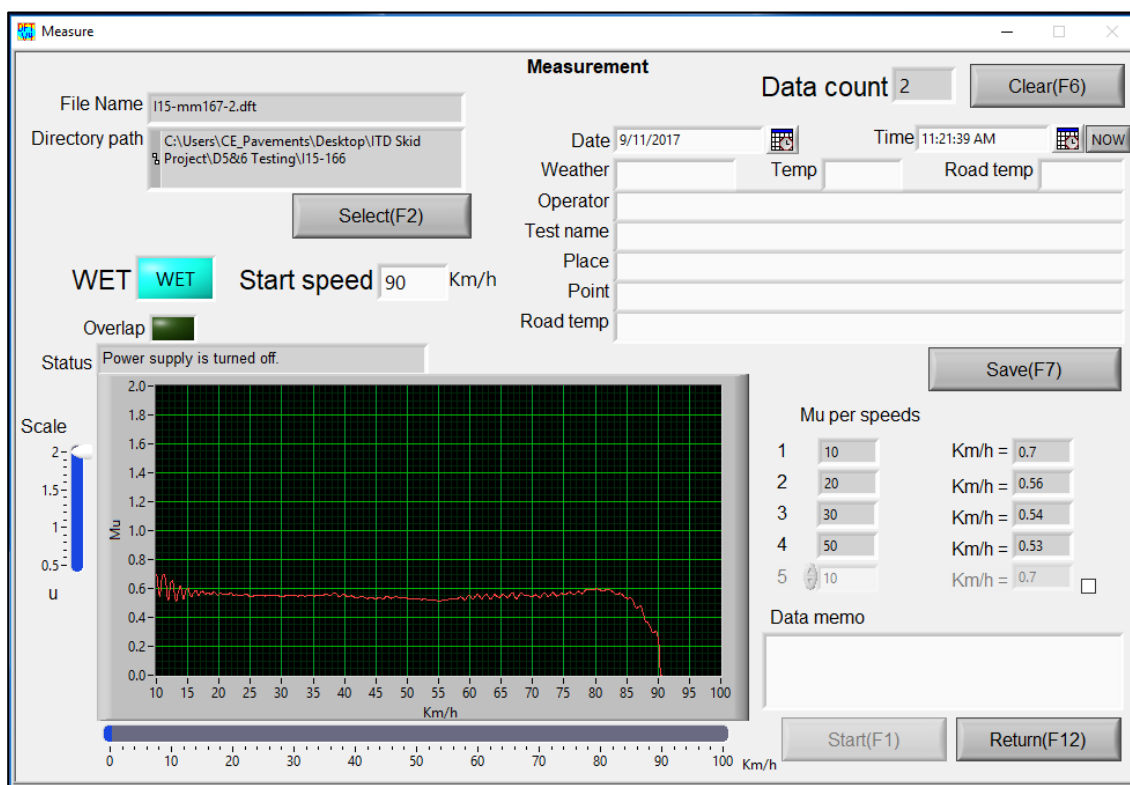


Figure 3.8. Coefficient of friction measurements by DFT software.

3.3.2 Measurement by Sand Patch Test

The sand patch test was used to measure the mean texture depth (MTD) of pavement surface at the same locations where the DFT was used to measure the microtexture as shown in Figure 3.9. Two sand patch tests were conducted at each location adjacent to the DFT measurements with a total of six tests at each site. The average MTD was calculated and used as a measure of surface macrotexture. Wind, rain and moisture may influence the results of the Sand Patch Test; therefore, the selected test spots were dry, and a box was used to shield the testing spot from wind if there was any. In some cases, a hot air blower was used to dry the pavement surface before testing.

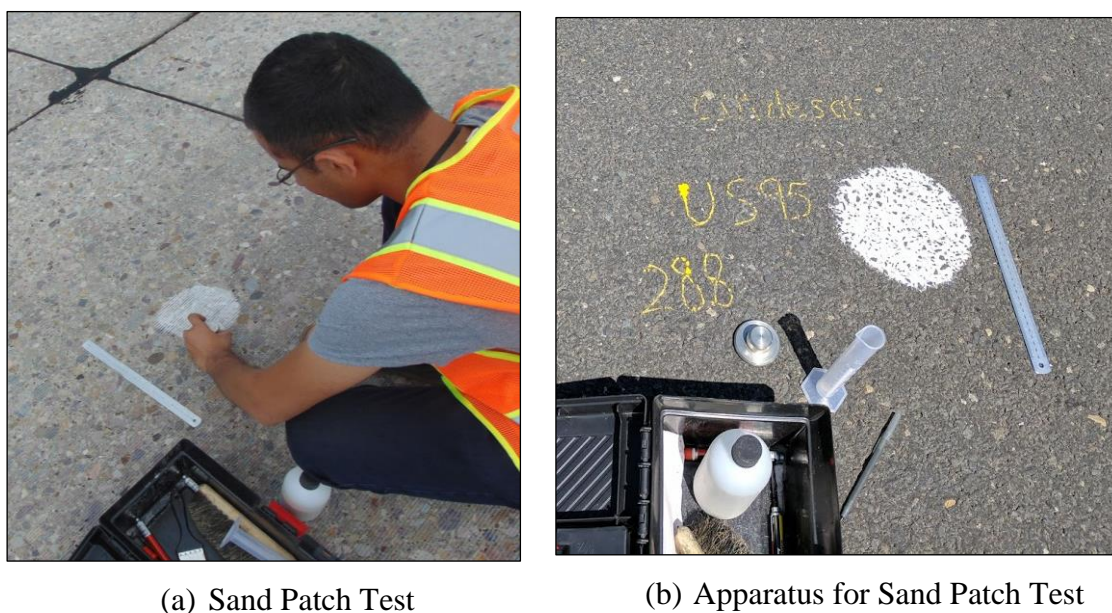
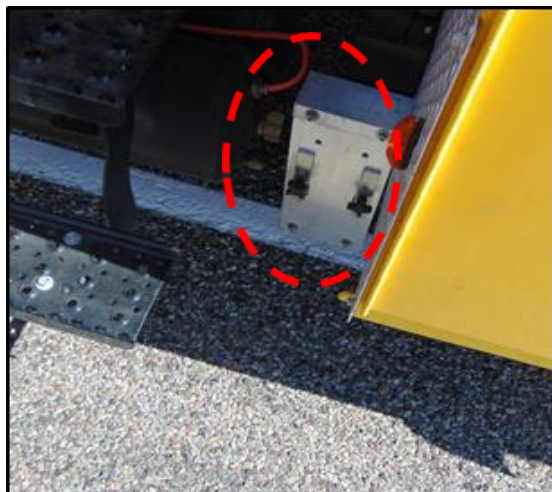


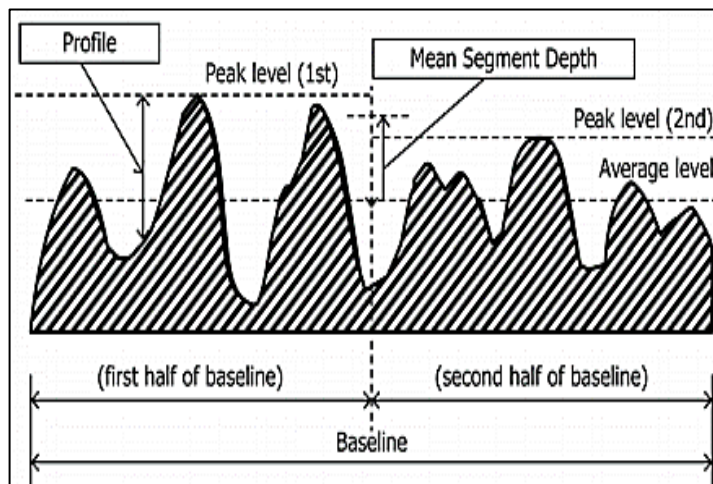
Figure 3.9. Sand patch test measurements.

3.3.3 Measurement using Laser Profiler

With advancements in laser-based technology, more accurate methods are now available to measure the pavement texture (Mataei *et al.* 2016). In this study, pavement macrotexture was also measured using a laser sensor installed on the skid truck as shown in Figure 3.10a. The pavement macrotexture is measured in terms of mean profile depth (MPD). The texture measurements were recorded simultaneously with skid number measurements using the skid trailer. The MPD is calculated in accordance with ASTM E1845 as shown in Figure 3.10b. Figure 3.11 shows examples of typical field testing of friction and texture.



a) Location of Laser Profiler in Skid Truck



b) Measurement of MPD (ASTM E 1845)

Figure 3.10. Measurement of MPD using laser profiler.



Figure 3.11. Examples of field testing.

CHAPTER 4 RESULTS AND DISCUSSION

4.1 Introduction

Several tests were conducted in the field including measuring skid numbers using the ITD skid trailer at various speeds (i.e., 20, 30, 40, 50, and 60 mph), measuring microtexture using the DFT device and macrotexture using the sand patch test and laser profiler. In Chapter 4, the data is analyzed, and the analyses performed to develop a statistical-based model to describe the change in skid with testing speed are described. In addition, the author conducted a sensitivity analyses of the model parameters to examine their effect on predicted skid numbers produced by the model.

4.2 Distribution of Friction (SN) And Texture (MPD) for the Test Sites

Figure 4.1 shows the average skid number values measured at 40 mph (standard test speed in Idaho) for all test sections and divided into three categories; HMA, seal coat, and concrete sites. It can be seen from Figure 4.1 that the seal coat sections had the highest skid number values compared to all other sections followed by the HMA surfaces. Figure 4.2 summarizes distribution of skid number measurements. The majority of the test sites (81%) have skid numbers of 40 or higher at 40 mph. A higher skid numbers indicates better resistance to skidding under wet conditions and improves safety.

Figure 4.3 shows the average MPD values for all test sections. The seal coat sections had the highest MPD which contributed to its higher skid number. MPD data from the laser profiler demonstrated that most sites have MPD between 2.0 mm and 0.50 mm with few sections outside this range as shown in Figure 4.4. A similar observation was made for the MTD values obtained using the sand patch test. Surfaces with higher MPD had higher MTD, and vice versa. Both MTD and MPD are used to describe the irregularities of pavement surface which is referred to as macrotexture. Two concrete sections had relatively high MPD. This is typical for textured concrete surface (e.g., longitudinal grooving).

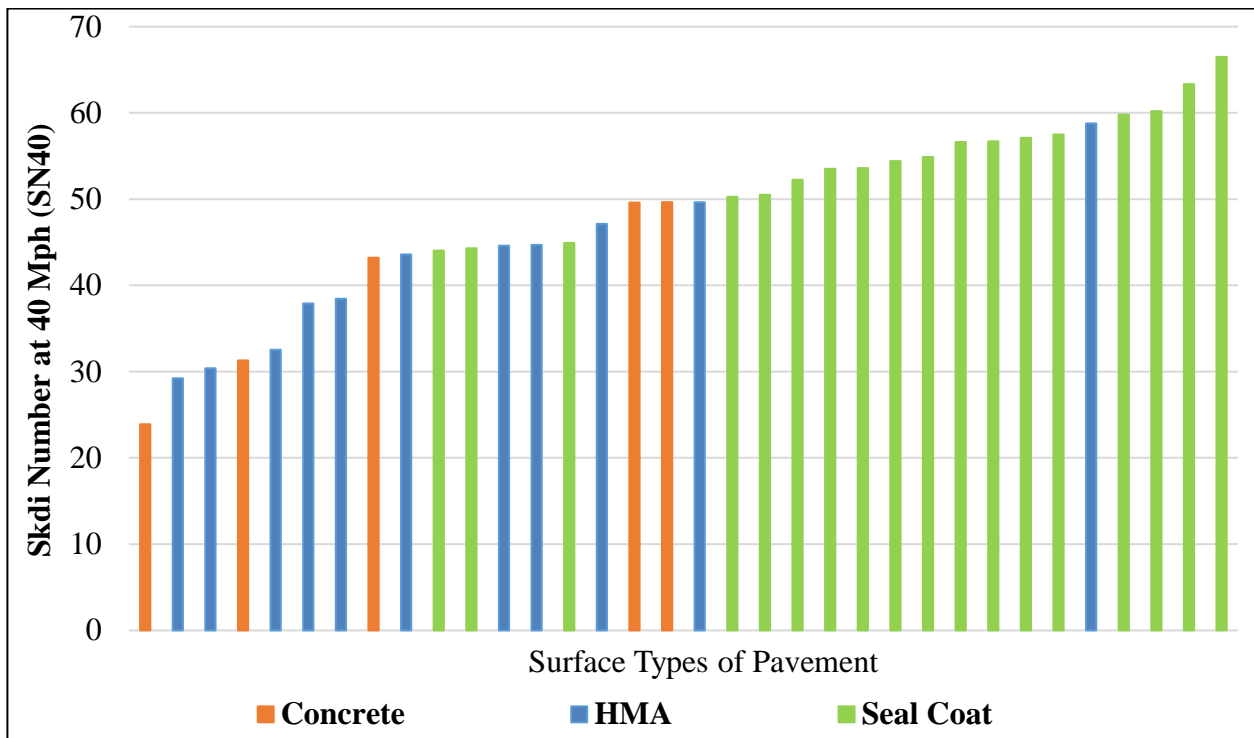


Figure 4.1. Skid number values at 40 mph for all test sections and road types examined in this study.

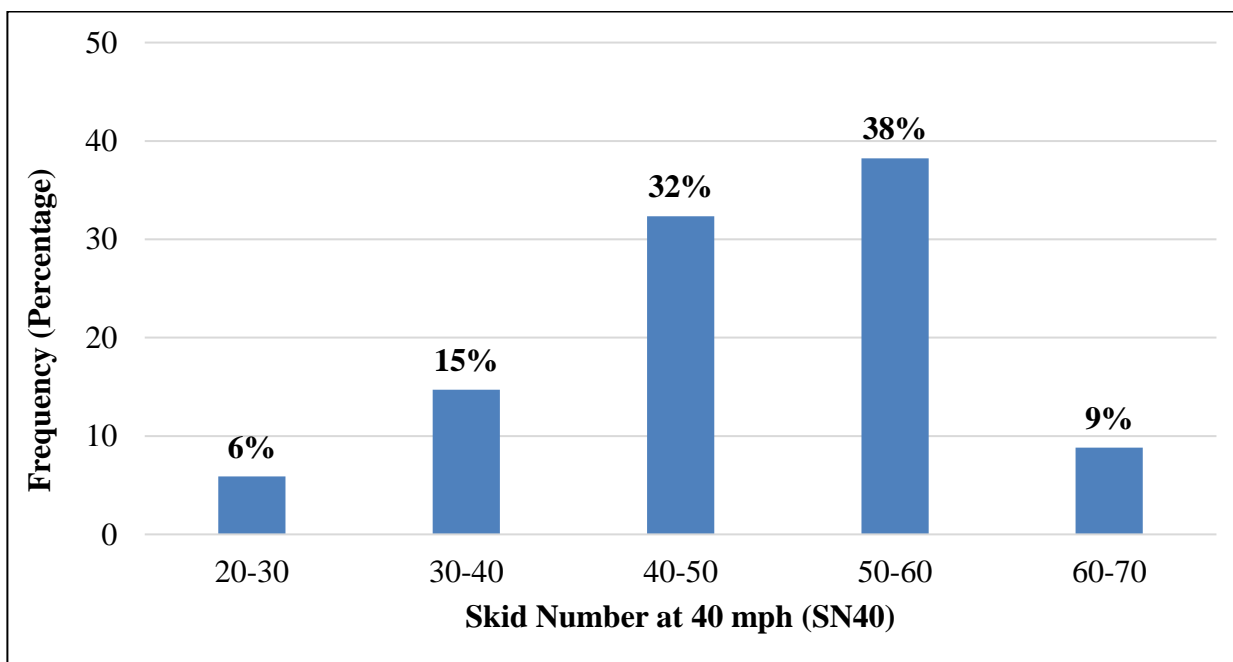


Figure 4.2. Distribution of skid number at 40 mph (SN40) for all test sections measured in this study.

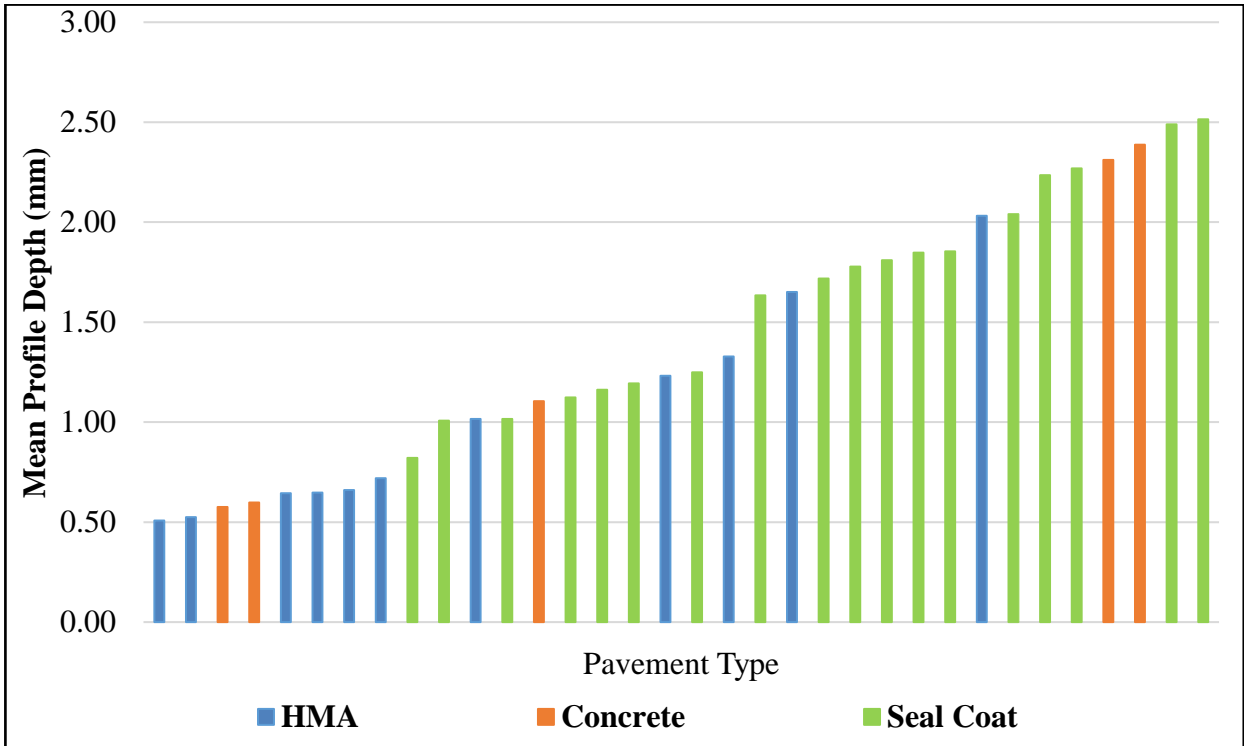


Figure 4.3. Mean Profile Depth (MPD expressed in mm) of the test sites and pavement types examined in this study.

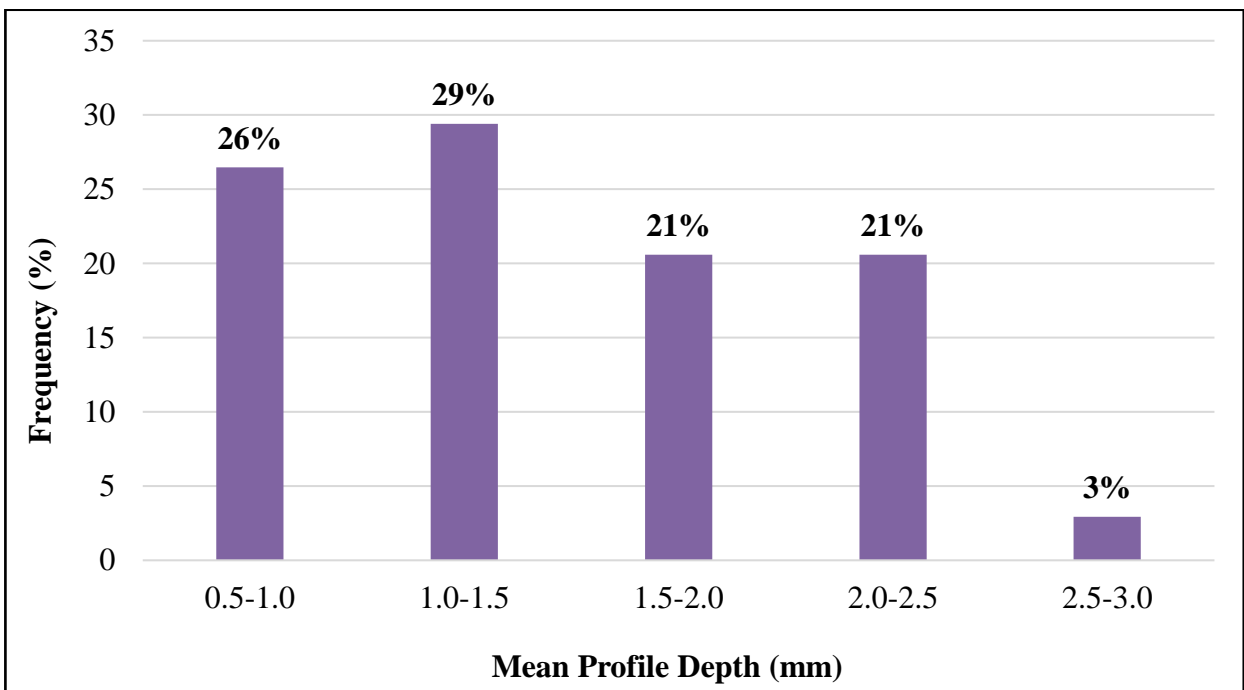


Figure 4.4. Distribution of MPD measurements for all test sections examined in this study.

4.3 Effect of Pavement Type on Friction Characteristics

An Analysis of Variance (ANOVA) was performed to examine the statistically significant difference ($P < 0.05$) among the various surface types (i.e., seal coat, HMA and concrete) in terms of pavement friction (SN40), pavement macrotexture (MPD) and microtexture (DFT). Tukey's Honestly Significant Differences (Tukey's HSD) results are presented in a form of letters.

Figure 4.5 graphically summarized the results of the Tukey's HSD of skid numbers obtained at 40 mph (SN40) for three pavement surfaces. There is no statistically significant difference in the skid numbers between surface types if they share the same letter (A, B, and C). The result indicates that SN40 values for seal coat are statistically different from both HMA and concrete at the 95% confidence interval while HMA and concrete share the same letter and so are not statistically different with respect to skid number. Figure 4.6 summarizes the MPD results where there was no statistical significant difference between mean profile depth for HMA and concrete or between concrete and seal coat; however, the Tukey's HSD results showed that there is a significant difference in MPD between the seal coat and HMA. The seal coat had a greater MPD value compared to the HMA surfaces evaluated in this study.

Tukey's HSD results presented in Figure 4.7 showed that there was no significant difference in the microtexture (i.e., DFT20) among different surface types since all of them share the same letter (i.e., A) at 95% confidence interval. The DFT20 values for various test sections had a small range which indicates insignificant difference in microtexture.

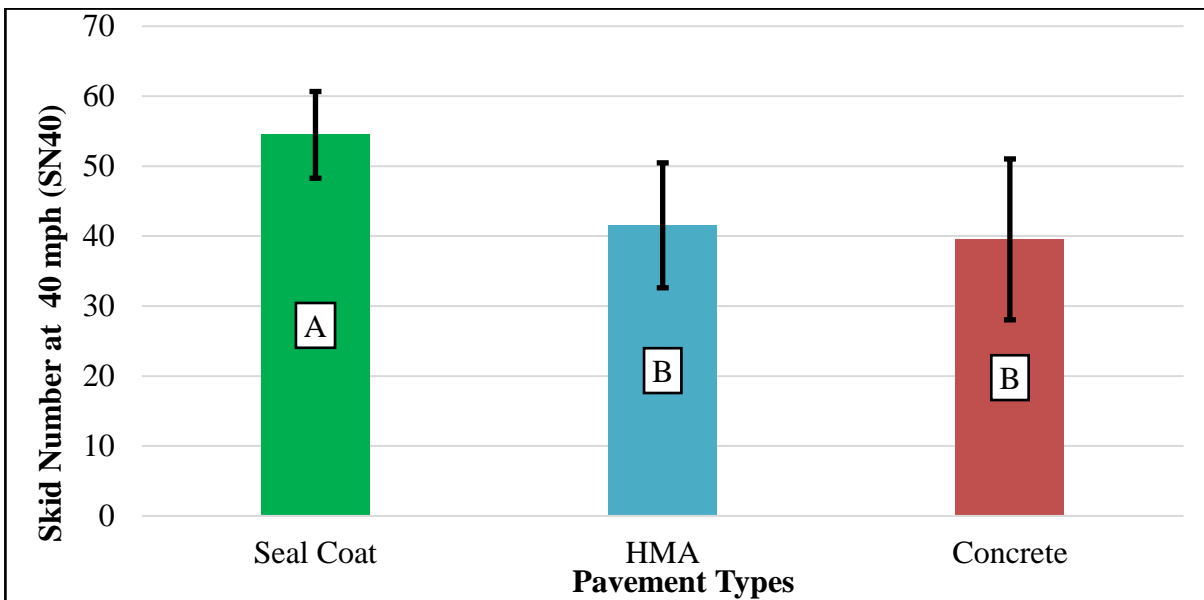


Figure 4.5. Average skid number measured at 40 mph for three pavement surfaces obtained from Tukey's HSD test. Categories with the different lettering (A, B, C) represents statistically significant difference.

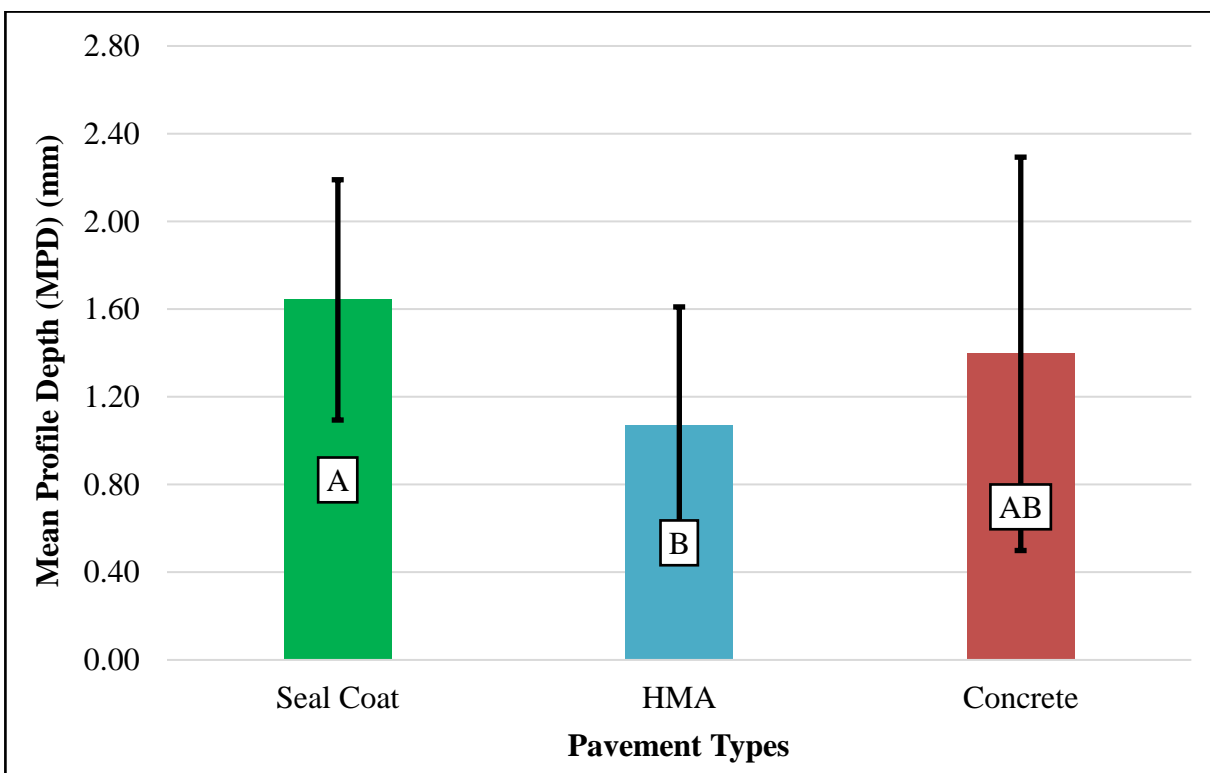


Figure 4.6. Average MPD for three pavement surfaces obtained from Tukey's HSD test. Categories with the different lettering (A, B, C) represents statistically significant difference.

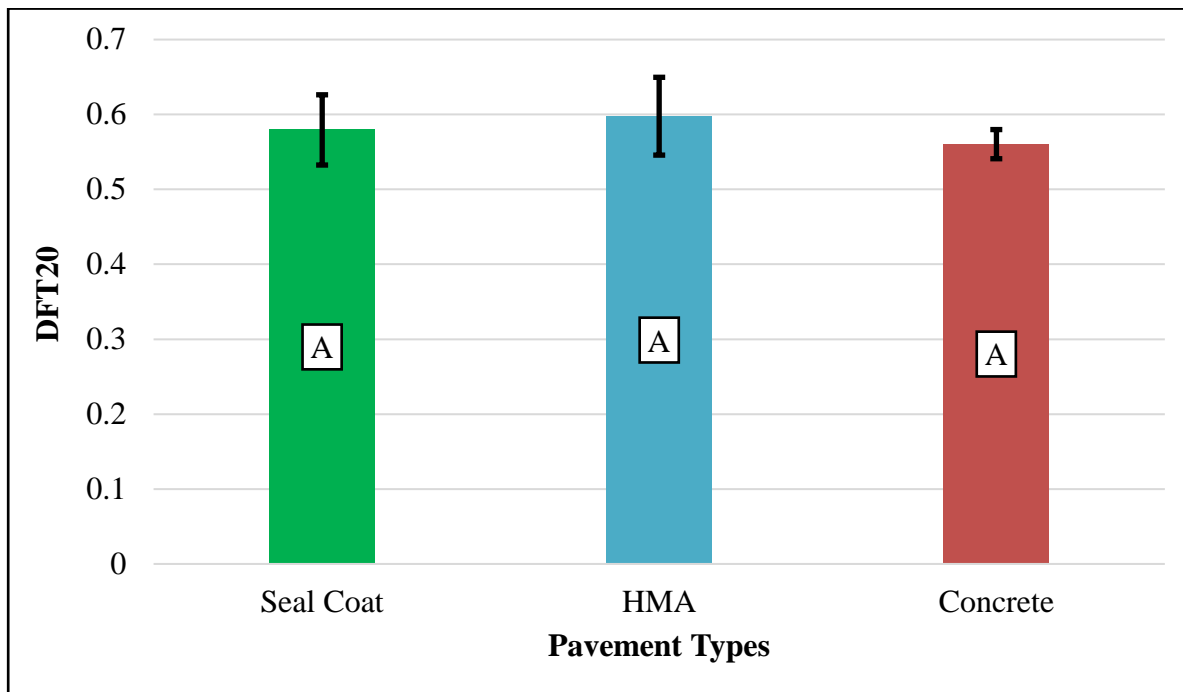


Figure 4.7. Average DFT20 values for three pavement surfaces obtained from Tukey's HSD test. Categories with the different lettering (A, B, C) represents statistically significant difference.

4.4 Variation in Skid Number Measurements

A skid trailer was used to collect several skid numbers on each run. The average skid number was calculated and considered to represent the skid resistance at a given speed. There is variation in the collected skid numbers since the surface is not uniform. The standard deviation of the skid numbers at 40 mph (SN40) for the test section in this study ranged from 0.82 to 13.11; meanwhile, most of the test sections (89%) had low standard deviation (<4).

Figure 4.8 shows the standard deviation with respect to the testing speed and mean profile depth. Overall, the standard deviation for the measured data was found to increase with the testing speed. The standard deviation for the measured skid number was 2.71 at 20 mph, which increased to 3.21 at 60 mph. No significant difference was found in standard deviation of skid number measurement with the mean profile depth of the test section.

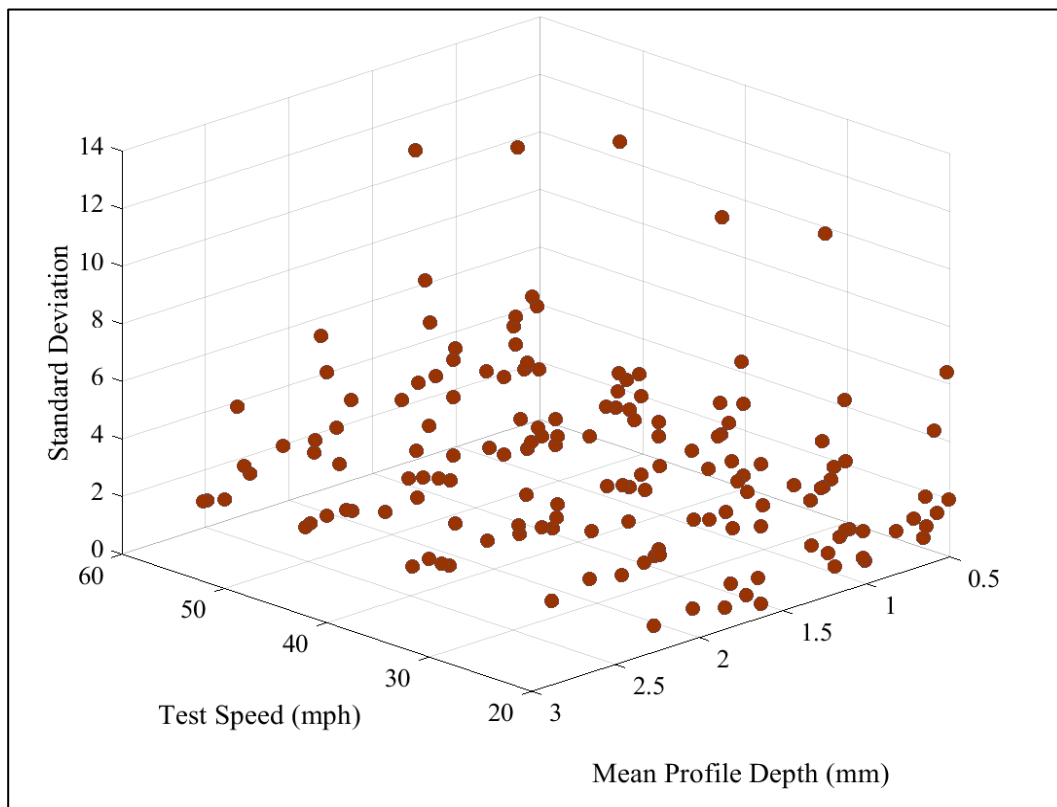


Figure 4.8. Standard deviation of measured skid number at 40 mph vs. speed and MPD.

4.5 Correlation between Friction, Speed and Texture

The measured skid numbers decreased with speed for all test sites as shown from Figure 4.9 to Figure 4.11. Most of the test sections and almost all HMA sections showed logarithmic reductions in skid number with speed. The R^2 for the correlation was greater than 0.9 for all test sites. Some researchers have reported a linear relationship between skid number and speed (Flintsch *et al.* 2010), while others found exponential decay with speed (Leu & Henry 1978; Kulakowski 1991). The change in skid numbers with speed was also found to be affected by the surface macrotexture (Hall *et al.* 2009) as discussed in Chapter 2. The skid number speed gradient (G_V) was calculated to quantify the decrease in skid number with testing speed. The G_V is defined in ASTM E867 as the rate of change in skid number per unit change in speed. In this study, the G_V was calculated between 20 mph and 60 mph, since most of the test were conducted over this range of testing speed. To maintain consistency in the G_V analysis, test sections where the skid testing could not be performed at either 20 mph or 60 mph were not considered in the G_V calculations. Figure 4.12 shows the relationship between the G_V and mean profile depths. The results demonstrated that the skid number skid gradient had a strong correlation with MPD; G_V decreases with increases in MPD. These results demonstrate that pavement surfaces with high MPD values have less change in skid number with speed compared to those with lower MPD values. This finding is supported by previous research by Hall *et al.* (2009) who concluded that the rate of change in skid number with speed is dependent on pavement macrotexture.

Figure 4.13 shows the relationship between mean texture depth (MTD) measured using the Sand Patch Test and the mean profile depth (MPD) measured using the laser profiler. The results suggest there is a strong linear relationship between MTD and MPD. One can predict MPD by measuring MTD if the laser profiler is not available due to its cost. These findings are in good agreement with previous studies in which MTD and MPD were found to have good correlation (China & James 2011; Yaacob *et al.* 2014; Praticò & Vaiana 2015; Hao *et al.* 2016; Mataei *et al.* 2016). It should be noted that this relationship was used in this study to estimate the MPD as a function of MTD for eight test sections where the researcher experienced some issues with the laser profiler.

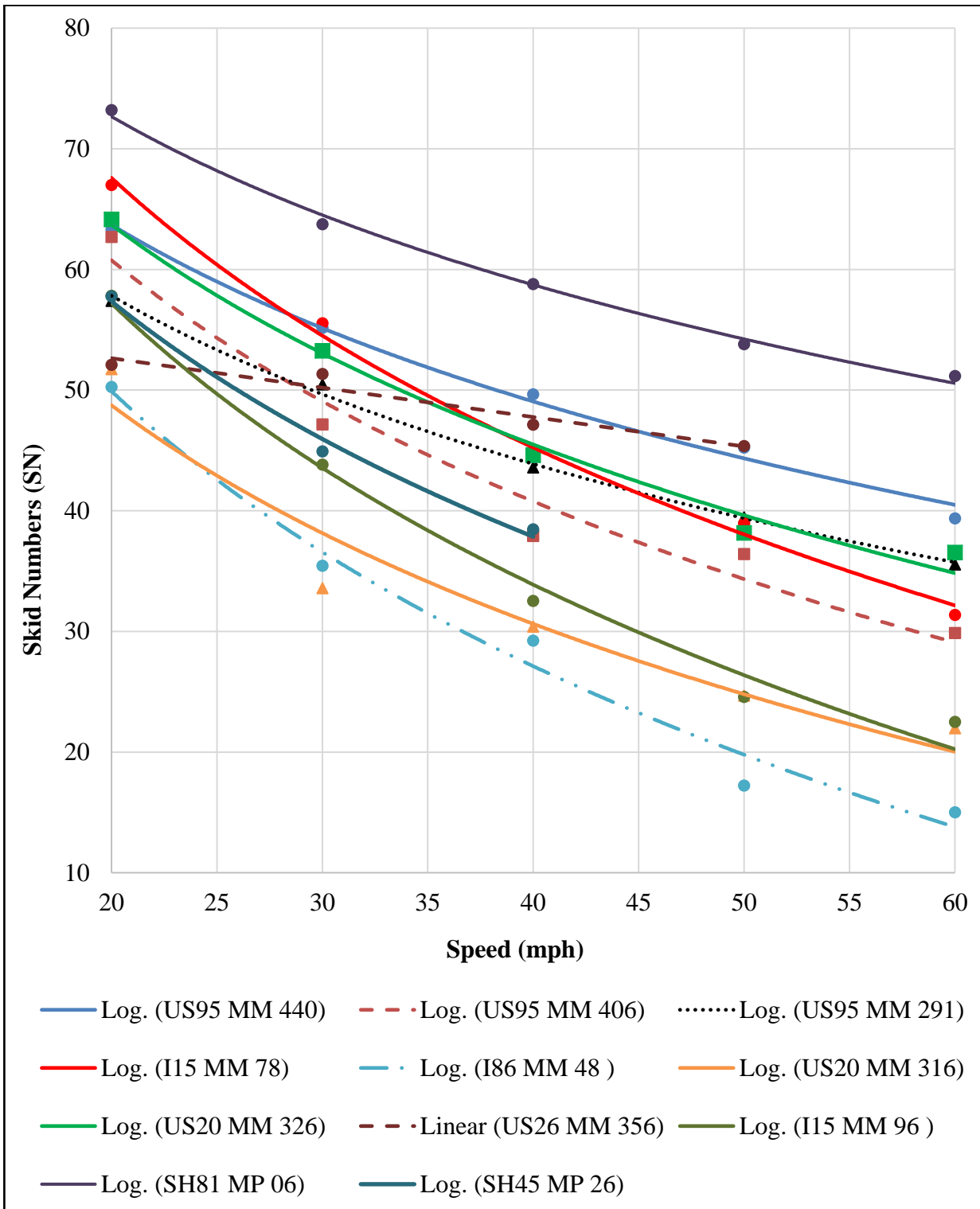


Figure 4.9. Relationship between skid number and speed on HMA test sections examined in this study.

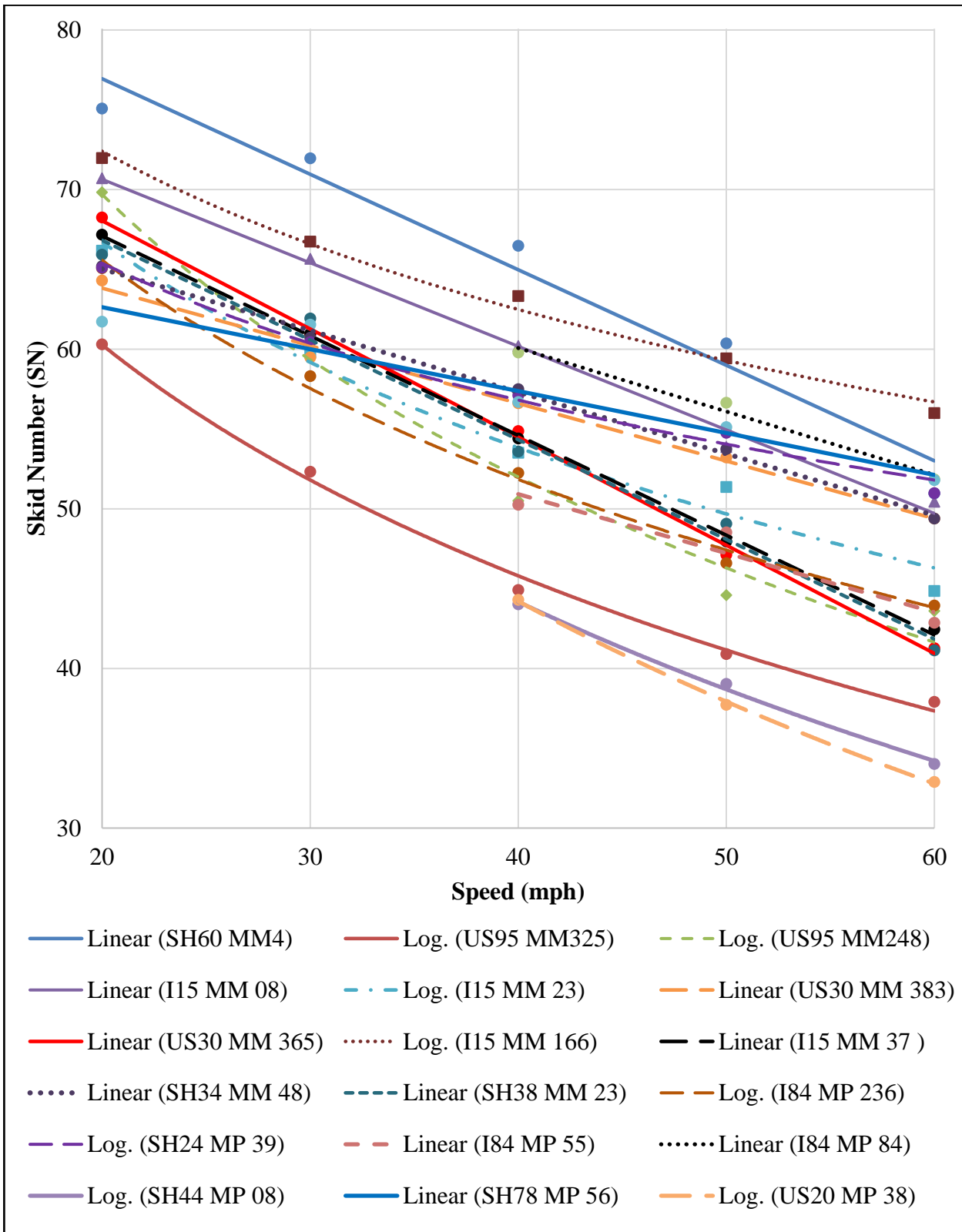


Figure 4.10. Relationship between skid number and speed on seal coat test sections examined in this study.

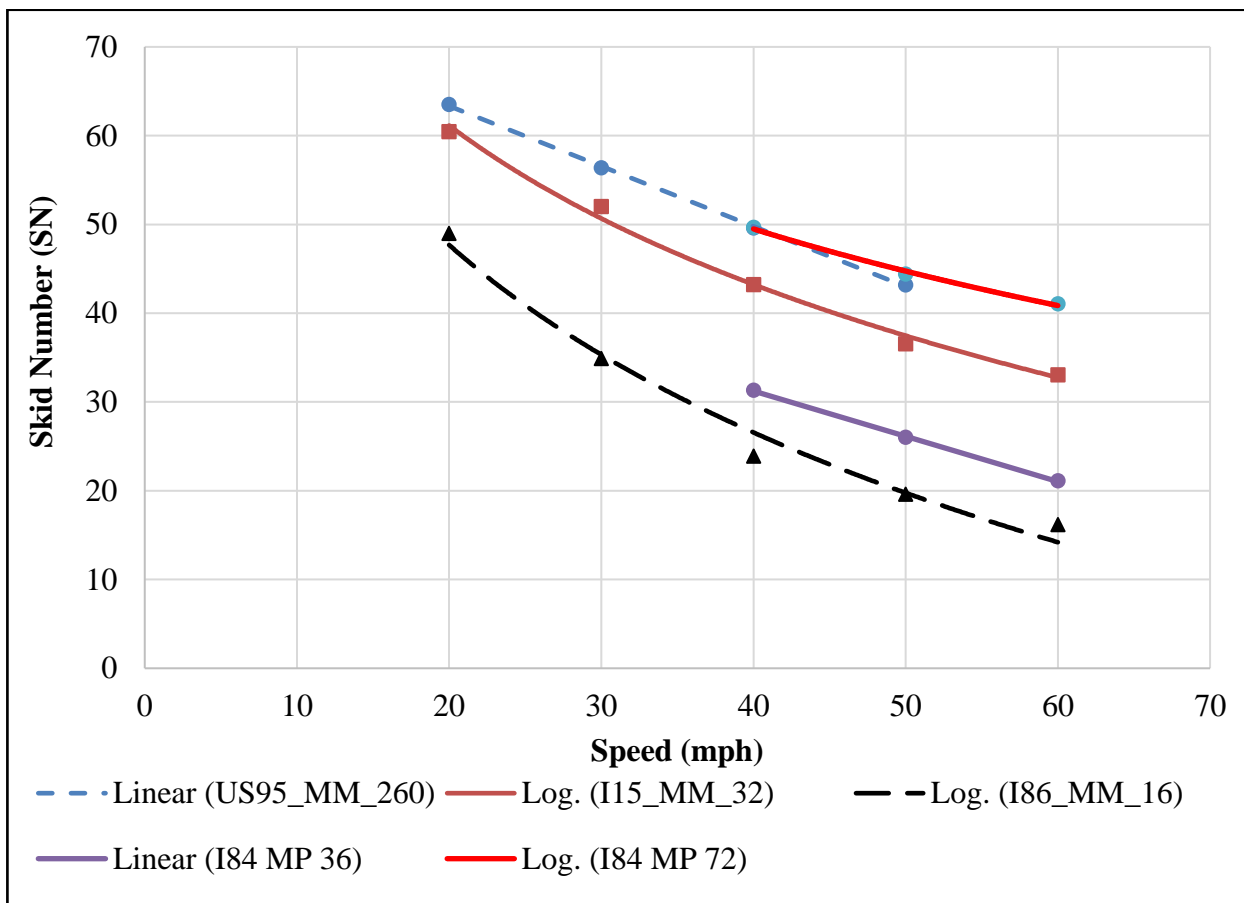


Figure 4.11. Relationship between skid number and speed on concrete test sections examined in this study.

Figure 4.14 shows that there is a logarithmic correlation with R^2 of 0.78 between skid numbers measured at 60 mph and MPD values for HMA. The R^2 value between the skid number and MPD improved with speed. The R^2 increased from 0.03 (at 20 mph) to 0.78 (at 60 mph). A similar trend was observed for the seal coat surfaces, where the R^2 value for the correlation between skid number and MPD increased from 0.01 at 20 mph to 0.16 at 60 mph. These findings are consistent with the literature since macrotexture is a more significant factor in determining skid number at higher speeds (Harwood *et al.* 1998). All plots of the relationship between skid number and mean profile depth for HMA and seal coat surfaces are provided in Appendix C. The DFT20 values did not show any correlation with the measured skid numbers at the various speeds (20, 30, 40, 50 and 60 mph) as demonstrated in Figure

4.15. It should be noted that most of the DFT20 measurements were between 0.52 and 0.63, suggesting that most of the test sections had good microtexture. All plots of DFT20 with skid numbers at various speeds are included in Appendix D.

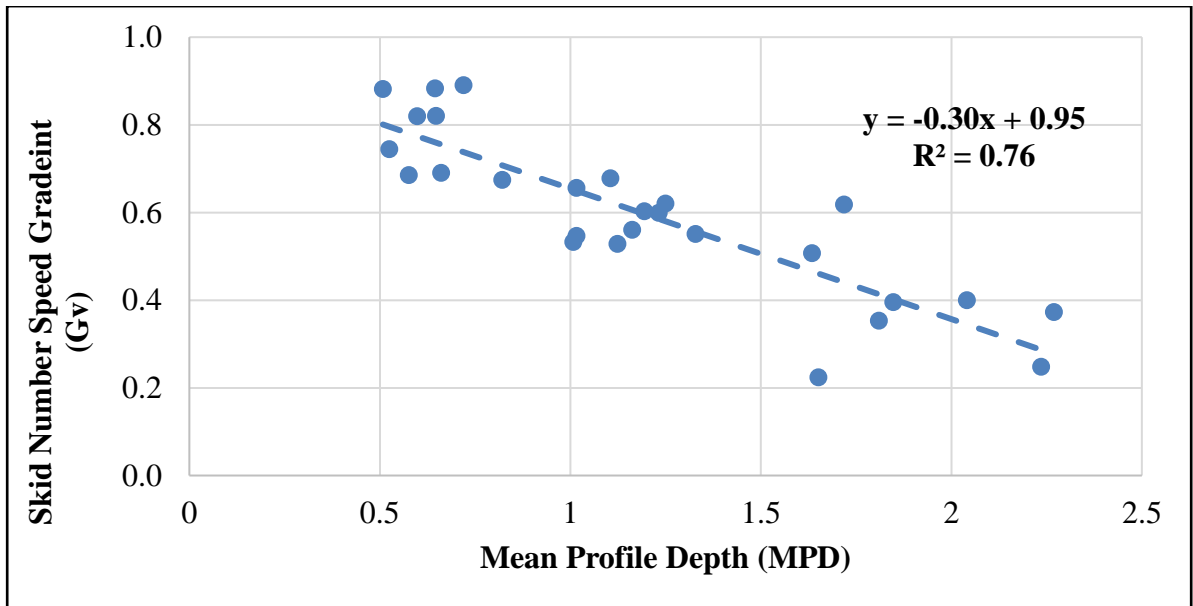


Figure 4.12. Correlation of skid number speed gradient (Gv) with macrotexture for all the pavement surface types examined in this study.

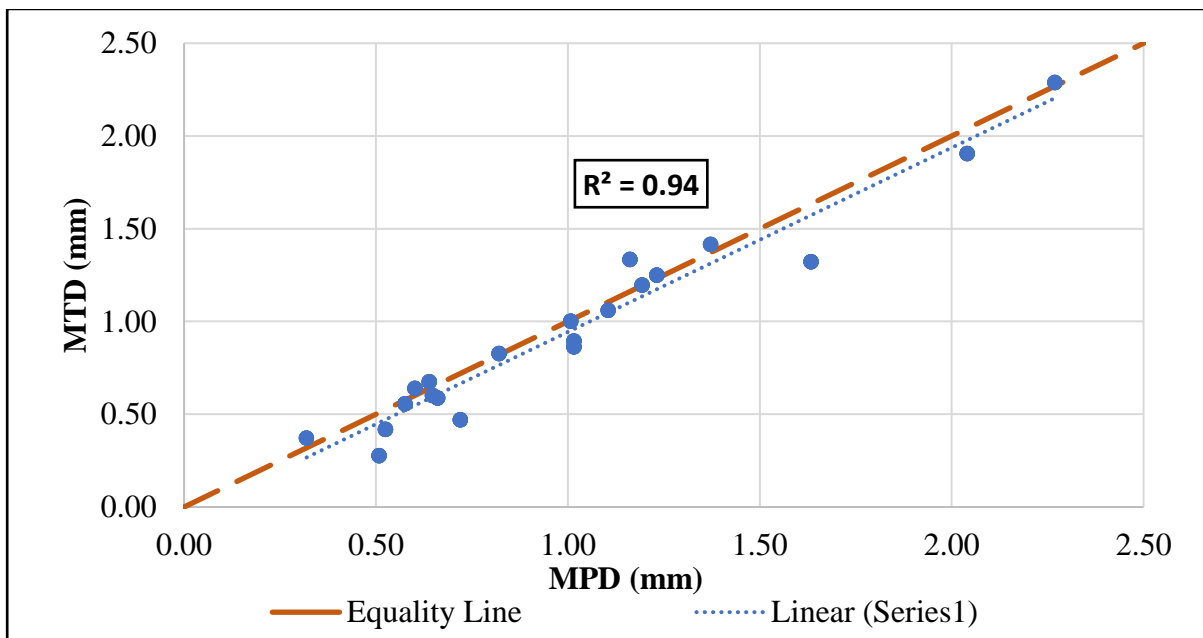


Figure 4.13. Correlation between mean texture depth and mean profile depth for all the pavement surface types examined in this study.

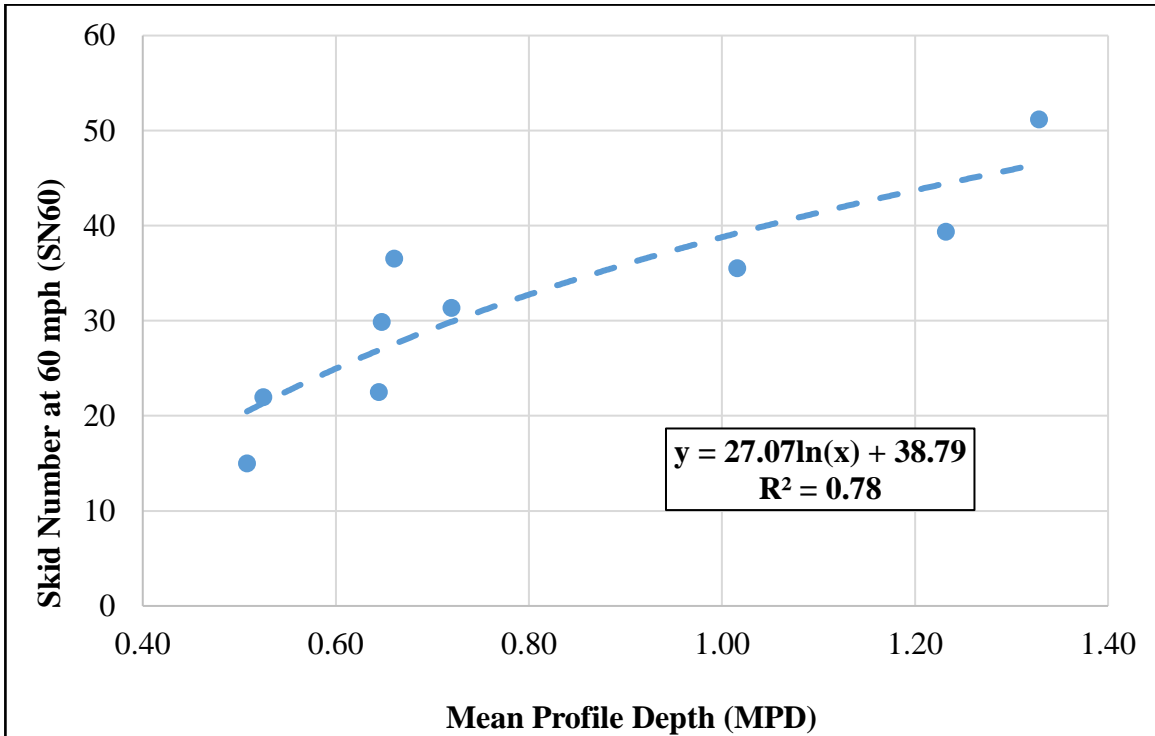


Figure 4.14. Skid number measured at 60 mph expressed as a logarithm of mean profile depth for HMA sections.

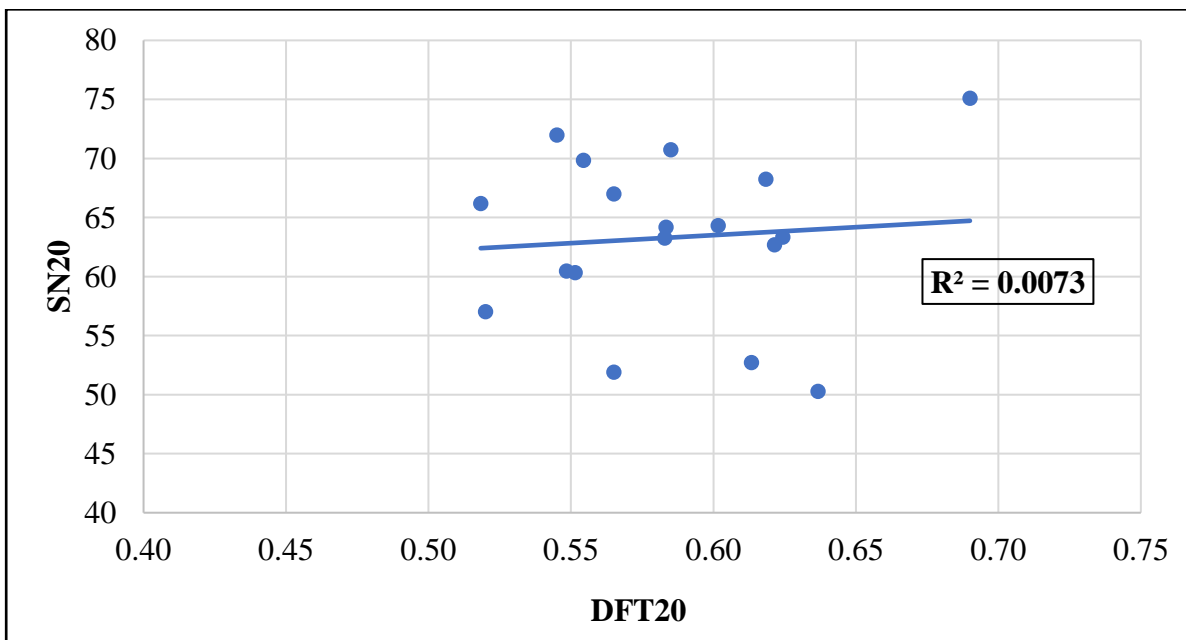


Figure 4.15. Skid numbers measured at 20 mph versus DFT20 values for the test sections examined in this study.

4.6 Development of Prediction Model

This study investigated the correlation between skid number measurements at different speeds and surface textures type. The texture measurements included macrotexture measured using laser profiler and Sand Patch Test and microtexture measured using DFT. The MPD can be measured simultaneously with skid testing unlike the MTD which requires traffic control. Since both MPD and MTD showed good correlation with one another, MPD was used to describe the macrotexture in this study.

The statistical program R in RStudio (RStudio 2015) environment was used to develop a model to describe the change in skid number as a function of surface texture. The results showed that the change in skid number can be described using Equation 4.1. It should be noted that DFT20 values were available for only 23 of the 34 test sections evaluated in this study since the use of DFT device in the field requires traffic control. Including the DFT values did not influence the rate of change in skid numbers with speed for this subset of test sections. Previous studies have demonstrated that changes in skid with speed is influenced by the macrotexture or mean profile depth and not microtexture (Hall *et al.* 2009).

The proposed model is presented in Equation 4.1.

$$SN_2 = 0.9991 * SN_1 - 22.2351 * \log (V_2/V_1) + 12.8467 * \log (MPD) * \log (V_2/V_1) \quad 4.1$$

where,

SN_2 = Predicted Skid number at desired speed (V_2 mph)

SN_1 = Measured Skid Number at any speed (V_1 mph)

V_2 = Desired reference speed at which the skid number is predicted

V_1 = Speed at which the skid number is measured using skid trailer

MPD = Mean Profile Depth of surface texture (mm)

The skid number measured at each speed was used with the MPD value to predict the skid numbers at other speeds. For example, the skid number measured at 30 mph was used to predict skid numbers measured at 20, 40, 50, and 60 mph. The predicted skid number values were within ± 5.6 of the measured skid number at the 95% confidence level. Figure 4.16 shows the predicted skid numbers versus the measured skid numbers.

The adjusted R^2 for the developed model is 0.95. The model presented in Equation 4.1 was developed based on 201 skid numbers measured in this study.

Table 4.1 summarizes the statistical parameters for the skid prediction model based on Equation 4.1.

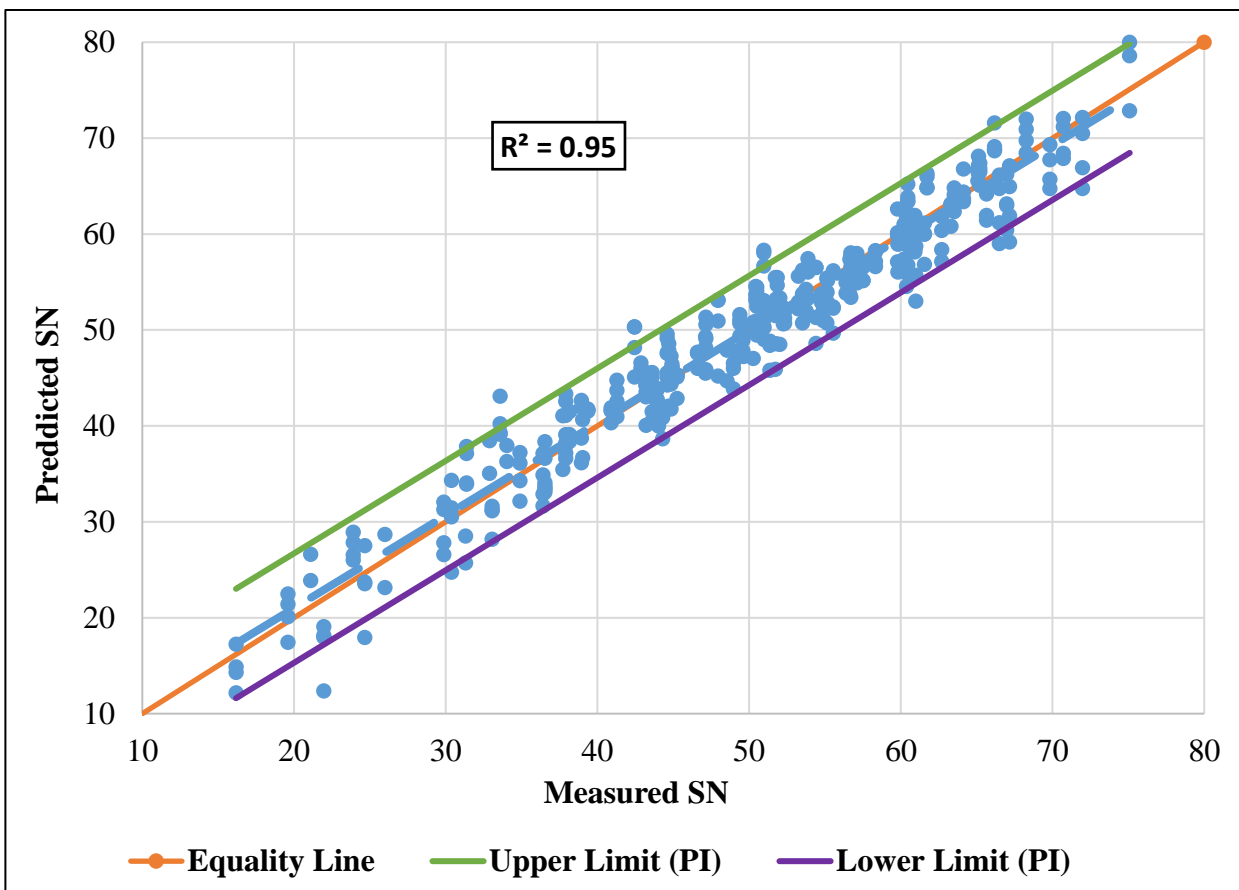


Figure 4.16. Predicted Versus Measured Skid Number (SN).

Table 4.1. Statistical Parameters for Model

Parameter	Value
Adjusted R -Square	0.95
Residual Standard Error	2.42
Number of Observations	201
Prediction Interval (95 % confidence)	± 5.7

Statistical checks were performed for the predictive model using R program in RStudio (RStudio 2015). The diagnostic checks were performed to statistically validate the prediction model including:

- Linear relationship between the outcome and the independent variable
- Normal distribution of the residuals
- Multi-collinearity between the independent variables
- Homoscedasticity

The diagnostic plot from R was used to verify the assumption of the multilinear regression analysis. Figure 4.17 shows the model residuals versus fitted values (predicted skid number) of the model. The R^2 for the developed model obtained from multilinear regression suggest that there is a strong linear relationship between the dependent and independent variables. Figure 4.17 demonstrate that there is no definite pattern between predicted values and residuals of the model, which means that there is no nonlinear relationship between the predicted and the predicting parameters of the model.

Figure 4.18 plots the normal probability of the residuals and is used to check whether or not the residuals follow standard normal distribution. These results demonstrate that the residuals formed an approximate straight line; the points are close and equally distributed on either side of the reference line. The linear regression assumes the residuals of the model are normally distributed, which was satisfied for the developed model.

The variation inflation factor (VIF) was used to check for possible correlation between the independent variables of the model. It is assumed that if VIF is less than five, there is no significant correlation between the independent variables (Murray *et al.* 2012; O'brien 2007). Table 4.2 presents the VIF values for the three independent parameters of the model. All of the parameters had VIF values less than 5 indicating that there is no multi-collinearity.

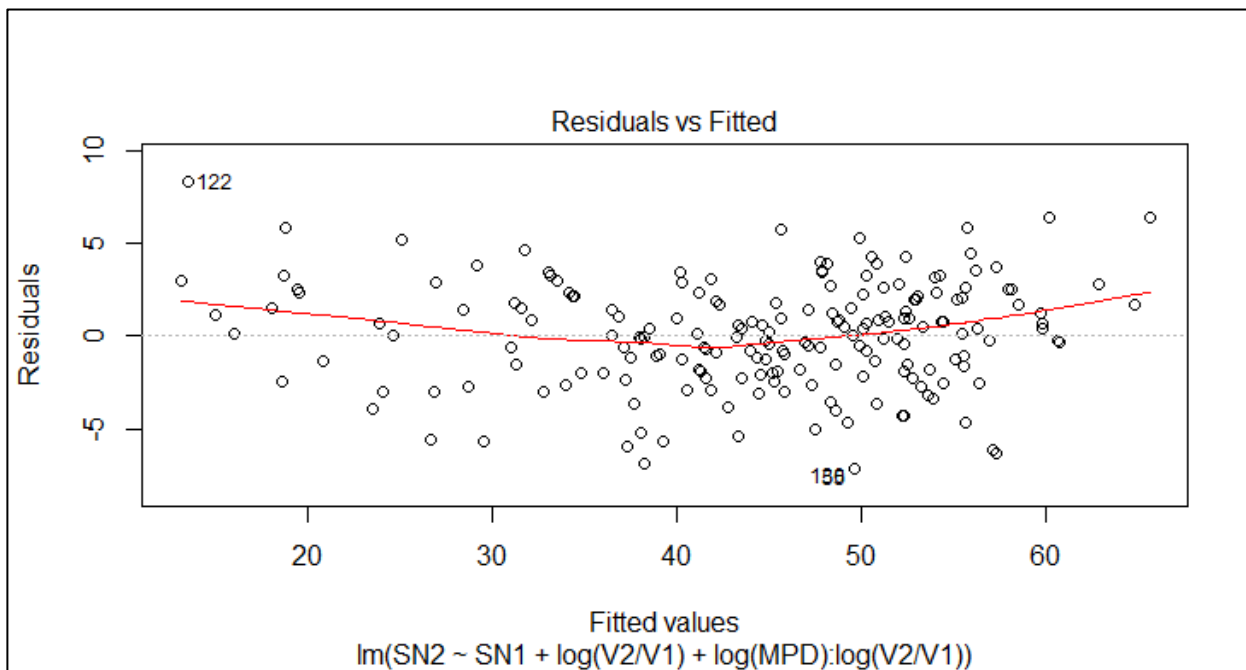


Figure 4.17. Residuals of the model plotted against the fitted values/predicted values of skid number from the model.

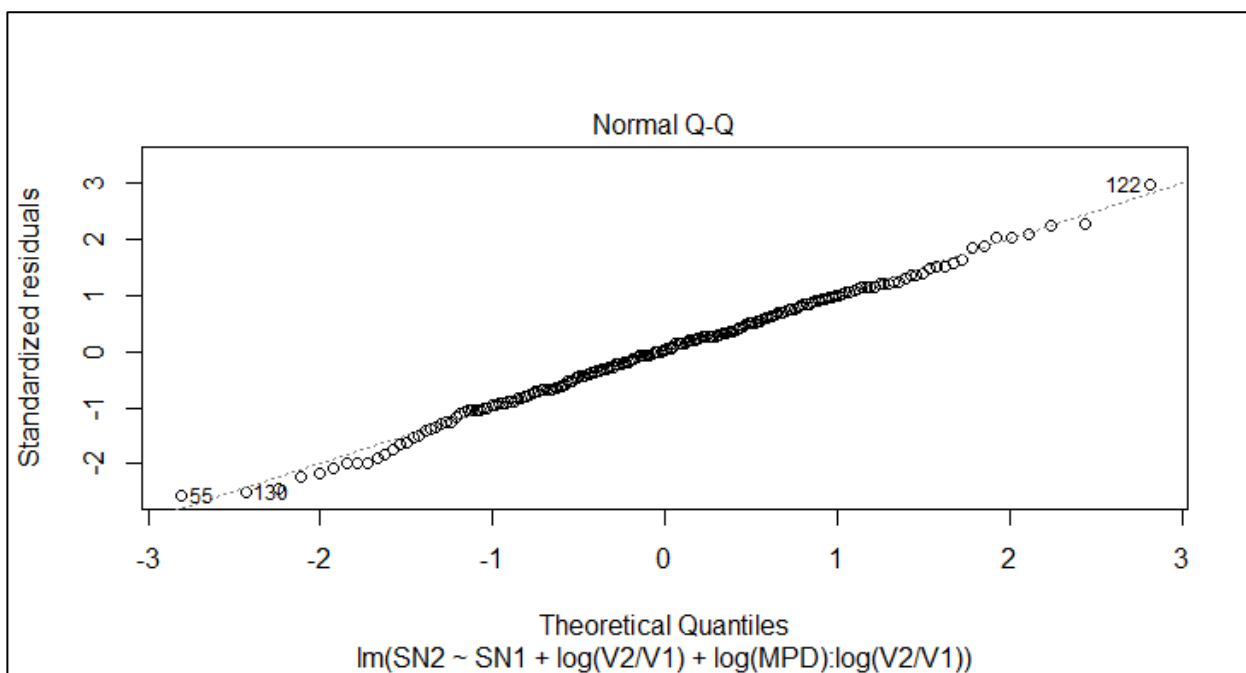


Figure 4.18. Plot of standardized residuals of the model versus theoretical quantiles also known as normal probability plot.

Table 4.2. VIF values for the independent variables in the model

SN ₁	Log (V ₂ /V ₁)	Log (V ₂ /V ₁) * log (MPD)
1.52	1.38	1.14

Figure 4.19 shows the scale or the spread location plot. This plot is used to check another assumption of multilinear regresssin which is homoscedasticity. Homoscedasticity is a condition in which all residuals of the model are similar across all independent variables (Statistics Solution 2013). A horizontal line with equally spaced points in a scale location plot indicates that the residuals are equally spread around the predictor variables. Figure 4.19 shows that this assumption of homescedasticity is satisfied and accepted for the proposed model.

Besides the verification of the model assumption, it is also necessary to ensure that the developed model is free from any data that can significantly change the model fit or the regression; such data points are called influential points. Figure 4.20 plots the residual versus leverage plot for the obtained prediction model. The data points are influential if they are outside the Cook's Cutoff distance and have high leverage; excluding or including those data points will change the regression model significantly. For the proposed model, all data points with higher leverage are well inside the Cook's distance as shown in Figure 4.20. These results demonstrate that the proposed model is free of influential data points.

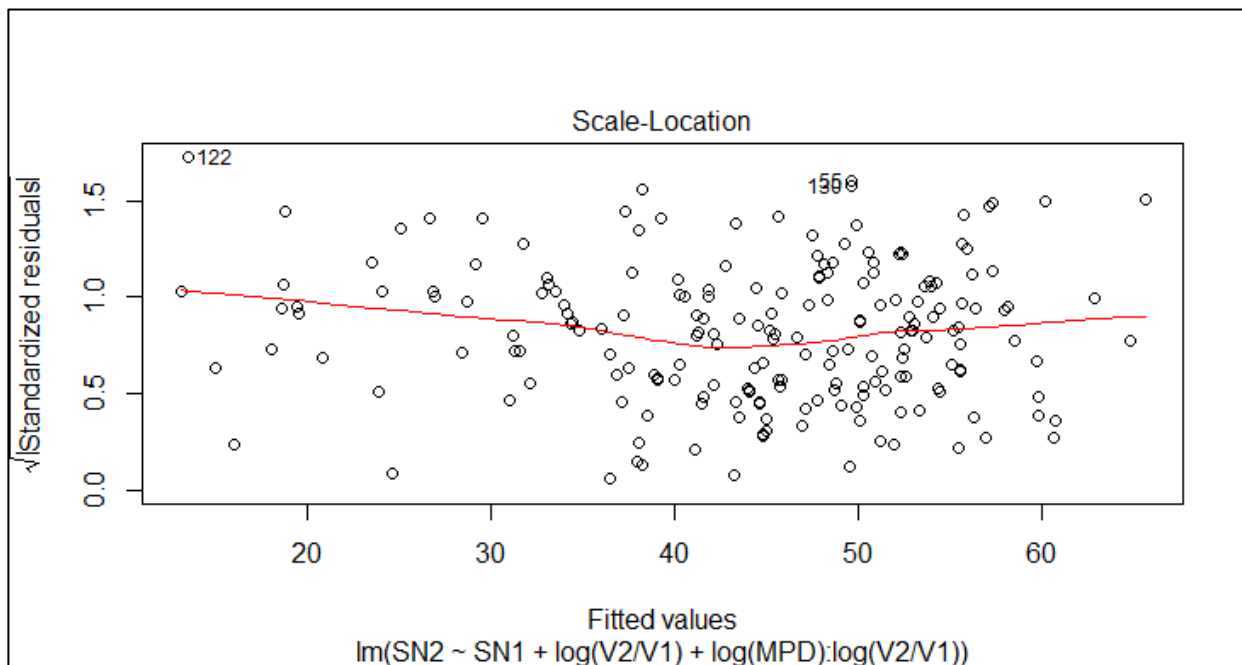


Figure 4.19. Plot of standardized residual of the model against the fitted values of the model (also known as scale location plot).

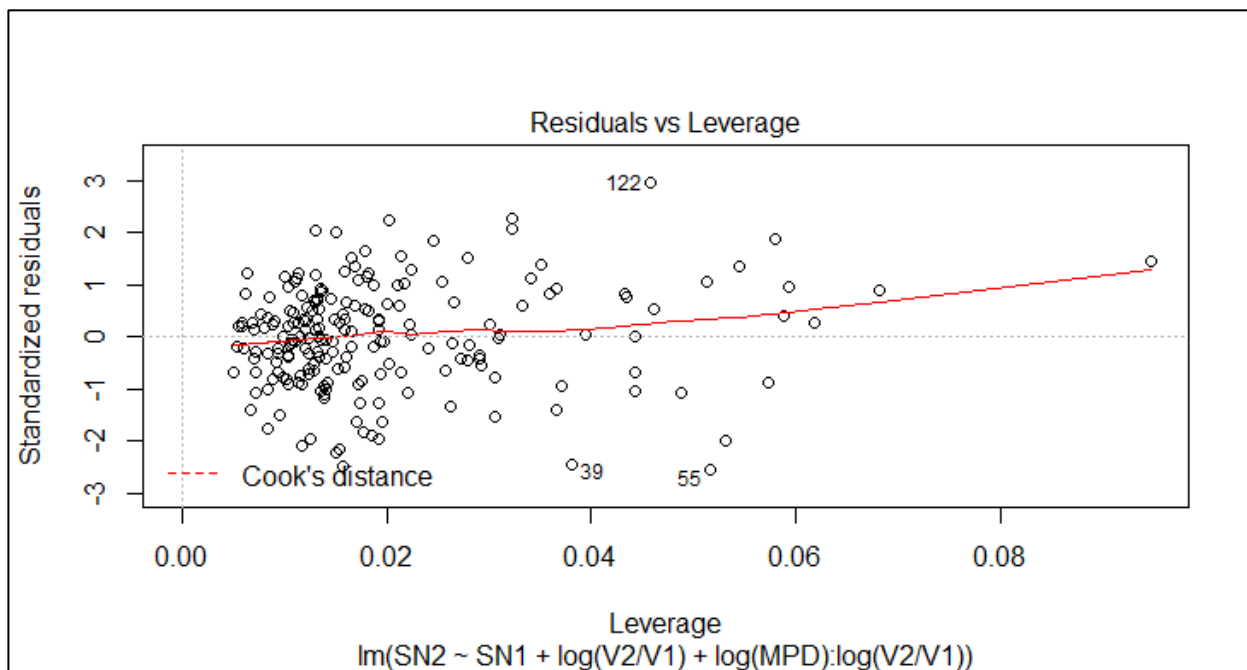


Figure 4.20. Plot of residuals versus leverage for the prediction model.

4.7 Model Validation

Eight test sections were used to validate the proposed prediction model. The skid measurements were collected at different speeds (i.e., 40, 50, and 60 mph). It was not possible to measure the skid at 20 and 30 mph for two sections due to safety of the crew; these measurements were collected at interstate and state highways where the posted speed limit is 70 mph or above. Figure 4.21 shows the distribution of the skid numbers at 40 mph for the test sections selected for validation. The sections cover a wide range of skid numbers like the sections used in the model development. Figure 4.22 shows the relationship between predicted skid numbers and the measured ones for both model development and validation points. The results demonstrate that most of the validation points for the model are within the 95% prediction interval of the proposed model. In addition, the R^2 for the validation is 0.94, which is nearly identical to the one for model development ($R^2 = 0.95$). These results clearly demonstrate that the model can be used to describe the change in skid number with speed as a function of mean profile depth.

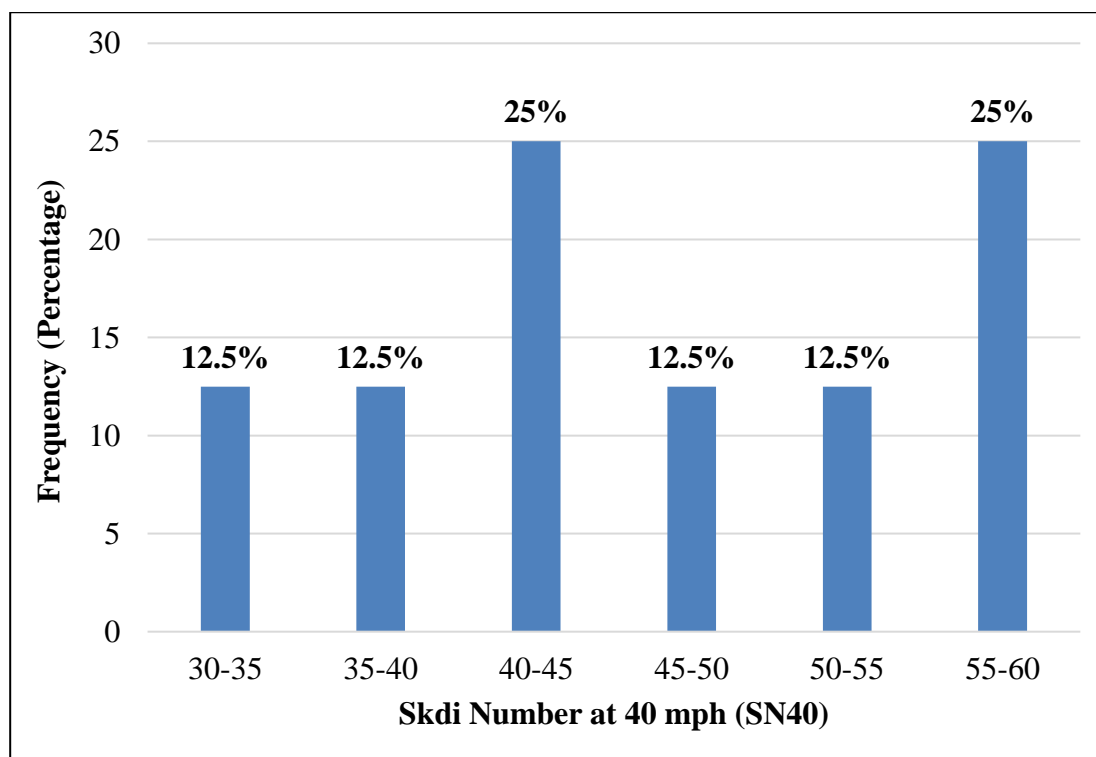


Figure 4.21. Distribution of SN for test sections selected for validation.

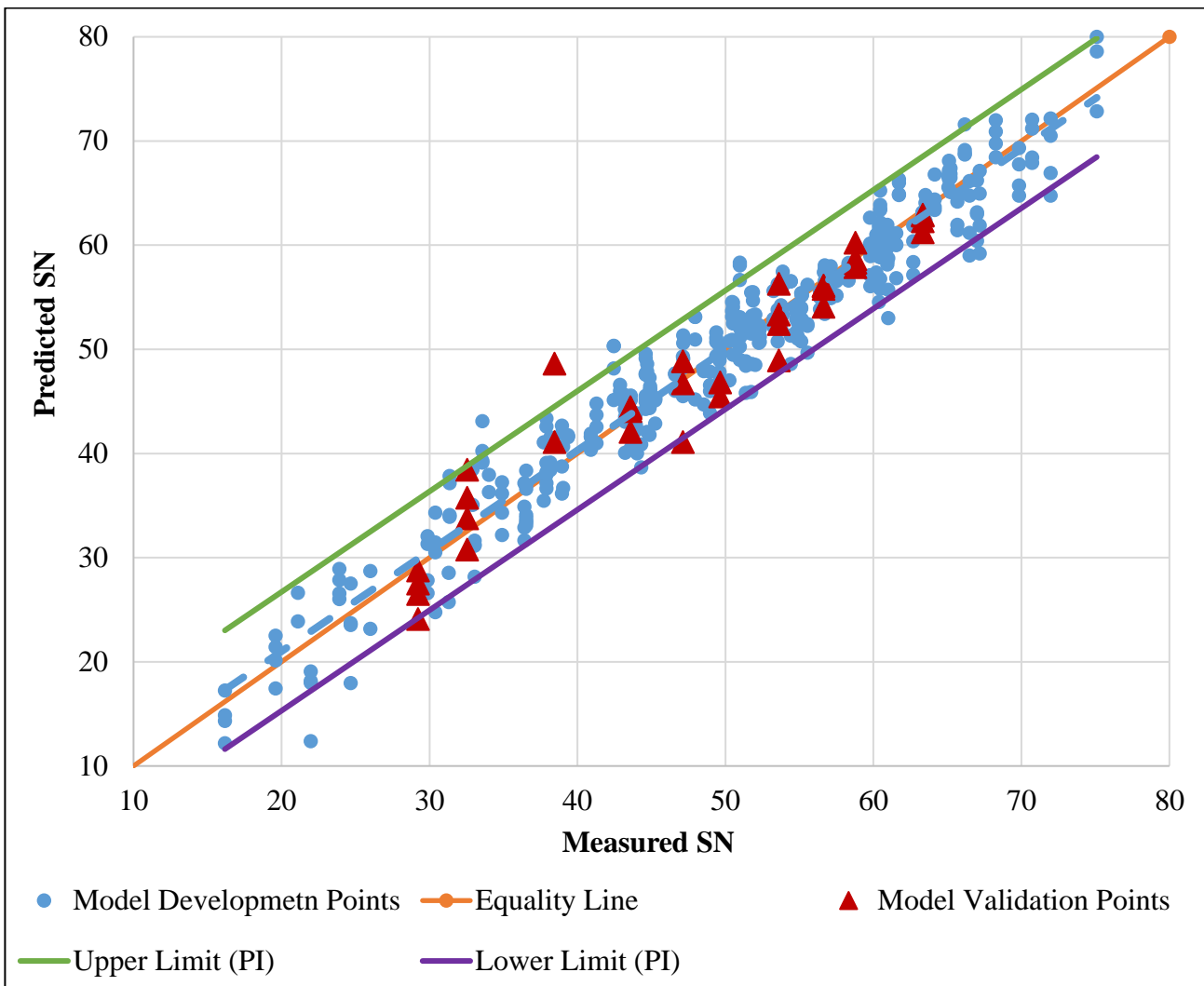


Figure 4.22. Predicted versus measured SN (Model Validation).

4.8 Individual Prediction Models

This study also investigated the development of separate prediction models for each pavement surface that was examined in this study (seal coat, HMA, and concrete). The objective was to assess any advantage of the separate models over the general model (Equation 4.1) in terms of model accuracy. The researcher used the same model parameters as in Equation 4.1 to describe the change in skid number with speed for each separate pavement surface. This section discusses the development of the separate prediction models and a comparison with the general model.

4.8.1 Model for Seal Coat Surface

Equation 4.2 presents the final proposed model for seal coat surfaces. Like the general model, the skid number at a reference speed is a function of measured skid number (SN_1), pavement macrotexture (MPD), and the ratio of reference speed (V_2) to test speed (V_1). A total of 113 data points were used for model development and 18 for model validation. Figure 4.23 shows the predicted and measured skid numbers for seal coat surfaces. As the general model, most of the data points used for model development and validation were within the 95% prediction interval of the proposed model.

$$SN_2 = 1.09 * SN_1 - 24.69 * \log (V_2/V_1) + 16.10 * MPD * \log (V_2/V_1) - 5.55 \quad 4.2$$

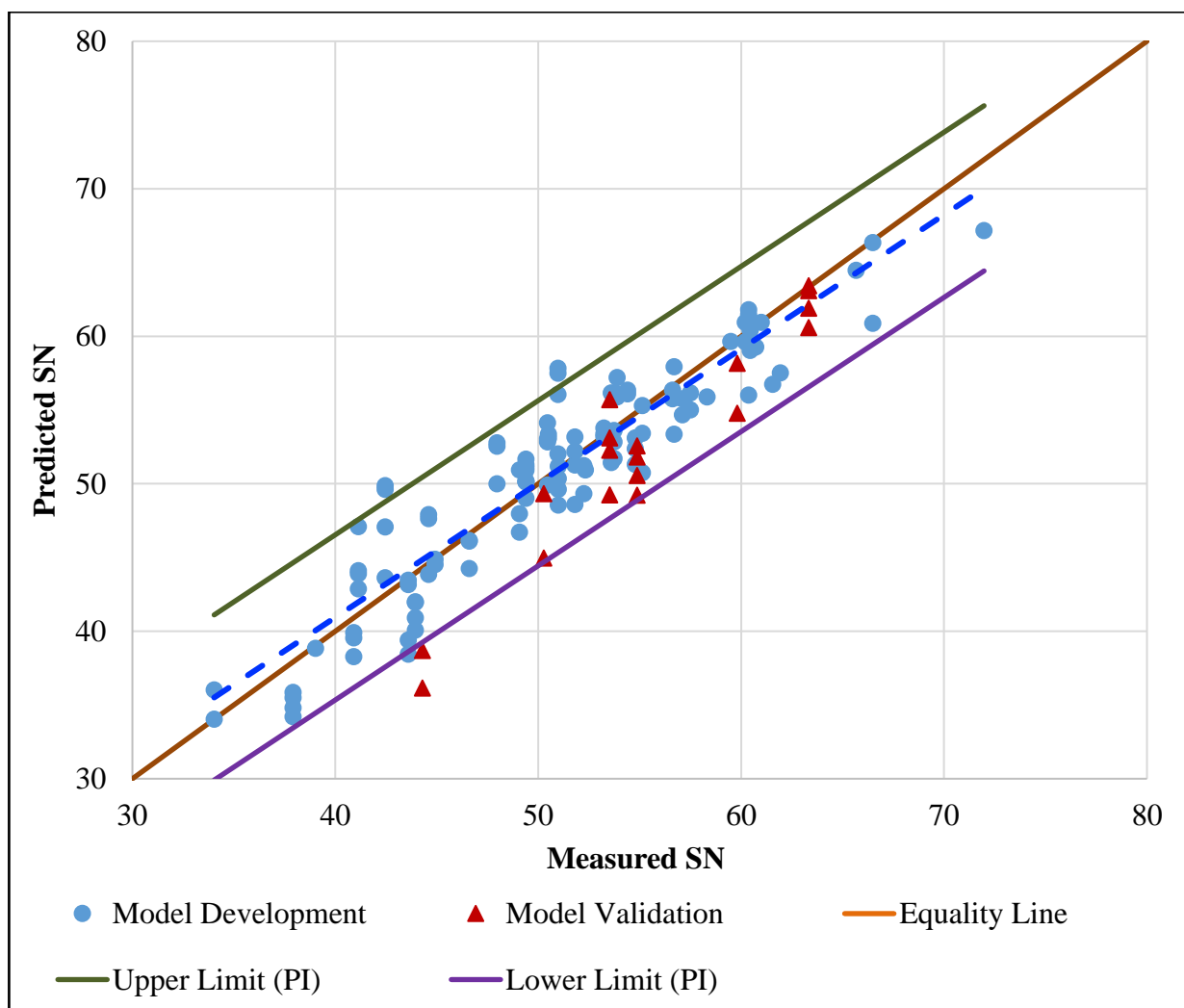


Figure 4.23. Predicted versus measured skid numbers for model development and validation of seal coat skid model.

4.8.2 Model for HMA Pavements

Equation 4.3 represents the prediction model for HMA pavements. The prediction model is similar to that of seal coat with slightly different values for the model parameters; 69 data points were used for model development and 12 for model validation. Figure 4.24 shows the model development and validation for HMA pavements. Although the HMA model used a smaller number of data points for model development and validation compared to the seal coat model, the R^2 (0.92) for the HMA was higher than that for the seal coat model ($R^2 = 0.69$). However, the seal coat model has the lower prediction interval (5.6) compared to that of HMA (6.98), suggesting lower variation in predicted skid numbers by the seal coat model. The model slightly overestimates the skid number below 40 mph and slightly underestimates it at speeds greater than 40 mph. With few validation data points, they all lie within the range of model development.

$$SN_2 = 0.79 * SN_1 - 18.84 * \log(V_2/V_1) + 11.92 * \log(MPD) * \log(V_2/V_1) + 8.62$$

4.3

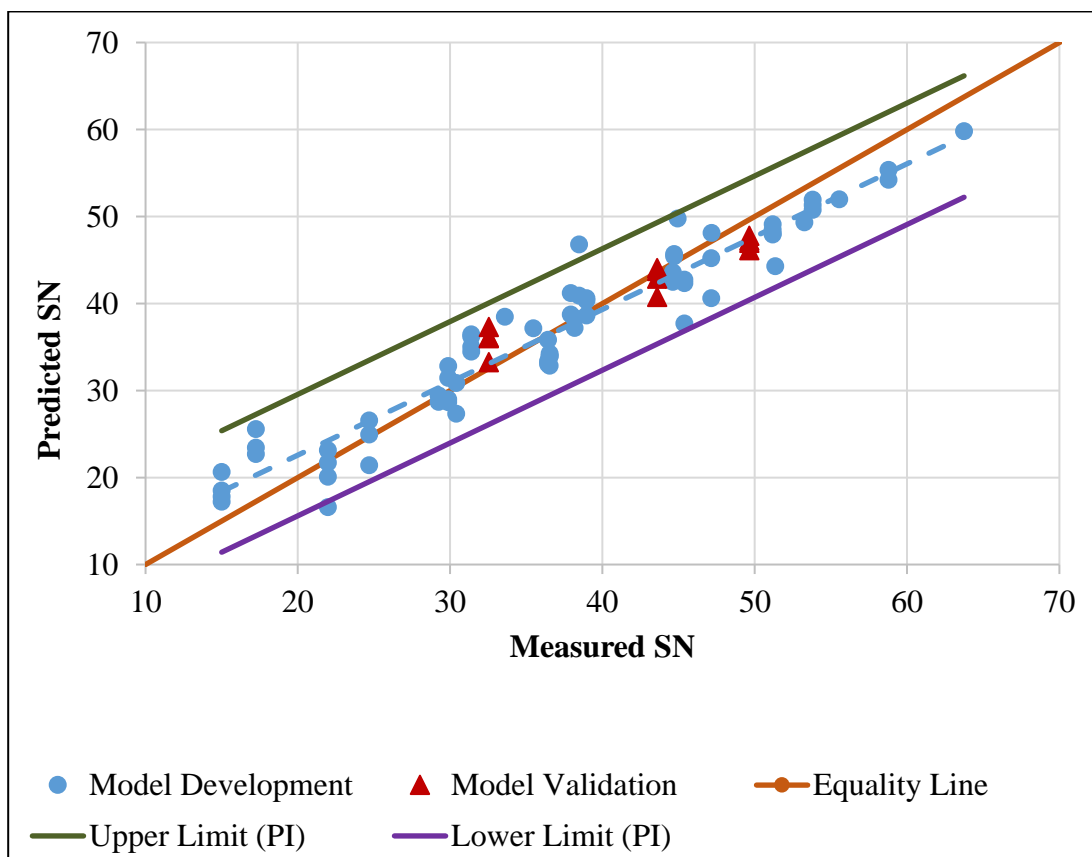


Figure 4.24. Predicted versus measured skid numbers for model development and validation of HMA skid model.

4.8.3 Concrete Skid Prediction Model

The model for the concrete pavement used the same parameters as the seal coat and HMA except for the intercept (constant) value as shown in Equation 4.4. The model intercept was found to be insignificant for concrete surfaces; so it was not included. The model development is similar to HMA with predictions slightly higher for speeds below 35 mph and slightly lower for speeds above 35 mph. The model validation data, however, were all in the lower range of model development as shown in Figure 4.25; 26 data points were used for model development and four for model validation. Due to the limited number of concrete sections included in this study, it is recommended to validate this model in the future with additional concrete pavement sites.

$$SN_2 = 0.88 * SN_1 - 19.70 * \log (V_2/V_1) + 11.74 * \log (MPD) * \log (V_2/V_1) \quad 4.4$$

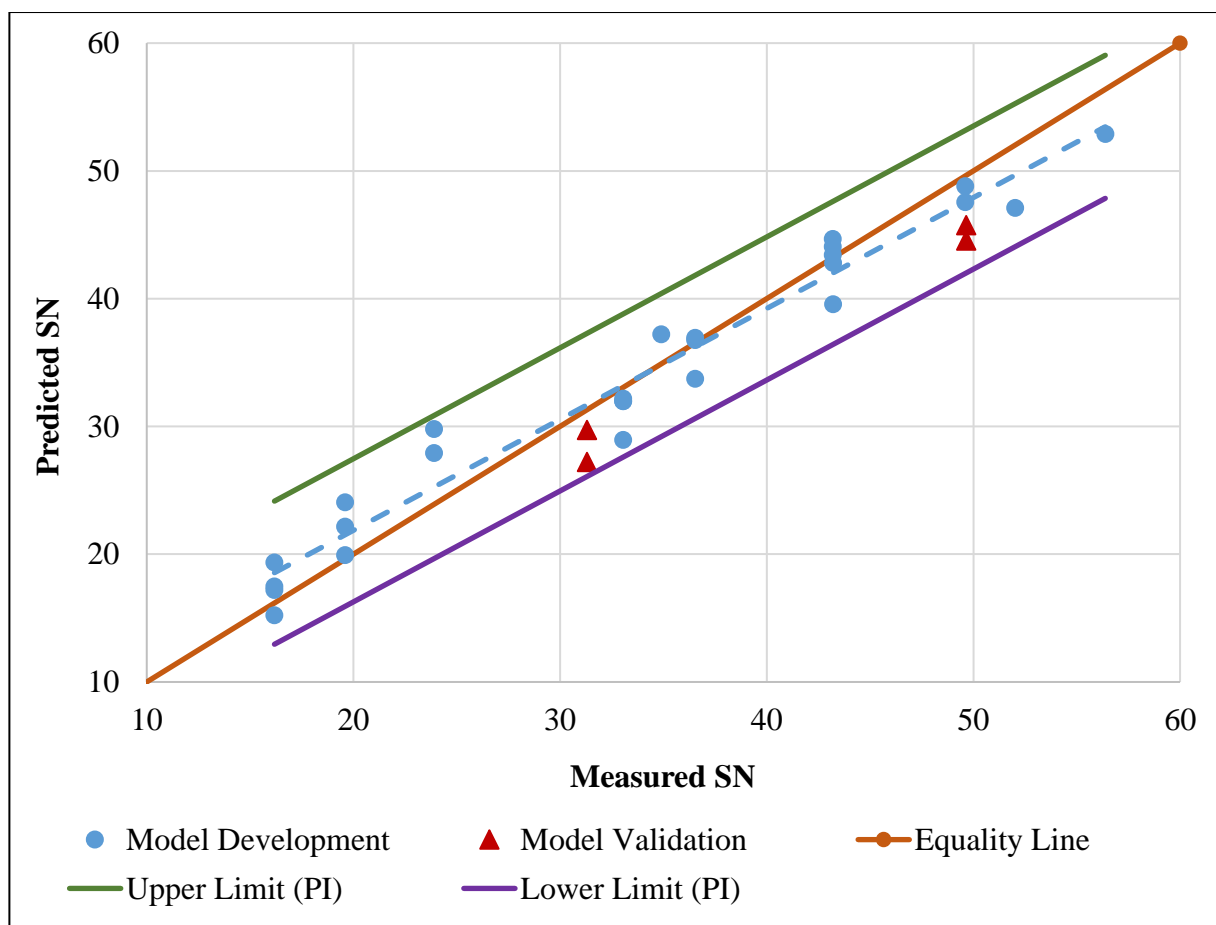


Figure 4.25. Predicted versus measured skid numbers for model development and validation of concrete skid model.

4.9 Comparison between Models

Table 4.3 summarizes the main statistical parameters of the individual and general models. The coefficient of determination (R^2) is about the same for all of the models except for the seal coat ($R^2 = 0.69$), which is considerably lower than for HMA ($R^2 = 0.92$) or concrete surfaces ($R^2 = 0.96$). The standard error of model coefficients was the lowest for the general model. The residual standard error was also lower for general model as compared to HMA and concrete model and slightly higher than seal coat model. The HMA and concrete models had higher residual standard errors compared to the seal coat and the general model. The number of data points used for model development and validation was 201 for the general model, but only 26 for the development and validation of the skid model for concrete. The prediction interval of skid for all models was similar (about ± 5.6), except for HMA which was higher (± 6.98). Comparing all parameters for the developed prediction models, it was found that the general model can be used to describe the change in skid with speed regardless the surface type with accuracy. The model was developed based on a large of data set with good R^2 of 0.94 and low residual standard error.

Table 4.3. Statistical Parameters for Individual and General Model

Prediction Model	General	Seal coat	HMA	Concrete
Model Coefficients	Estimates / Standard Error of Model Coefficients			
a	1.00 / 0.03	1.09 / 0.05	0.79 / 0.04	0.88 / 0.06
b	-22.24 / 0.79	-24.69 / 1.48	-18.84 / 1.56	-19.70 / 3.06
c	12.85 / 1.09	16.10 / 2.25	11.92 / 2.29	11.74 / 5.17
d	1.88 / 1.31	-5.55 / 2.65	8.62 / 2.11	4.73 / 2.78
Parameters of Prediction Model				
Adjusted R -Square	0.94	0.86	0.92	0.96
Residual Standard Error	2.95	2.78	4.02	3.17
Number of Observations	201	113	69	26
Prediction Interval (95 % confidence level)	± 5.7	± 5.6	± 6.98	± 5.6

4.10 Sensitivity Analysis of the Model

The proposed prediction model presented in Equation 4.1 is a function of three input parameters; measured skid resistance (SN_1) at a given speed (V_1), desired reference speed (V_2) at which the skid number needs to be calculated (SN_2), and the mean profile depth (MPD) of the tested surface. The velocity ratio (V_2/V_1) term combines both speeds (i.e., V_1 and V_2). Each of these input parameters affects the predicted skid number (SN_2). A sensitivity analysis was performed to study the effect of input parameters on the predicted skid number. The MATLAB software (MATLAB 2010) was used to create a three-dimension surface plot to show the variation in predicted skid number (SN_2) due to the change in input parameters. The results of the sensitivity analysis are shown in Figure 4.26 to Figure 4.28.

Figure 4.26 shows an example of variation in predicted skid number (SN_2) with velocity ratio (V_2/V_1), and MPD. In this example, the measured skid number (SN_1) was remained constant at 60. The results demonstrated that SN_2 was higher than SN_1 (i.e., 60) when the velocity ratio (V_2/V_1) was less than one [i.e., the reference speed (V_2) is lower than test speed (V_1)], and SN_2 was lower than SN_1 (i.e., 60) when the velocity ratio (V_2/V_1) was greater than one [i.e., the reference speed (V_2) is higher than test speed (V_1)]. These findings are in good agreement with the change in skid number with test speed as shown in Figure 4.9 through Figure 4.11. In addition, Figure 4.26 shows that the MPD affects the change in SN_2 with velocity ratio. The SN_2 was higher than SN_1 when the velocity ratio was smaller than 1 at various MPD values; however, the difference between SN_2 and SN_1 was higher at low MPD values compared to the difference at high MPD values. Similarly, SN_2 was lower than SN_1 when the velocity ratio was greater than 1 at various MPD values and the difference between SN_2 and SN_1 was higher at low MPD values compared differences at high MPD values. These results are consistent with observations in the field (Figure 4.12) when the skid number speed gradient (G_v) decreased with an increase in MPD.

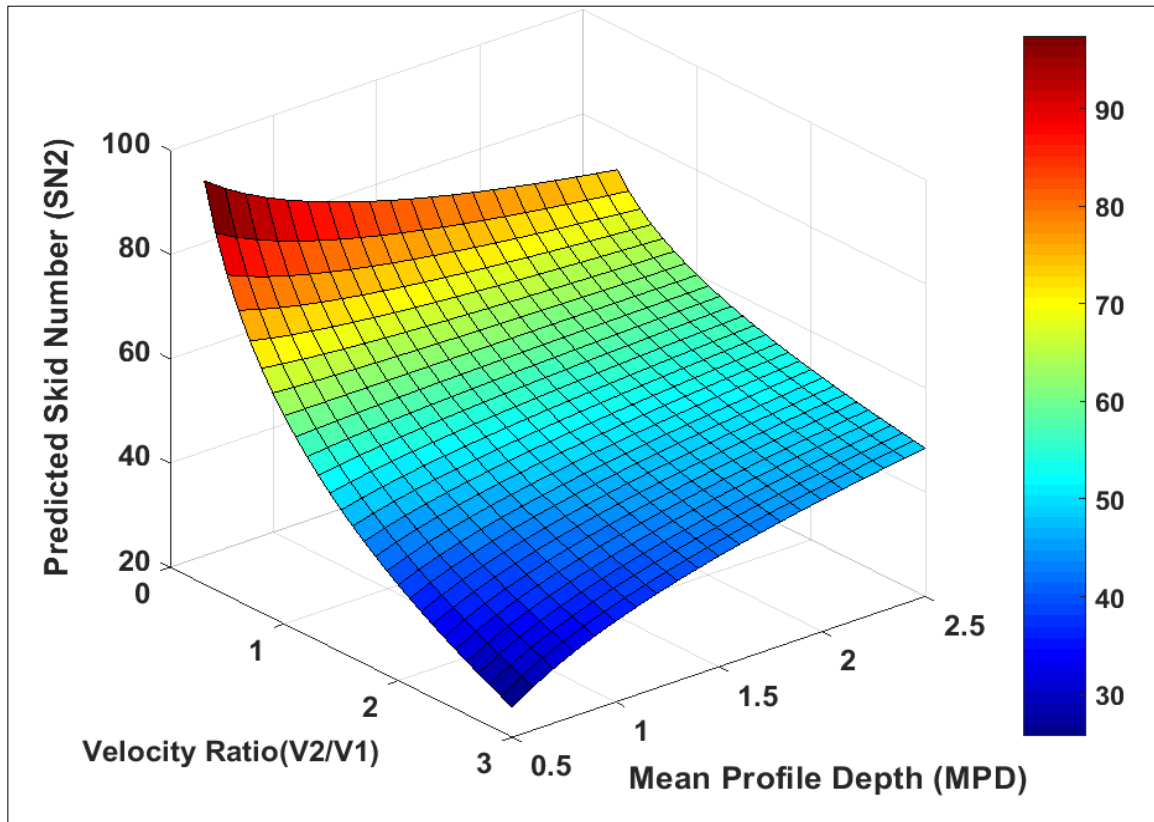


Figure 4.26. Change in predicted skid number with velocity ratio and mean profile depth

Note: the SN_1 is maintained constant at 60.

Figure 4.27 shows an example of variation in predicted skid number (SN_2) with velocity ratio (V_2/V_1), and measured skid number (SN_1). In this example, the MPD was maintained at 1.5 mm. The results demonstrate that the predicted skid number (SN_2) increased with measured skid number (SN_1). SN_2 had a linear relationship with SN_1 , while SN_2 had a nonlinear relationship with the velocity ratio.

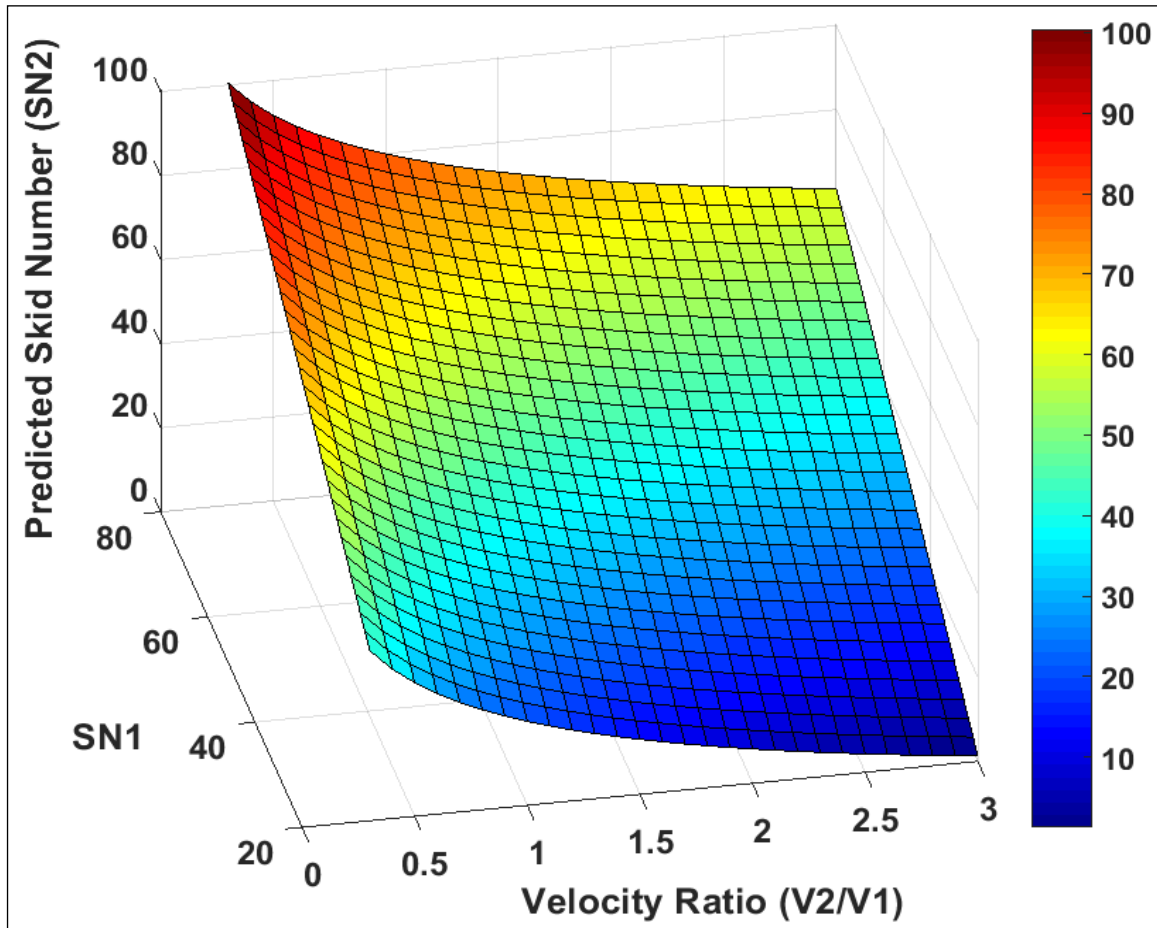


Figure 4.27. Change in predicted skid number with velocity ratio and measured skid number.

Note: the MPD is maintained at 1.5 mm.

Figure 4.28 shows an example of variation in predicted skid number (SN_2) with velocity ratio (V_2/V_1), and mean profile depth (MPD). In this example, the velocity ratio (V_2/V_1) was remained constant at 1.5. At this velocity ratio, the SN_2 is always lower than SN_1 . The results of Figure 4.28 demonstrate that the difference between SN_2 and SN_1 is lower at higher MPD values. These results are consistent with the field measurements presented in Figure 4.12.

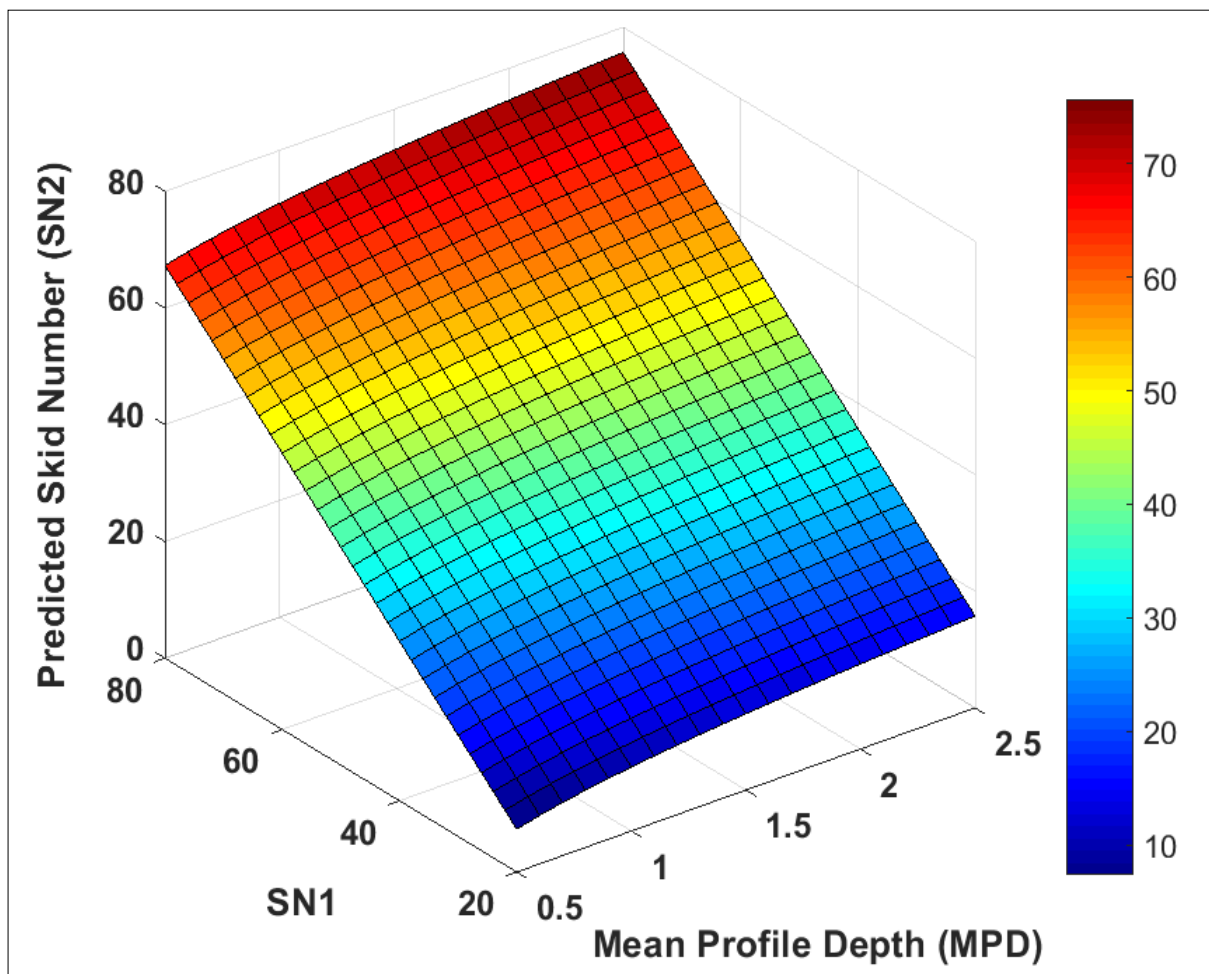


Figure 4.28. Change in predicted skid number with measured skid number and mean profile depth. Note: the velocity ratio is constant at 1.5.

CHAPTER 5 DEVELOPMENT OF THE SKID PREDICTION SOFTWARE

5.1 Overview

This chapter presents the development of an Excel-based Visual Basic application to facilitate the use of the proposed skid model (Equation 4.1) developed in this study. The Excel-based software simplifies the analysis and enables ITD engineers to use the developed skid prediction model to convert skid number measurements collected at any speed between 20 mph and 60 mph to a value at a reference speed (e.g., 40 mph). The software can be used to import the skid measurements at various test speeds and MPD data as recorded by the ITD pavement friction tester and use such information to calculate the skid number at a reference speed specified by the user. The software removes erroneous data and displays the average skid number and MPD measured along the test section as well as the calculated skid number at the desired speed. By default, the desired reference speed is set at 40 mph, but the user can change it to any other speed as needed. The accuracy of the software was verified by comparing the results obtained from the software to the similar calculations performed in Excel. Figure 5.1 shows the interface of the software.

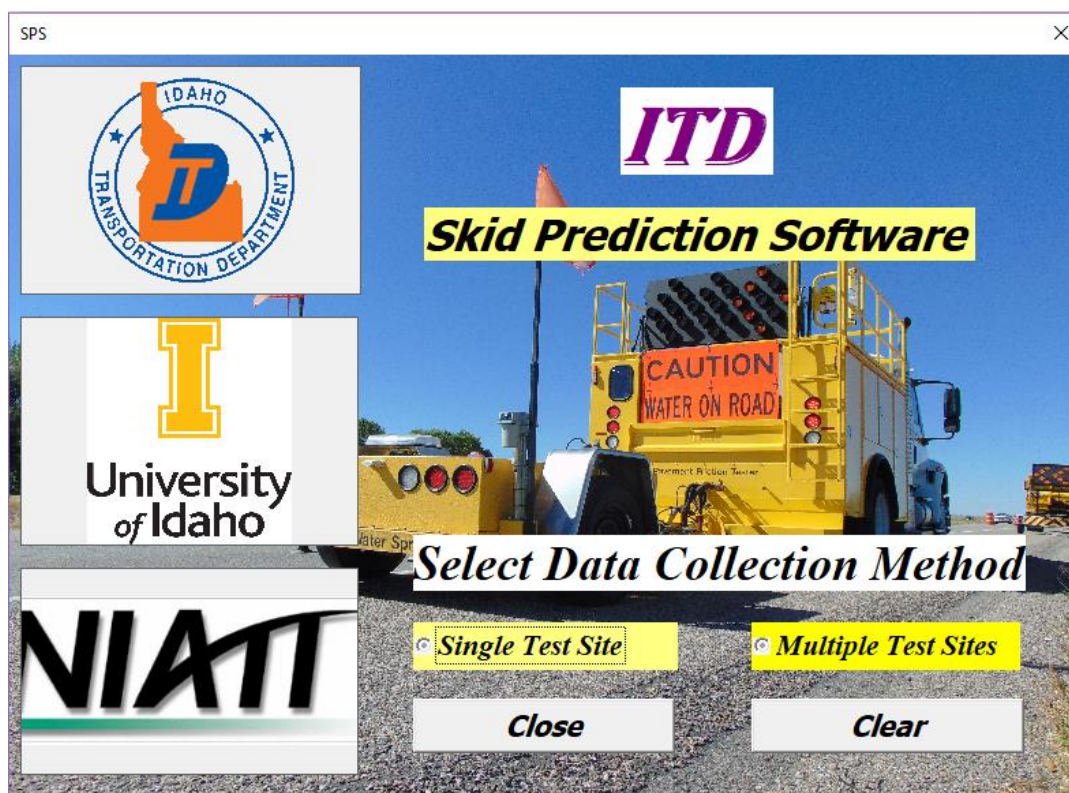


Figure 5.1. Skid prediction software interface

As shown in Figure 5.1, there are two modes for running the software--single test site or multiple test sites, depending on the type of data collected and objective of the skid measurements. These two options are discussed in this section.

5.2 Single Test Site

The interface for the single test site mode is shown in Figure 5.2. The user should select this mode under the following circumstances:

- If the objective of the skid testing is to collect several skid friction and texture measurements (e.g., 7 or 10 measurements along the test section) to calculate a representative value for skid number and MPD at a reference speed, and
- If the test surfaces have identical characteristics (i.e., surface type, mix design, material properties, texture pattern, etc.)

Figure 5.2. Interface of the single test site mode

5.2.1 Command Buttons

There are several command buttons in the software that are coded to perform specific functions (Figure 5.2). The command buttons and their respective functions are briefly described and summarized in Table 5.1.

Table 5.1. Command buttons and their function

Command	Functions
Browse Skid data	Browse and select skid measurement data collected using the skid trailer
Browse MPD data	Browse and select the mean profile depth measurement data collected using the laser sensor installed on the skid truck
Import Skid Data	Imports the selected skid data file into Excel, removes the outliers (highly deviated data) and calculates the average skid number
Import MPD Data	Imports the selected texture data file into Excel, removes the outliers (highly deviated data) and calculates the average MPD
Calculate SN	Calculates the skid number at the reference speed provided by a user using the prediction model (Equation 4.1) embedded in the software
Reset	Clears all the commands and inputs and restores the software to the initial status to run additional analysis
Close	Closes the program

5.2.2 Software Outputs

Table 5.2 summarizes the main outcomes of the single test site mode that include (1) average skid number, (2) average MPD, (3) average test speed, (4) reference speed, and (5) calculated skid number. Appendix E provides an example of single test site skid analysis.

Table 5.2. Single test site mode outputs

Output	Definition
Average SN	Displays the average skid number for various skid number measurements imported into the software. This is the SN_1 parameter used in Equation 4.1
Average MPD (mm)	Displays the average mean profile depth (mm) for various MPD measurements imported into the software. This is the MPD input parameter used in Equation 4.1. It should be noted that the MPD is measured in inches by the laser sensor and it is converted to mm in the software.
Average Test Speed (mph)	Displays the average test speed at which the skid numbers were measured using the skid trailer. It is expressed in mile per hour. This is the V_1 input parameter used in Equation 4.1.
Reference Speed (mph)	This is where the reference speed is specified by the user. The predicted skid number is calculated at the reference speed. It is expressed in mile per hour. This is the V_2 input parameter used in Equation 4.1.
Calculated Skid Number	Displays the skid number calculated from the prediction model (Equation 4.1) embedded in the software. This is the SN_2 parameter used in Equation 4.1

5.3 Multiple Test Site

The interface for the multiple test sites mode is shown in Figure 5.3. The user should select this mode if the objective is to collect continuous friction and texture measurements which is the typical practice at ITD. This mode has similar command buttons and outputs as the single test site mode. A user can browse and import the skid and MPD data into the software as recorded by the skid friction tester. Also, the user can specify the reference speed. A default value of 40 mph (current reference speed used by ITD) is selected. Upon importing the skid and texture data and specifying the reference speed, the skid number can be calculated at the reference speed by selecting “Calculate Skid Number” command button. One major difference between the single and multiple test site interface is the output display of predicted

skid number. While the single test site mode displays the predicted skid number on the interface itself, the multiple test sites interface permits the user to save and export the data to a separate Excel file. This is useful to a user because the output data from the multiple sites interface consists of multiple rows and columns of data unlike a single value as in single site analysis. After completing the analysis, the user has the option either to run another calculation or to quit the application as indicated by the command buttons in the software.

Figure 5.4 shows a typical input file (skid number) measured using the ITD skid friction tester. A similar file is obtained for MPD. Figure 5.5 displays typical output of the multiple test sites mode in Excel format. The output files include the station number, milepost, test speed, measured skid number at the test speed, mean profile depth and finally the predicted skid number at the desired reference speed set by a user. Appendix E provides an example of multiple test sites skid analysis.

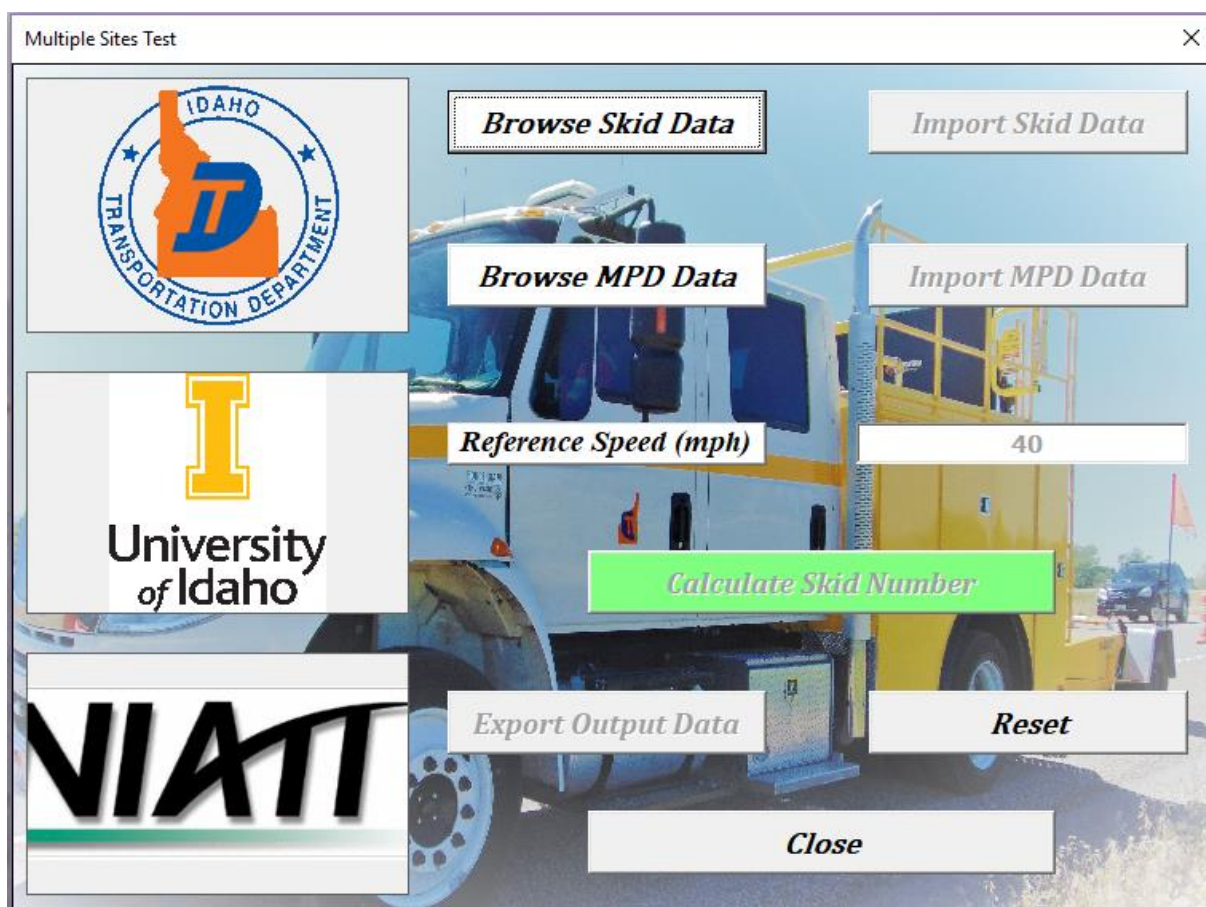


Figure 5.3. Interface of the multiple test sites mode

```

07_26_17_S60D0004_20 - Notepad
File Edit Format View Help
5100, FILE NAME & SYSTEM MODEL      :C:\Minn\07_26_17_S60D0004_20.SKS  1295 Paveme
5101, SOFTWARE VERSION              :V8000901-601.007
5102, TIME (hh:mm:ss)               :14:57:45
5103, DATE (mm/dd/yyyy)             :WEDNESDAY 7/26/2017
5104, SYSTEM UNITS                   :US (ENGLISH)
5105, TEST TYPE                     :STANDARD
5106, TARGET SPEED (mph)            :20.0
5107, TEST WHEEL                    :LEFT
5108, TEST LUBRICANT                :WET
5109, DATA FILTER                  :5-POINT
5110, CYCLE TYPE                    :AUTO
5111, CYCLE DWELL DISTANCE (miles)  :|                               :
5182, Unit 203254 (Operator - Driver) :STEVE/TREK
5183, Const./Resurf. Mo./Yr.        :07/06
5184, Ave\g. Daily Traffic (ADT)    :
5185, Avg. Texture EDT (.000 in)   :
5186, Site Comments                 : concrete study
5250, -----
5250,
5250,           W
5250,           E A M M % A
5250, R           W T V I A S E
5250, T O L       H / G N X P S P T V F
5250, E U D A     E D           E L E E L
5250, S T I N     E R S S S A I E M N O
5250, T E R E     MP/S TIME L Y N N N K P D P T W
5250, ---|-----|---|-----|-----|---|---|-----|---|-----|---|-----|---
5500, 1, US95,N, 0, 4.000,14:59,L,W, 76.4, 72, 80, 99.40, 14, 20.0, 95, UI, 14
5232, 1, 47.228590, -116.961017
5502, 1, 121.4,108.2,129.0
5500, 2, US95,N, 0, 3.962,14:59,L,W, 75.3, 73, 78,103.24, 12, 20.3, 95, , 14
5232, 2, 47.228590, -116.961847
5502, 2, 125.7,98.9,129.1
5500, 3, US95,N, 0, 3.924,14:59,L,W, 75.2, 72, 78,101.44, 15, 20.3, 95, , 15
5232, 3, 47.228590, -116.962567
5502, 3, 123.2,95.9,128.4
5500, 4, US95,N, 0, 3.886,14:59,L,W, 74.8, 71, 78,102.23, 14, 20.2, 95, , 15
5232, 4, 47.228588, -116.963408
5502, 4, 124.4,96.7,128.7

```

Figure 5.4. Typical input file (SN) for the software obtained from skid truck

The screenshot shows the Microsoft Excel interface with the following data table displayed:

	A	B	C	D	E	F
1	Station Number	Mile Post	Speed	Measured SN	Mean Profile Depth	Predicted SN
2	219	0	41.9	27.3	0.09	27.81
3	220	0.5	40.4	46.7	0.087	46.78
4	221	1	40.5	40.9	0.087	41.01
5	222	1.5	40.6	39.2	0.082	39.35
6	223	2	21.3	54	0.084	46.07
7	224	2.5	19.9	73.8	0.08	64.57
8	225	3	39.8	46.8	0.074	46.69
9	226	3.5	31.2	53.5	0.075	49.98
10	227	4	39.6	52.9	0.074	52.71
11	228	4.5	40.2	51.6	0.081	51.62

Figure 5.5. Output of the multiple test site mode

CHAPTER 6 CONCLUSIONS AND RECOMMENDATIONS

6.1 Summary

Idaho Transportation Department (ITD) requires a minimum skid number of 35 measured at 40 mph to ensure adequate friction levels for pavements in Idaho. Since the skid number changes with testing speed, it is important to collect skid number measurements at a reference speed (e.g., 40 mph for ITD); however, field operations may not permit the collection of skid resistance measurement at the reference speed. This study aimed to develop a method that can be used to convert the skid number collected at any speed between 20 mph and 60 mph to the corresponding skid number at a reference speed.

In this study, the frictional characteristics of 34 pavement sections across Idaho were determined, including HMA, seal coat, and concrete pavement sites. The skid number was measured at five different speeds (20, 30, 40, 50, and 60 mph) using a locked wheel skid trailer with a smooth tire. In addition, the MPD of test sites was measured using a laser profiler and Sand Patch Test. The microtexture was quantified indirectly by measuring the coefficient of friction using the DFT.

The results revealed a logarithmic relationship between measured skid number and testing speed. Based on the data collected in this study, a statistical model was developed to describe the change in skid number with speed. The model uses the MPD data and skid number measurements at a given speed and calculates the skid number at a reference speed specified by the user. The predicted skid numbers correlated well with the measured values. The model was further validated with skid data from an additional eight test sites that were not used in the model development. Again, good correlation was observed between the measured and predicted skid numbers .

An Excel-based utility software was developed that can be used to import the skid measurements and texture data collected by the ITD pavement friction tester and calculate the skid number at a reference speed. The outcome of this study will assist ITD pavement engineers to collect skid measurements at a safe speed when field operations do not allow data collection at higher speeds. In addition, some interstate highways have a speed limit up to 80

mph, and the skid measurements are collected at 40 mph which imposes hazards to motorists. The skid number can be collected at higher speeds (e.g., 60 mph) and be converted to the corresponding values at a reference speed. In addition, it will expedite the data collection since the skid can be collected at higher speeds especially on the interstate highways.

6.2 Findings

This section summarizes the main findings of this study.

6.2.1 Skid and Texture Data Analysis

- Seal coat test sections exhibited relatively higher skid resistance and macrotexture values compared to the HMA and concrete test sections. The higher mean profile depth of the seal coat test sections contributed to the higher skid numbers and were found to be statistically different from the HMA pavements both in terms of macrotexture and skid resistance. There was no significant difference between HMA and concrete surfaces. All test sections (seal coat, HMA, and concrete) had comparable microtexture values.
- A strong linear correlation ($R^2 = 0.95$) was found between the mean profile depth measured using a laser sensor attached to the skid truck and mean texture depth measured using the Sand Patch Test. Such correlations can be used to estimate the mean profile depth from the mean texture depth data. The laser sensor has several advantages over the sand patch test since it allows continuous data collection and doesn't require traffic control. The Sand Patch Test is cheaper but can be used to measure the macrotexture at only limited spots since it requires lane closure.
- In general, a logarithmic trend was found between the measured skid number and test speed. Although the R^2 for the logarithmic relationship was higher than 0.9 for all test sections, the linear trend between measured skid resistance and test speed was also significant. The R^2 for the logarithmic trend was higher than the linear trend for HMA and concrete sections, while the linear trend had higher R^2 for seal coat sections.
- The skid number decreased with test speed for all test sections. The rate of change in skid number was a function of the macrotexture of the test section. Sections with higher macrotexture exhibited less reduction in skid resistance with speed compared

with sections with low macrotexture that had a more dramatic decrease in skid number with speed.

- The skid number had a fair correlation ($R^2 = 0.78$ for HMA and $R^2 = 0.16$ for seal coat at 60 mph) with the macrotexture; however, skid number is a function of both macrotexture and macrotexture. This study was concerned with the change in skid number with speed which was found to be controlled by the macrotexture. The results are in good agreement with the findings of previous research studies.
- The test sections evaluated in this study had comparable microtextures. The coefficients of friction measured using the DFT device at 20 km/hr, ranged from 0.51 to 0.67. Higher microtextures result in higher skid numbers. The microtexture was not significant in affecting the change in skid number with speed.

6.2.2 Development of Skid Prediction Model

- A general statistical-based model was proposed to describe changes in skid number with speed of various surfaces including seal coat, HMA, and concrete. In addition, separate models were developed for each pavement surface. Such models were a function of measured skid number value (SN_1), a ratio of reference to test speed (V_2/V_1), and surface mean profile depth. Several statistical checks and analyses of measured and predicted skid values for model development and validation concluded that the general model is able to predict the change in skid number with speed.
- The results demonstrated a strong correlation between the predicted skid number and the measured ones. Most of the validation points were within the 95% prediction intervals of the proposed model. These results demonstrate that the model can be used to describe the change in skid number with speed as a function of mean profile depth. In addition, the results showed that skid number speed gradient decreased with the increase in MPD. The predicted skid number had a positive linear relationship with the measured skid number when the mean profile depth is kept constant, while the predicted skid number had nonlinear relationship with the test speed.

6.2.3 Development of a Skid Prediction Software

- An Excel-based utility was developed on a Visual Basic platform to facilitate the process of analyzing the friction and texture data collected using the ITD pavement

friction tester and calculating the skid number at a reference speed. The software extracts the needed information and values from the raw data files and considers the reference speed as specified by the user to estimate the skid number at this speed.

- The software removes erroneous data, provides warnings for the wrong inputs by the user, gives the user the option to re-import the data, and uses the proposed model to predict the skid number at a desired reference speed. The output from the software is displayed in the interface itself for the single test site mode. It provides an option to the user to save the outputs from the software in excel formats for multiple test sites mode.

6.3 Recommendations for Future Research

- Additional test sections from various pavement surfaces can be evaluated to further validate the model.
- Test sections with a wider range of microtexture should be included to investigate the effects of microtexture on the change of skid number with speed.
- Generate a database for the aggregate properties used in pavement construction in the state. Such a database should include aggregate texture and its resistance to abrasion and polishing.
- Skid prediction models should be developed to be used in the mix design stage to ensure adequate skid resistance over the service life of pavements. Such a model should utilize aggregate properties and mix design and predict skid number with time.
- Additional skid resistance data can be collected to examine the effect of traffic level on skid resistance for various pavement surfaces (e.g., seal coat, HMA, concrete).
- The effects of studded tires on skid resistance of various HMA mix design should be examined.

References

- Abe, H., Tamai, A., Henry, J. J., & Wambold, J. (2001). Measurement of Pavement Macrottexture with Circular Texture Meter. *Transportation Research Record: Journal of the Transportation Research Board*, 1764(1), 201–209.
- Al-Assi, M., & Kassem, E. (2017). Evaluation of Adhesion and Hysteresis Friction of Rubber–Pavement System. *Applied Sciences*, 7(10), 1029–1041.
<https://doi.org/10.3390/app7101029>
- Aldagari, S., Al-Assi, M., Kassem, E., Chowdhury, A., & Masad, E. (2018). Prediction Models for Skid Resistance of Asphalt Pavements and Seal Coat. *Proceedings of Transportation Research Board 97th Annual Meeting*, Washington DC, United States, January 7-11.
- American Society of Testing and Materials (ASTM) E274 / E274M-15. Standard Test Method for Skid Resistance of Paved Surfaces Using a Full-Scale Tire. (2015). *ASTM International, West Conshohocken, PA*.
- American Society of Testing and Materials (ASTM) E1551-16. Standard Specification for a Size 4.00-8 Smooth Tread Friction Test Tire. (2016). *ASTM International, West Conshohocken, PA*.
- American Society of Testing and Materials (ASTM) E1845-15. Standard Practice for Calculating Pavement Macrottexture Mean Profile Depth. (2015). *ASTM International, West Conshohocken, PA*.
- American Society of Testing and Materials (ASTM) E1859 / E1859M-11. Standard Test Method for Friction Coefficient Measurements Between Tire and Pavement Using a Variable Slip Technique. (2015). *ASTM International, West Conshohocken, PA*.
- American Society of Testing and Materials (ASTM) E1911-09ae1. Standard Test Method for Measuring Paved Surface Frictional Properties Using the Dynamic Friction Tester. (2018). *ASTM International, West Conshohocken, PA*.

American Society of Testing and Materials (ASTM) E2157-15. Standard Test Method for Measuring Pavement Macrotexture Properties Using the Circular Track Meter. (2015). *ASTM International, West Conshohocken, PA.*

American Society of Testing and Materials (ASTM) E303-93. Standard Test Method for Measuring Surface Frictional Properties Using the British Pendulum Tester. (2018). *ASTM International, West Conshohocken, PA.*

American Society of Testing and Materials (ASTM) E501-08. Standard Specification for Standard Rib Tire for Pavement Skid-Resistance Tests. (2015). *ASTM International, West Conshohocken, PA.*

American Society of Testing and Materials (ASTM) E524-08 . Standard Specification for Standard Smooth Tire for Pavement Skid-Resistance Tests. (2015). *ASTM International, West Conshohocken, PA.*

American Society of Testing and Materials (ASTM) E670-09. Standard Test Method for Testing Side Force Friction on Paved Surfaces Using the Mu-Meter. (2015). *ASTM International, West Conshohocken, PA.*

American Society of Testing and Materials (ASTM) E867-06. Standard Terminology Relating to Vehicle-Pavement Systems. (2012). *ASTM International, West Conshohocken, PA.*

American Society of Testing and Materials (ASTM) E965-15. Standard Test Method for Measuring Pavement Macrotexture Depth Using a Volumetric Technique. (2015). *ASTM International, West Conshohocken, PA.*

Åström, H., & Wallman, C.-G. (2001). Friction Measurement Methods And The Correlation Between Road Friction And Traffic Safety: A Literature Review. *Digitala Vetenskapliga Arkivet Vti.*

Beautru, Y., Kane, M., Cerezo, V., & Do, M.-T. (2011). Effect of thin water film on tire/road friction. In *Young Researchers Seminar (YRS 2011)*, Copenhagen, Denmark, June 8-10.

- Bitelli, G., Simone, A., Girardi, F., & Lantieri, C. (2012). Laser Scanning on Road Pavements: A New Approach for Characterizing Surface Texture. *Sensors*, 12(7), 9110–9128.
- Bowden, F. P., & Tabor, D. (1950). The Friction and lubrication of solids. *Oxford University Press*. doi:10.1002/asl
- Byrd, T. (1981). MacDonald and Lewis Training Course: Skid Resistance Measurements and Design, Instructor Notebook. *US Department of Transportation, Federal Highway Administration, and National Highway Institute*, Vol. 10.
- Cairney, P. (1997). Skid Resistance and Crashes: A Review of the Literature. *Research Report ARR 311, Australian Road Research Board (ARRB)*, Australia.
- China, S., & James, D. E. (2011). Comparison of laser-based and sand patch measurements of pavement surface macrotexture. *Journal of Transportation Engineering*, 138(2), 176–181.
- Chowdhury, M. A., Khalil, M. K., Nuruzzaman, D. M., & Rahaman, M. L. (2011). The effect of sliding speed and normal load on friction and wear property of aluminum. *Int. J. Mech. Mechatron. Eng*, 11(01), 53–57.
- Corsello, P. (1993). *Evaluation of surface friction guidelines for Washington state highways*. Defense Technical Information Center, University of Seattle, Seattle.
- Cybernetics, I. (2000). *Skid\Friction Testing System*. Pennsylvania Department of Transportation, Pennsylvania. Accessed on 7/14/2018, <http://www.dot.state.pa.us/public/Bureaus/BOMO/Roadway%20Testing%20&%20Inventory/Equipment/Internet%20PDF/SKID.pdf>
- Dunford, A. (2013). *Friction and the texture of aggregate particles used in the road surface course*. PhD. Dissertation, University of Nottingham.
- Federal Aviation Administration. (1971). *Measurement of Runway Friction Characteristics on Wet, Icy or Snow Covered Runways*. Progress Report No. FS-I60-65-68-I, Federal Aviation Administration.

- Flintsch, G., de León Izeppi, E., McGhee, K., & Najafi, S. (2010). Speed adjustment factors for locked-wheel skid trailer measurements. *Transportation Research Record: Journal of the Transportation Research Board*, (2155), 117–123.
- Flintsch, G., McGhee, K., Izeppi, E. D. L., & Najafi, S. (2012). *The Little Book of Tire Pavement Friction*, Pavement Surface Properties Consortium1.
- Fuentes, L. G. (2009). *Investigation of the Factors Influencing Skid Resistance and the International Friction Index*. PhD. Dissertation, Department of Civil and Environmental Engineering, University of South Florida.
- Hall, J. W., Kelly L. Smith, & Paul Christopher Littleton. (2008). *Texturing of concrete pavements*. NCHRP Report 634, National Cooperative Highway Research Program, Transportation Research Board, Washington, D.C., <https://doi.org/10.17226/14318>
- Hall, J. W., Smith, K. L., Titus-Glover, L., Wambold, J. C., Yager, T. J., & Rado, Z. (2009). *Guide for pavement friction*. Final Report *NCHRP Project 01-43*, National Cooperative Highway Research Program, Transportation Research Board. Washington, D.C., <https://doi.org/10.17226/23038>
- Hanson, D. I., & Prowell, B. D. (2005). Evaluation of circular texture meter for measuring surface texture of pavements. *Transportation Research Record*, 1929 (1), 88–96. <https://doi.org/10.1177/0361198105192900111>
- Hao, X., Sha, A., Sun, Z., Li, W., & Zhao, H. (2016). Evaluation and comparison of real-time laser and electric sand-patch pavement texture-depth measurement methods. *Journal of Transportation Engineering*, 142(7). [https://doi.org/10.1061/\(ASCE\)TE.1943-5436.0000842](https://doi.org/10.1061/(ASCE)TE.1943-5436.0000842).
- Harwood, D., Blackburn, R., Kulakowski, B., & Kibler, D.(1998). *Wet weather exposure measures*. Federal Highway Administration, Kansas City, Kansas.
- Henry, J. J. (1986). Tire wet-pavement traction measurement: A state-of-the-art review. In *The tire pavement interface*, ASTM International.

- Henry, J. J. (2000). *Evaluation of pavement friction characteristics*. NCHRP Synthesis of Highway Practice 291, National Cooperative Highway Research Program, Transportation Research Board. Washington, D.C.
- Henry, J. J., & Wambold, J. C. (1992). Use of smooth-treaded test tire in evaluating skid resistance. *Transportation Research Record*, (1348), 35–42 .
- Horne, W. B., & Buhlmann, F. (1983). A method for rating the skid resistance and micro/macrottexture characteristics of wet pavements. In *Frictional Interaction of Tire and Pavement*, ASTM International.
- Jackson, N. M. (2008). *Harmonization of texture and skid-resistance measurements*. Research Report FL/DOT/SMO/08-BDH-23, Florida Department of Transportation, Jacksonville, Florida.
- Jayawickrama, P., & Thomas, B. (1998). Correction of field skid measurements for seasonal variations in Texas. *Transportation Research Record*, 1639(1), 147–154.
<https://doi.org/10.3141%2F1639-16>
- Kassem, E., Awed, A., Masad, E. A., & Little, D. N. (2013). Development of Predictive Model for Skid Loss of Asphalt Pavements. *Transportation Research Record*, **2372**(1), 83–96. <https://doi.org/10.3141%2F2372-10>
- Kulakowski, B. T. (1991). Mathematical Model of Skid Resistance as a Function of Speed. *Transportation Research Record: Journal of the Transportation Research Board*, 1311(1), 26–32.
- Lebens, M. A., & Troyer, B. (2012). *Porous asphalt pavement performance in cold regions*. Final Report No. MN/RC 2012-12, Minnesota Department of Transportation, Minnesota.
- Leu, M. C., & Henry, J. J. (1978). Prediction of skid resistance as a function of speed from pavement texture measurements. *Transportation Research Record*, 666(8), 7–13.
- Li, S. (2005). Consideration in Developing a Network Pavement Inventory Friction Test Program for a State Highway Agency. *Journal of Testing and Evaluation*, 33.

- Lu, Q., Steven, B., & No, F. (1971). Friction testing of pavement preservation treatments: literature review. Technical Memorandum No. UCPRC-TM-2006-10, California Department of Transportation.
- Luo, Y. (2003). Effect of Pavement Temperature on Frictional Properties of Hot Mix Asphalt Pavement Surfaces at Virginia Smart Road. *MSc. Thesis., Virginia Polytechnic Institute and State University.*
- Martino, M. M., & Weissmann, J. (2008). *Evaluation of Seal Coat Performance Using Macro-texture Measurements.* Report Number FHWA/TX-08/0-5310-3, Texas Department of Transportation, Research and Technology Implementation Office, Austin, TX.
- Masad, E., Rezaei, A., Chowdhury, A., & Freeman, T. J. (2010). *Field evaluation of asphalt mixture skid resistance and its relationship to aggregate characteristics,* Texas Transportation Institute.
- Mataei, B., Zakeri, H., Zahedi, M., & Nejad, F. M. (2016). Pavement Friction and Skid Resistance Measurement Methods: A Literature Review. *Open Journal of Civil Engineering*, 6(04), 537-565.
- MATLAB. (2010). version 7.10.0 (R2010a), The MathWorks Inc. Natick, Massachusetts.
- Moore, D. F. (1975). *The Friction of Pneumatic Tyres.* Elsevier Scientific Publishing Company, New York .
- Moyer, R. A. (1943). Motor Vehicle Operating Costs, Road Roughness and Slipperiness of Various Bituminous and Portland Cement Concrete Surfaces. *Highway Research Board Proceedings*, Missouri, Decemeber 1-4, 22, 13-52.
- Moyer, R. A. (1959). Historical background of skid resistance measurement-American experience. In *Al-Rayhane, 1st international skid prevention conference,* Charlottesville, Virginia.

- Murray, L., Nguyen, H., Lee, Y.-F., Remmenga, M. D., & Smith, D. W. (2012). Variance inflation factors in regression models with dummy variables. *Proceedings of Applied Statistics in Agriculture*, Manhattan, Kansas, April 29 - May 1.
- Noyce, D. A., Bahia, H. U., Yambó, J. M., & Kim, G. (2005). *Incorporating Road Safety into Pavement Management: Maximizing Asphalt Pavement Surface Friction for Road Safety Improvements*. Midwest Regional University Transportation Center.
- O'brien, R. M. (2007). A caution regarding rules of thumb for variance inflation factors. *Quality & Quantity*, 41(5), 673–690.
- Poorbaugh, J. (2017). Idaho Transportation System Pavement Performance-2017 Report, (208).
- Praticò, F. G., & Vaiana, R. (2015). A study on the relationship between mean texture depth and mean profile depth of asphalt pavements. *Construction and Building Materials*, 101, 72–79.
- Oh, Soon Mi, David R. Ragland, & Ching-Yao Chan (2010). Evaluation of Traffic and Environment Effects on Skid Resistance and Safety Performance of Rubberized Open-grade Asphalt Concrete. Final Report for Task Order 6218, California PATH Research Projects, California Department of Transportation.
- Rizenbergs, R. L., Burchett, J. L., & Napier, C. T. (1973). "Skid resistance of pavements" in *Skid Resistance of Highway Pavements*, ed. R. Wilcox, West Conshohocken, PA. ASTM International, 138-159. <https://doi.org/10.1520/STP38898S>.
- RStudio, I. (2015). RStudio: Integrated Development for R.
- Saito, K., Horiguchi, T., Kasahara, A., Abe, H., & Henry, J. J. (1996). Development of portable tester for measuring skid resistance and its speed dependency on pavement surfaces. *Transportation Research Record*, 1536(1), 45–51.
- Schallamach, A. (1971). How does rubber slide? *Wear*, 17(4), 301–312. [https://doi.org/10.1016/0043-1648\(71\)90033-0](https://doi.org/10.1016/0043-1648(71)90033-0)

Shahin, M. Y. (1994). *Pavement Management for Airports, Roads, and Parking Lots*. Chapman & Hall, One Penn Plaza, New York, NY, United States.

Statistics Solution. (2013). Retrieved December 2, 2019, from <https://www.statisticssolutions.com/homoscedasticity/>

Yaacob, H., Hassan, N. A., Hainin, M. R., & Rosli, M. F. (2014). Comparison of sand patch test and multi laser profiler in pavement surface measurement. *Jurnal Teknologi*, **70**(4), 103-106.

Zimmer, R., & Fernando, E. (2013). Evaluation of Skid Measurements Used by TxDOT: Technical Report, **7**(2). Retrieved from <http://tti.tamu.edu/documents/0-6619-1.pdf>
<http://www.ntis.gov>

APPENDIX A TEST DATA

Table A.1. Skid Measurement Data

Section ID	Test Speed (mph)	Average SN	Standard Deviation of SN
1	20	75.09	0.95
	30	71.97	1.11
	40	66.49	1.33
	50	60.37	1.48
	60	50.97	6.12
2	20	63.31	1.49
	30	55.16	1.75
	40	49.64	1.47
	50	45.24	2.59
	60	39.36	2.65
3	20	62.69	2.39
	30	47.15	3.11
	40	37.91	3.25
	50	36.41	2.45
	60	29.87	2.89
4	20	60.31	1.94
	30	52.33	2.67
	40	44.92	3.60
	50	40.90	6.69
	60	37.91	4.61
5	20	69.83	1.88
	30	60.45	3.02
	40	50.50	3.28
	50	44.60	1.28
	60	43.60	3.05
6	20	63.52	2.09
	30	56.38	2.20
	40	49.60	1.07
	50	43.19	1.72
7	20	57.40	0.94
	30	50.47	0.86
	40	43.59	2.77
	50	39.46	2.20
	60	35.55	1.76

Table A.1. Skid Measurement Data (continued)

Section ID	Test Speed (mph)	Average SN	Standard Deviation of SN
8	20	70.72	0.49
	30	65.66	1.19
	40	60.20	1.08
	50	53.88	2.06
	60	50.45	2.78
9	20	66.17	0.82
	30	59.78	1.55
	40	53.52	1.73
	50	51.37	1.58
	60	44.86	3.44
10	20	60.46	1.67
	30	52.02	2.08
	40	43.21	1.10
	50	36.54	1.68
	60	33.05	2.13
11	20	66.99	1.75
	30	55.54	1.19
	40	44.70	1.08
	50	38.94	2.06
	60	31.37	1.88
12	20	50.26	2.01
	30	35.45	2.14
	40	29.23	2.96
	50	17.23	2.02
	60	15.00	1.76
13	20	64.31	0.90
	30	59.49	0.59
	40	56.62	0.64
	50	53.23	1.36
	60	49.39	1.71
14	20	68.26	1.50
	30	60.93	1.90
	40	54.88	1.92
	50	47.13	1.20
	60	41.28	2.29

Table A.1. Skid Measurement Data (continued)

Section ID	Test Speed (mph)	Average SN	Standard Deviation of SN
15	20	71.98	1.07
	30	66.74	0.93
	40	63.33	1.07
	50	59.43	0.85
	60	56.00	1.98
16	20	51.73	6.45
	30	33.58	4.29
	40	30.39	4.45
	50	24.67	2.82
	60	21.97	3.99
17	20	64.14	0.97
	30	53.25	1.49
	40	44.61	2.12
	50	38.16	1.90
	60	36.53	3.56
18	20	52.09	1.43
	30	51.34	0.98
	40	47.13	0.75
	50	45.37	1.24
19	20	67.18	0.96
	30	60.99	0.88
	40	54.41	0.92
	50	47.96	1.44
	60	42.45	1.99
20	20	57.81	1.35
	30	43.82	1.52
	40	32.54	2.14
	50	24.57	3.07
	60	22.50	3.85
21	20	48.97	4.57
	30	34.90	1.70
	40	23.90	2.46
	50	19.60	2.77
	60	16.18	1.92

Table A.1. Skid Measurement Data (continued)

Section ID	Test Speed (mph)	Average SN	Standard Deviation of SN
22	20	65.20	0.75
	30	60.72	0.68
	40	57.50	0.94
	50	53.74	1.02
	60	49.39	1.81
23	20	65.93	12.63
	30	61.93	12.00
	40	53.60	13.44
	50	49.07	12.05
	60	41.13	10.75
24	20	65.08	2.09
	30	58.32	2.80
	40	52.25	1.63
	50	46.60	2.08
	60	43.95	2.67
25	20	73.20	1.94
	30	63.74	1.64
	40	58.78	1.63
	50	53.80	1.54
	60	51.17	2.24
26	20	65.11	1.51
	30	60.45	2.48
	40	57.11	2.22
	50	54.78	1.64
	60	50.98	5.35
27	40	31.30	0.78
	50	26.00	3.02
	60	21.10	3.82
28	40	50.27	4.12
	50	48.53	1.23
	60	42.87	0.91

Table A.1. Skid Measurement Data (continued)

Section ID	Test Speed (mph)	Average SN	Standard Deviation of SN
29	40	49.65	1.08
	50	44.40	1.39
	60	41.05	0.77
30	40	59.80	1.00
	50	56.65	1.32
	60	51.85	0.92
31	40	44.03	3.98
	50	39.03	3.37
	60	34.03	4.05
32	20	57.78	4.16
	30	44.93	2.58
	40	38.45	4.28
33	20	61.73	3.31
	30	61.55	3.89
	40	56.70	2.02
	50	55.13	1.25
	60	51.80	1.36
34	40	44.30	1.26
	50	37.73	2.64
	60	32.90	1.37

Table A.2. Texture Measurement Data

Section ID	MPD (mm)	MTD (mm)	DFT20
1	1.194	1.196	0.69
2	1.232	1.249	0.62
3	0.648	0.601	0.62
4	1.162	1.334	0.55
5	1.016	0.862	0.55
6	1.105	1.059	0.58
7	1.016	0.893	0.52
8	1.634	1.322	0.59
9	1.008	1.001	0.52
10	0.576	0.555	0.55
11	0.720	0.469	0.62
12	0.508	0.277	0.64
13	2.269	2.287	0.6
14	0.821	0.827	0.57
15	2.040	1.904	0.55
16	0.525	0.418	0.61
17	0.660	0.587	0.58
18	1.651	1.415	0.57
19	1.718	1.635	
20	0.645	0.561	0.65
21	0.598	0.514	0.55
22	1.848	1.765	
23	1.249	1.166	
24	1.124	1.040	0.6
25	1.328	1.245	0.63
26	1.810	1.727	0.58
27	2.311		
28	2.515		
29	2.388		
30	2.489		
31	1.778		
32	2.032		
33	2.235		
34	1.854		

APPENDIX B DATA FOR MODEL DEVELOPMENT AND VALIDATION

Table B.1. Model Development Data

Section ID	V1	SN1	MPD	V2	SN2
1	20	75.09	1.19	30	71.97
1	20	75.09	1.19	40	66.49
1	20	75.09	1.19	50	60.37
1	20	75.09	1.19	60	50.97
2	20	63.31	1.23	30	55.16
2	20	63.31	1.23	40	49.64
2	20	63.31	1.23	50	45.24
2	20	63.31	1.23	60	39.36
3	20	62.69	0.65	30	47.15
3	20	62.69	0.65	40	37.91
3	20	62.69	0.65	50	36.41
3	20	62.69	0.65	60	29.87
4	20	60.31	1.16	30	52.33
4	20	60.31	1.16	40	44.92
4	20	60.31	1.16	50	40.90
4	20	60.31	1.16	60	37.91
5	20	69.83	1.02	30	60.45
5	20	69.83	1.02	40	50.50
5	20	69.83	1.02	50	44.60
5	20	69.83	1.02	60	43.60
6	20	63.52	1.10	30	56.38
6	20	63.52	1.10	40	49.60
6	20	63.52	1.10	50	43.19
8	20	70.72	1.63	30	65.66
8	20	70.72	1.63	40	60.20
8	20	70.72	1.63	50	53.88
8	20	70.72	1.63	60	50.45
9	20	66.17	1.01	30	59.78
9	20	66.17	1.01	40	53.52
9	20	66.17	1.01	50	51.37
9	20	66.17	1.01	60	44.86
10	20	60.46	0.58	30	52.02
10	20	60.46	0.58	40	43.21
10	20	60.46	0.58	50	36.54
11	20	66.99	0.72	30	55.54
11	20	66.99	0.72	40	44.70
11	20	66.99	0.72	50	38.94
11	20	66.99	0.72	60	31.37

Table B.1. Model Development Data (continued)

Section ID	V1	SN1	MPD	V2	SN2
14	20	68.26	0.82	30	60.93
14	20	68.26	0.82	40	54.88
14	20	68.26	0.82	50	47.13
14	20	68.26	0.82	60	41.28
16	20	51.73	0.52	30	33.58
16	20	51.73	0.52	40	30.39
16	20	51.73	0.52	50	24.67
16	20	51.73	0.52	60	21.97
17	20	64.14	0.66	30	53.25
17	20	64.14	0.66	40	44.61
17	20	64.14	0.66	50	38.16
17	20	64.14	0.66	60	36.53
19	20	67.18	1.72	30	60.99
19	20	67.18	1.72	40	54.41
19	20	67.18	1.72	50	47.96
19	20	67.18	1.72	60	42.45
21	20	48.97	0.60	30	34.90
21	20	48.97	0.60	40	23.90
21	20	48.97	0.60	50	19.60
21	20	48.97	0.60	60	16.18
22	20	65.20	1.85	30	60.72
22	20	65.20	1.85	40	57.50
22	20	65.20	1.85	50	53.74
22	20	65.20	1.85	60	49.39
24	20	65.08	1.12	30	58.32
24	20	65.08	1.12	40	52.25
24	20	65.08	1.12	50	46.60
24	20	65.08	1.12	60	43.95
26	20	65.11	1.81	30	60.45
26	20	65.11	1.81	40	57.11
26	20	65.11	1.81	50	54.78
26	20	65.11	1.81	60	50.98
33	20	61.73	2.24	30	61.55
33	20	61.73	2.24	40	56.70
33	20	61.73	2.24	50	55.13
33	20	61.73	2.24	60	51.80
1	30	71.97	1.19	40	66.49
1	30	71.97	1.19	50	60.37
1	30	71.97	1.19	60	50.97

Table B.1. Model Development Data (continued)

Section ID	V1	SN1	MPD	V2	SN2
2	30	55.16	1.23	40	49.64
2	30	55.16	1.23	50	45.24
2	30	55.16	1.23	60	39.36
3	30	47.15	0.65	40	37.91
3	30	47.15	0.65	50	36.41
3	30	47.15	0.65	60	29.87
4	30	52.33	1.16	40	44.92
4	30	52.33	1.16	50	40.90
4	30	52.33	1.16	60	37.91
5	30	60.45	1.02	40	50.50
5	30	60.45	1.02	50	44.60
5	30	60.45	1.02	60	43.60
6	30	56.38	1.10	40	49.60
6	30	56.38	1.10	50	43.19
8	30	65.66	1.63	40	60.20
8	30	65.66	1.63	50	53.88
8	30	65.66	1.63	60	50.45
9	30	59.78	1.01	40	53.52
9	30	59.78	1.01	50	51.37
9	30	59.78	1.01	60	44.86
10	30	52.02	0.58	40	43.21
10	30	52.02	0.58	50	36.54
10	30	52.02	0.58	60	33.05
11	30	55.54	0.72	40	44.70
11	30	55.54	0.72	50	38.94
11	30	55.54	0.72	60	31.37
14	30	60.93	0.82	40	54.88
14	30	60.93	0.82	50	47.13
14	30	60.93	0.82	60	41.28
16	30	33.58	0.52	40	30.39
16	30	33.58	0.52	50	24.67
16	30	33.58	0.52	60	21.97
17	30	53.25	0.66	40	44.61
17	30	53.25	0.66	50	38.16
17	30	53.25	0.66	60	36.53
19	30	60.99	1.72	40	54.41
19	30	60.99	1.72	50	47.96
19	30	60.99	1.72	60	42.45

Table B.1. Model Development Data (continued)

Section ID	V1	SN1	MPD	V2	SN2
21	30	34.90	0.60	40	23.90
21	30	34.90	0.60	50	19.60
21	30	34.90	0.60	60	16.18
22	30	60.72	1.85	40	57.50
22	30	60.72	1.85	50	53.74
22	30	60.72	1.85	60	49.39
24	30	58.32	1.12	40	52.25
24	30	58.32	1.12	50	46.60
24	30	58.32	1.12	60	43.95
26	30	60.45	1.81	40	57.11
26	30	60.45	1.81	50	54.78
26	30	60.45	1.81	60	50.98
33	30	61.55	2.24	40	56.70
33	30	61.55	2.24	50	55.13
33	30	61.55	2.24	60	51.80
1	40	66.49	1.19	50	60.37
1	40	66.49	1.19	60	50.97
2	40	49.64	1.23	50	45.24
2	40	49.64	1.23	60	39.36
3	40	37.91	0.65	50	36.41
3	40	37.91	0.65	60	29.87
4	40	44.92	1.16	50	40.90
4	40	44.92	1.16	60	37.91
5	40	50.50	1.02	50	44.60
5	40	50.50	1.02	60	43.60
6	40	49.60	1.10	50	43.19
8	40	60.20	1.63	50	53.88
8	40	60.20	1.63	60	50.45
9	40	53.52	1.01	50	51.37
9	40	53.52	1.01	60	44.86
10	40	43.21	0.58	50	36.54
10	40	43.21	0.58	60	33.05
11	40	44.70	0.72	50	38.94
11	40	44.70	0.72	60	31.37
14	40	54.88	0.82	50	47.13
14	40	54.88	0.82	60	41.28
16	40	30.39	0.52	50	24.67
16	40	30.39	0.52	60	21.97

Table B.1. Model Development Data (continued)

Section ID	V1	SN1	MPD	V2	SN2
17	40	44.61	0.66	50	38.16
17	40	44.61	0.66	60	36.53
19	40	54.41	1.72	50	47.96
19	40	54.41	1.72	60	42.45
21	40	23.90	0.60	50	19.60
21	40	23.90	0.60	60	16.18
22	40	57.50	1.85	50	53.74
22	40	57.50	1.85	60	49.39
24	40	52.25	1.12	50	46.60
24	40	52.25	1.12	60	43.95
26	40	57.11	1.81	50	54.78
26	40	57.11	1.81	60	50.98
27	40	31.30	2.31	50	26.00
27	40	31.30	2.31	60	21.10
28	40	50.27	2.51	50	48.53
28	40	50.27	2.51	60	42.87
30	40	59.80	2.49	50	56.65
30	40	59.80	2.49	60	51.85
31	40	44.03	1.78	50	39.03
31	40	44.03	1.78	60	34.03
33	40	56.70	2.24	50	55.13
33	40	56.70	2.24	60	51.80
34	40	44.30	1.85	50	37.73
34	40	44.30	1.85	60	32.90
1	50	60.37	1.19	60	50.97
2	50	45.24	1.23	60	39.36
3	50	36.41	0.65	60	29.87
4	50	40.90	1.16	60	37.91
5	50	44.60	1.02	60	43.60
8	50	53.88	1.63	60	50.45
9	50	51.37	1.01	60	44.86
10	50	36.54	0.58	60	33.05
11	50	38.94	0.72	60	31.37
14	50	47.13	0.82	60	41.28
16	50	24.67	0.52	60	21.97
17	50	38.16	0.66	60	36.53
19	50	47.96	1.72	60	42.45
21	50	19.60	0.60	60	16.18
22	50	53.74	1.85	60	49.39

Table B.1. Model Development Data (continued)

Section ID	V1	SN1	MPD	V2	SN2
24	50	46.60	1.12	60	43.95
26	50	54.78	1.81	60	50.98
27	50	26.00	2.31	60	21.10
28	50	48.53	2.51	60	42.87
30	50	56.65	2.49	60	51.85
31	50	39.03	1.78	60	34.03
33	50	55.13	2.24	60	51.80
34	50	37.73	1.85	60	32.90

Table B.2. Model Validation Data

V1	SN1	MPD	V2	SN2
20	57.40	1.02	40	43.59
30	50.47	1.02	40	43.59
50	39.46	1.02	40	43.59
60	35.55	1.02	40	43.59
20	50.26	0.51	40	29.23
30	35.45	0.51	40	29.23
50	17.23	0.51	40	29.23
60	15.00	0.51	40	29.23
20	64.31	2.27	40	56.62
30	59.49	2.27	40	56.62
50	53.23	2.27	40	56.62
60	49.39	2.27	40	56.62
20	71.98	2.04	40	63.33
30	66.74	2.04	40	63.33
50	59.43	2.04	40	63.33
60	56.00	2.04	40	63.33
20	52.09	1.65	40	47.13
30	51.34	1.65	40	47.13
50	45.37	1.65	40	47.13
20	57.81	0.64	40	32.54
30	43.82	0.64	40	32.54
50	24.57	0.64	40	32.54
60	22.50	0.64	40	32.54
20	65.93	1.25	40	53.60
30	61.93	1.25	40	53.60
50	49.07	1.25	40	53.60
60	41.13	1.25	40	53.60
20	73.20	1.33	40	58.78
30	63.74	1.33	40	58.78
50	53.80	1.33	40	58.78
60	51.17	1.33	40	58.78
50	44.40	2.39	40	49.65
60	41.05	2.39	40	49.65
20	57.78	2.03	40	38.45
30	44.93	2.03	40	38.45

APPENDIX C RELATION BETWEEN SN AND MPD

HMA SECTIONS

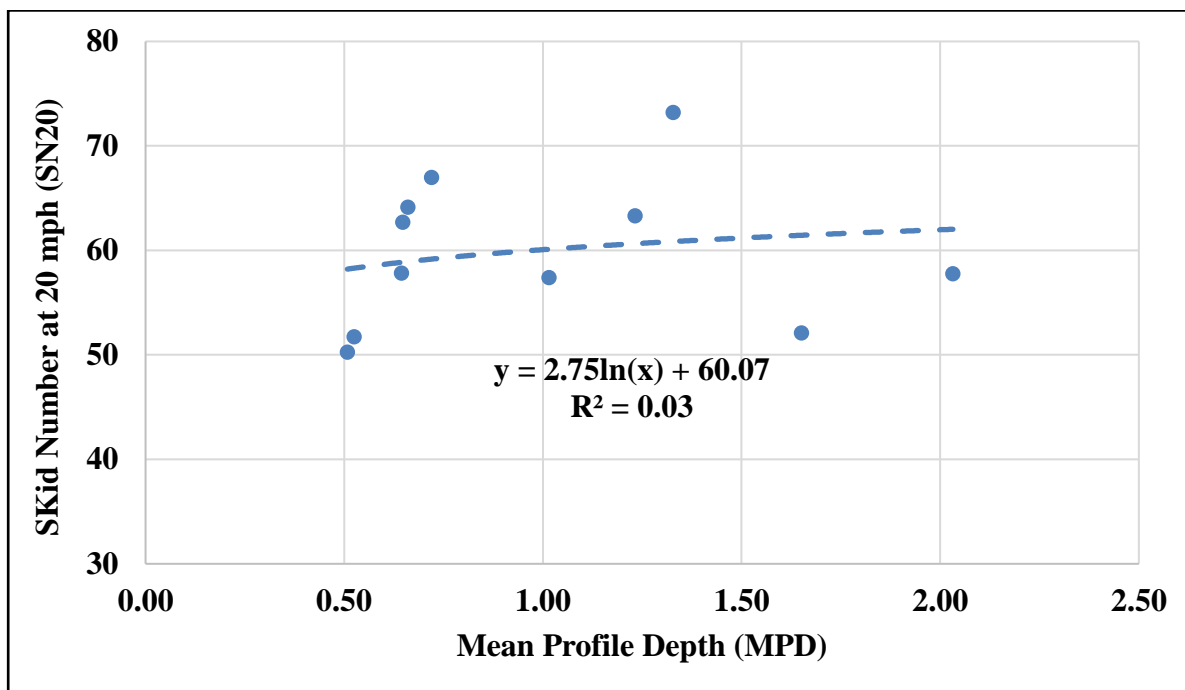


Figure C.1. Relationship between skid number at 20 mph (SN20) and mean profile depth

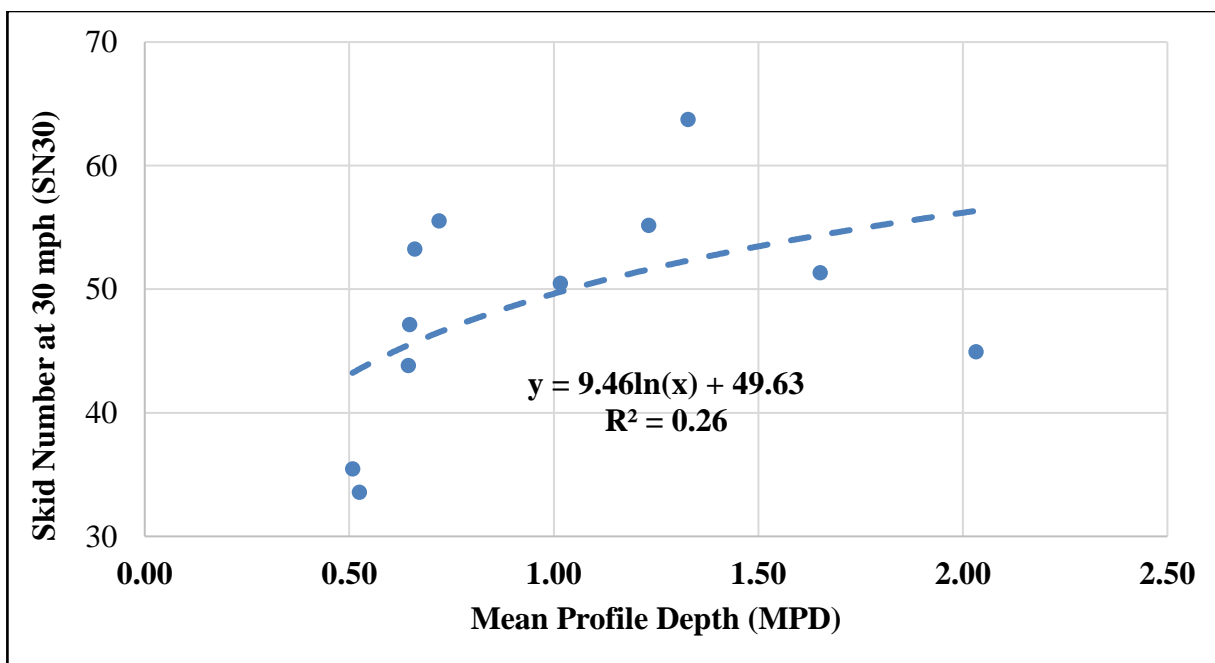


Figure C.2. Relationship between skid number at 30 mph (SN30) and mean profile depth

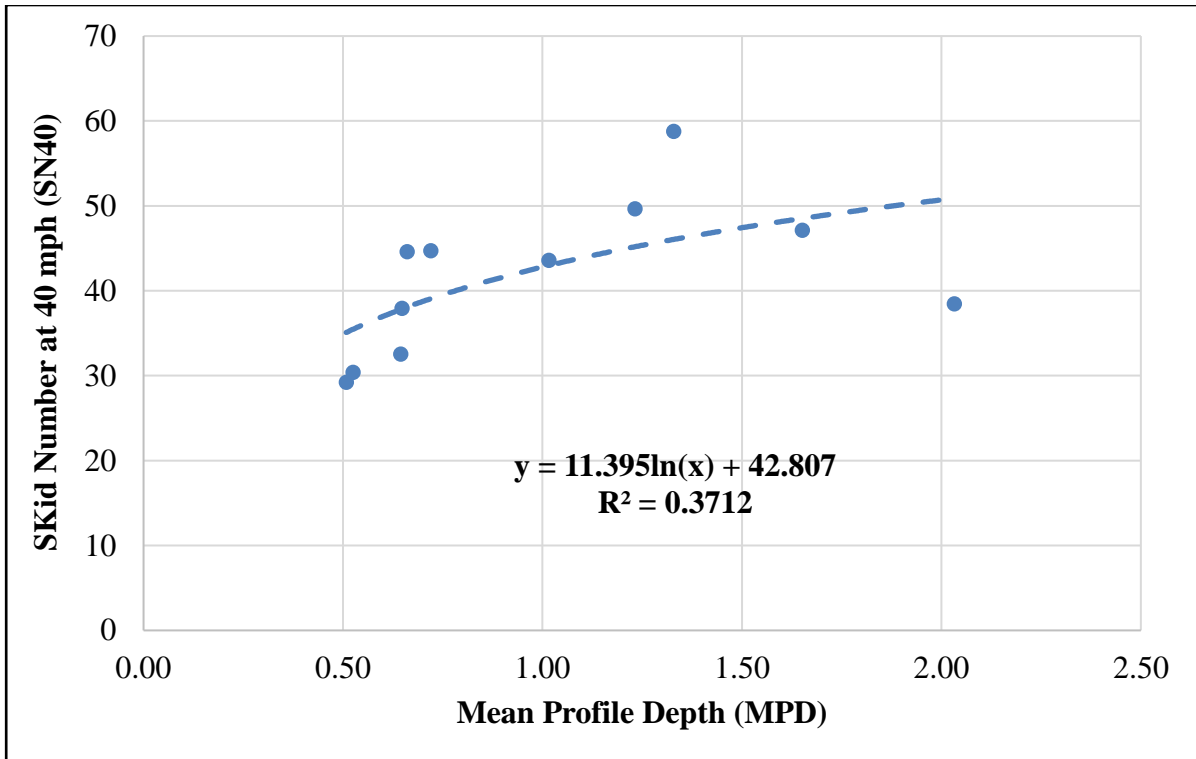


Figure C.3. Relationship between skid number at 40 mph (SN40) and mean profile depth

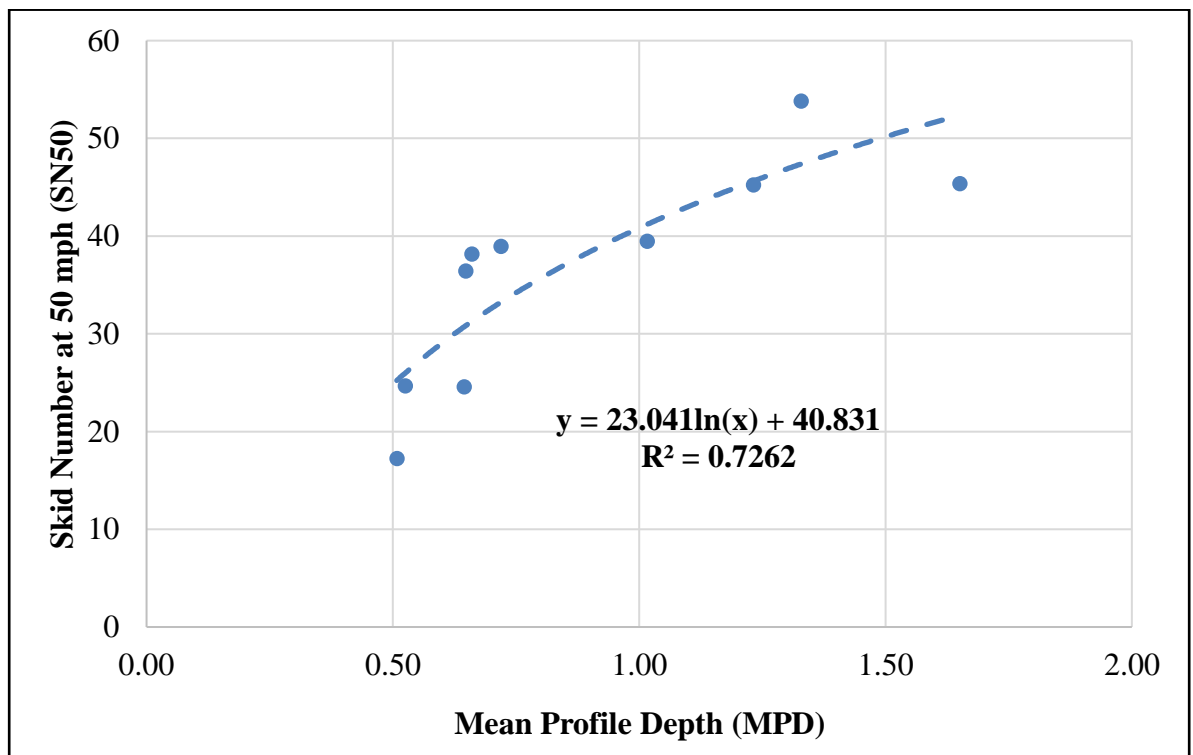


Figure C.4. Relationship between skid number at 50 mph (SN50) and mean profile depth

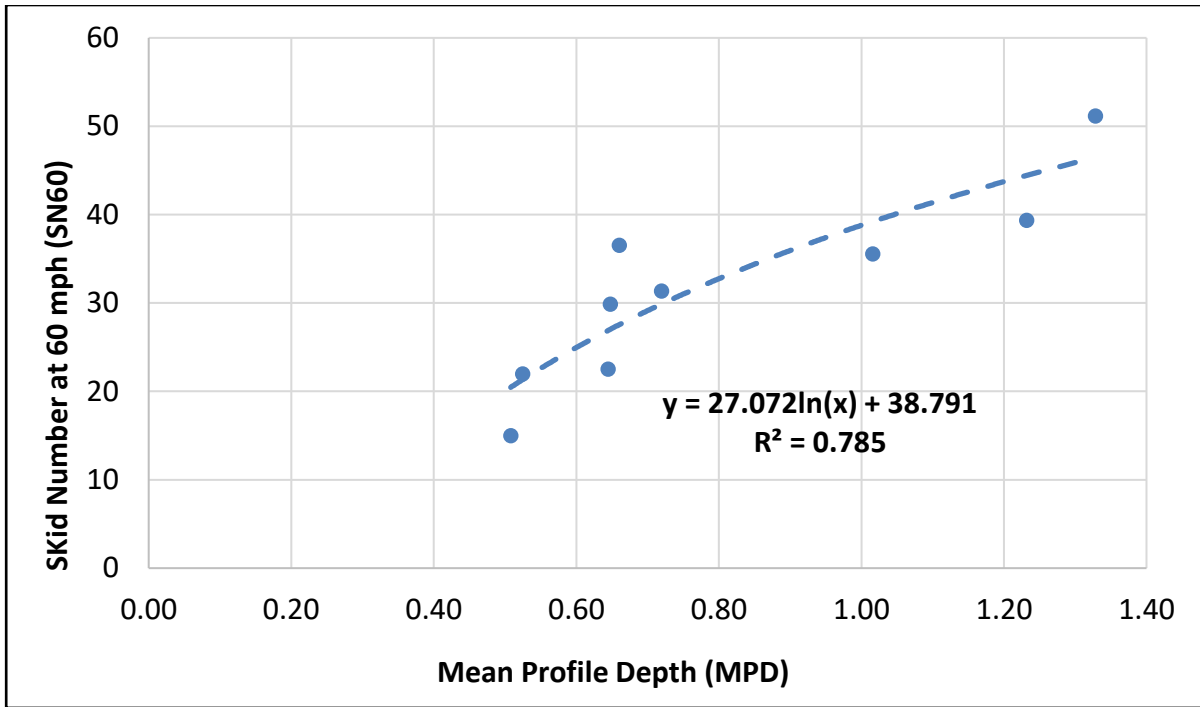


Figure C.5. Relationship between skid number at 60 mph (SN60) and mean profile depth

SEAL COAT SECTIONS

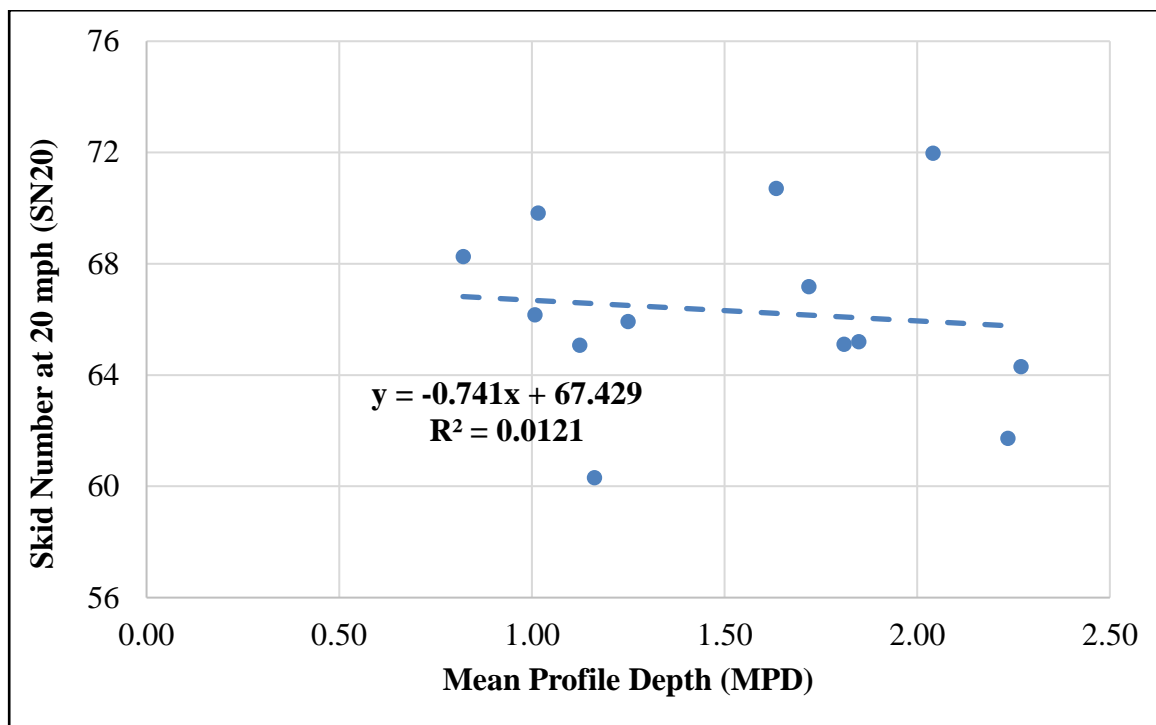


Figure C.6. Relationship between skid number at 20 mph (SN20) and mean profile depth

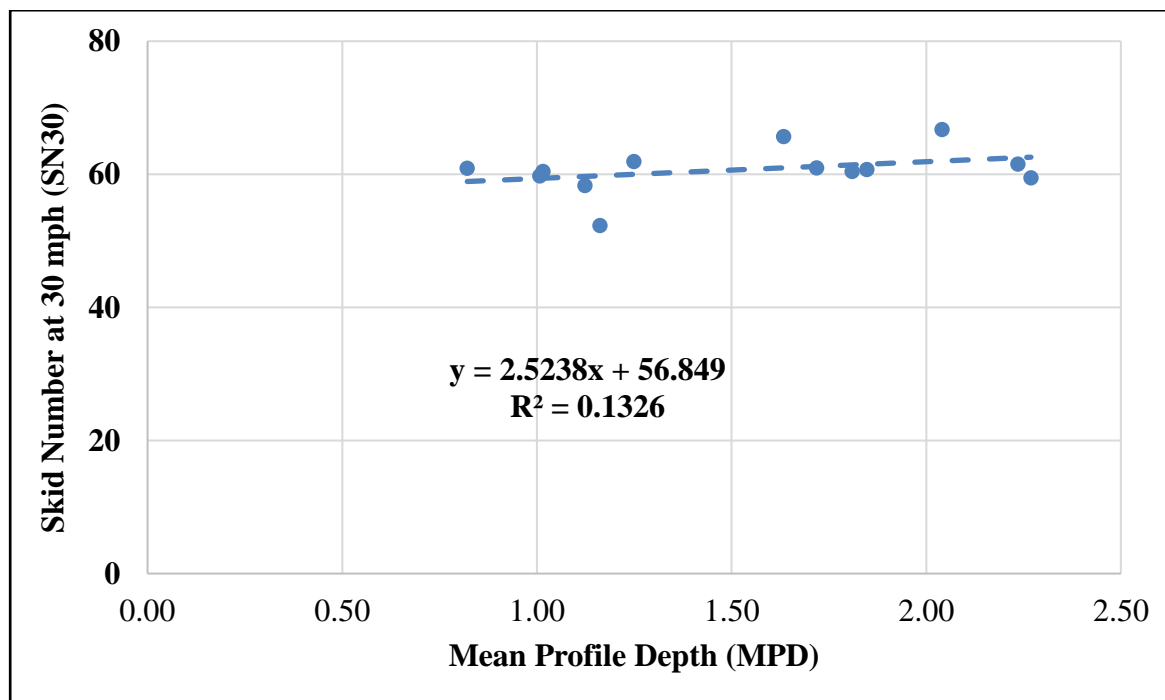


Figure C.7. Relationship between skid number at 30 mph (SN30) and mean profile depth

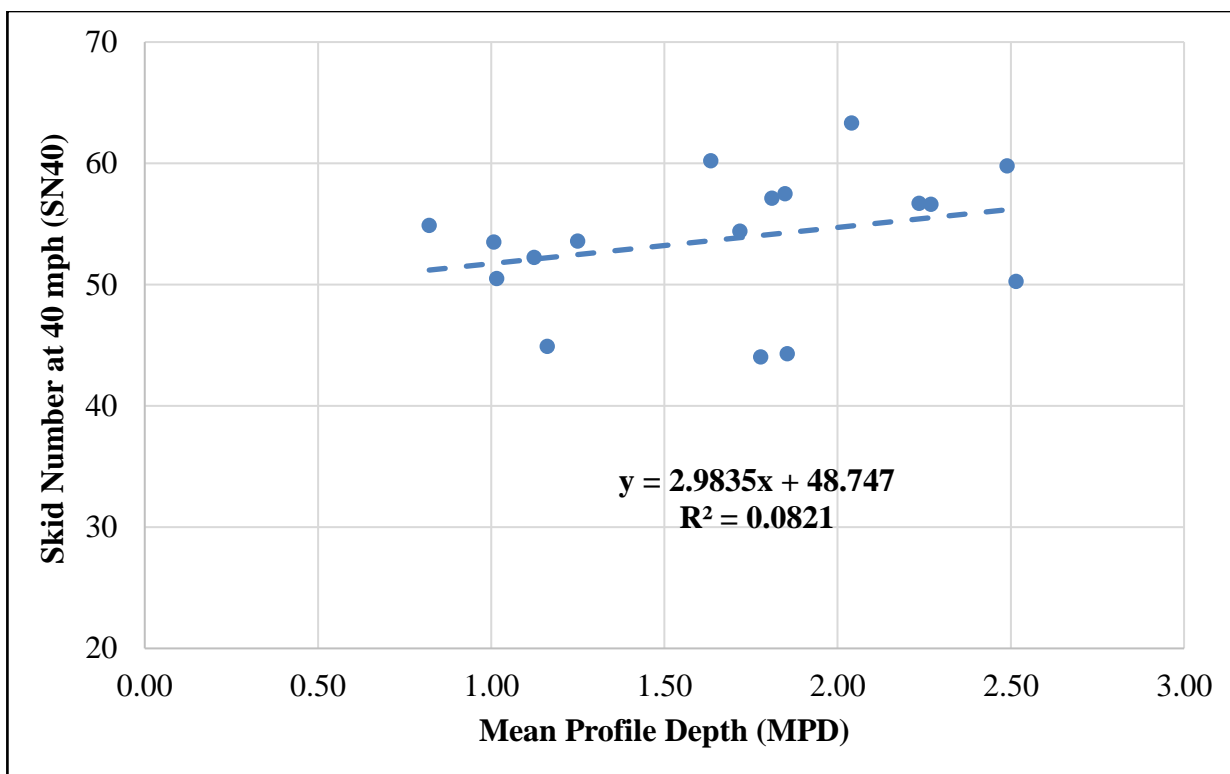


Figure C.8. Relationship between skid number at 40 mph (SN40) and mean profile depth

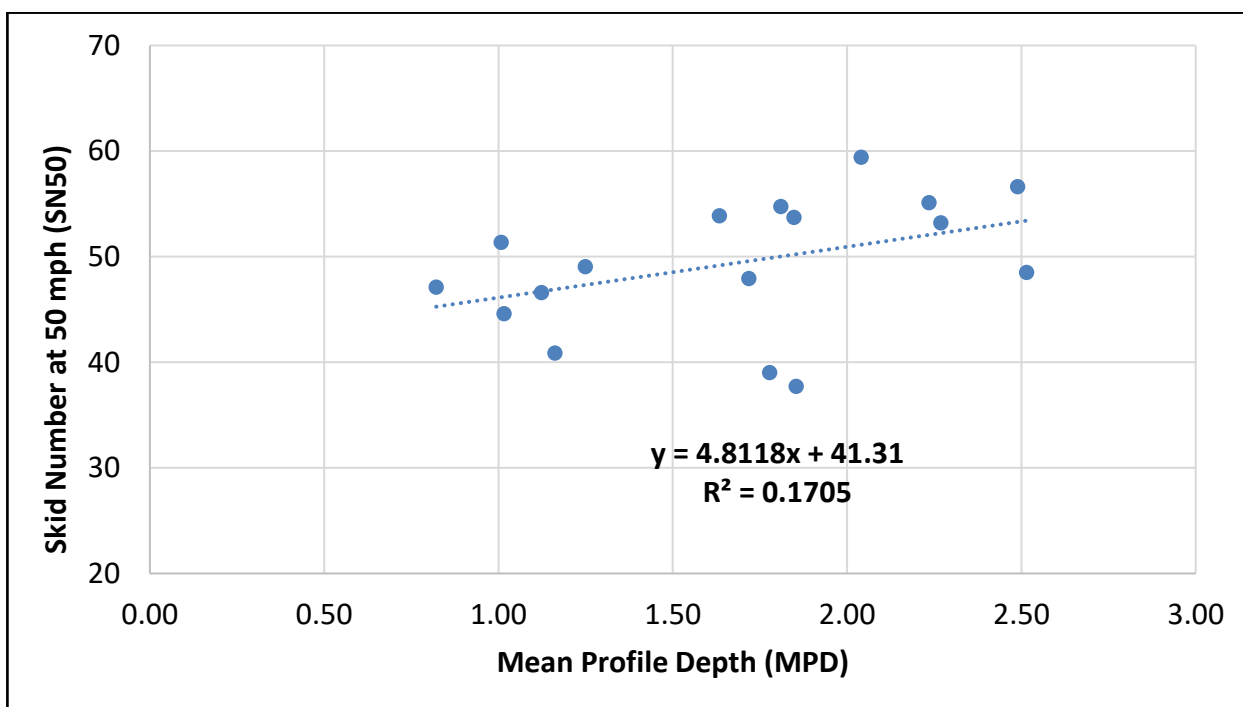


Figure C.9. Relationship between skid number at 50 mph (SN50) and mean profile depth

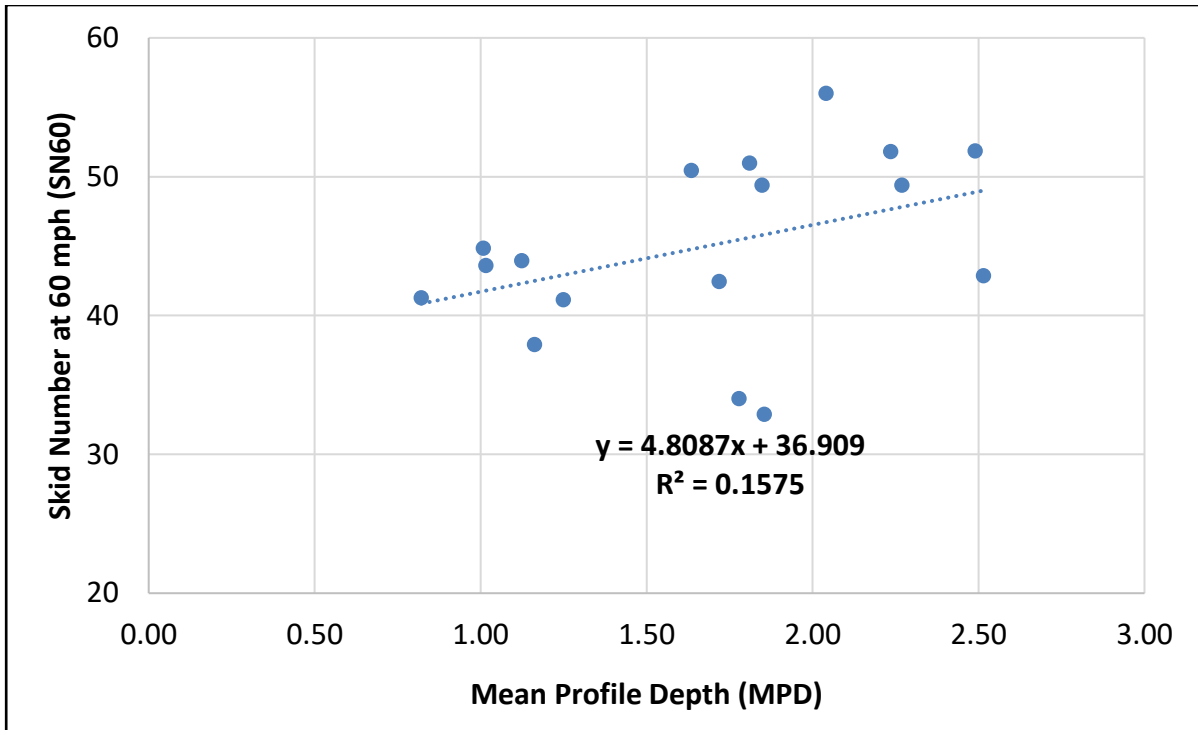


Figure C.10. Relationship between skid number at 60 mph (SN60) and mean profile depth

APPENDIX D RELATIONSHIP BETWEEN SKID NUMBER (SN) AND DFT20

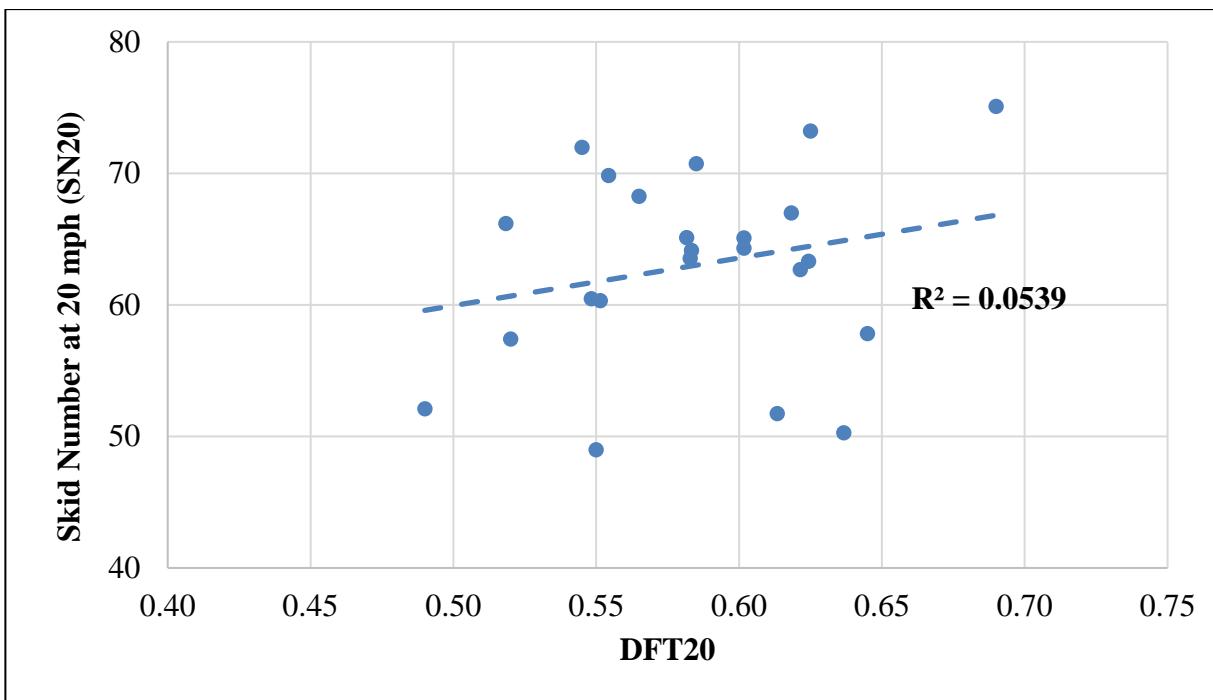


Figure D.1. Relationship between skid number at 20 mph (SN20) and DFT20

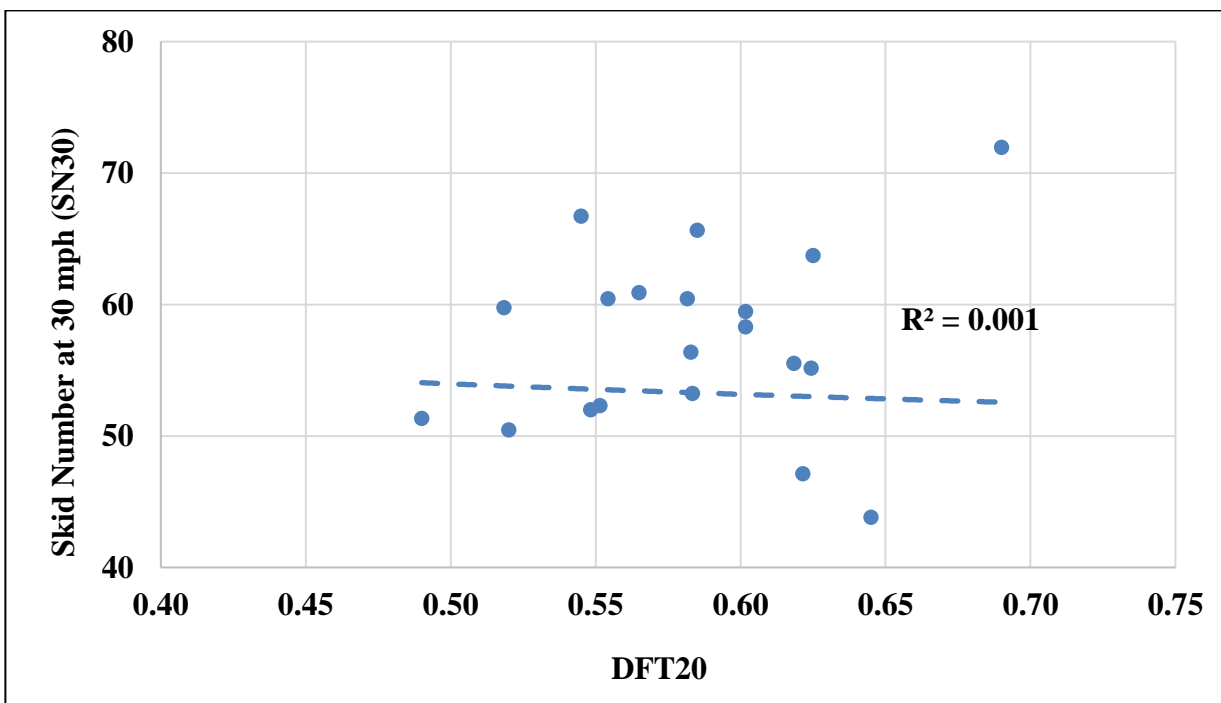


Figure D.2. Relationship between skid number at 30 mph (SN30) and DFT20

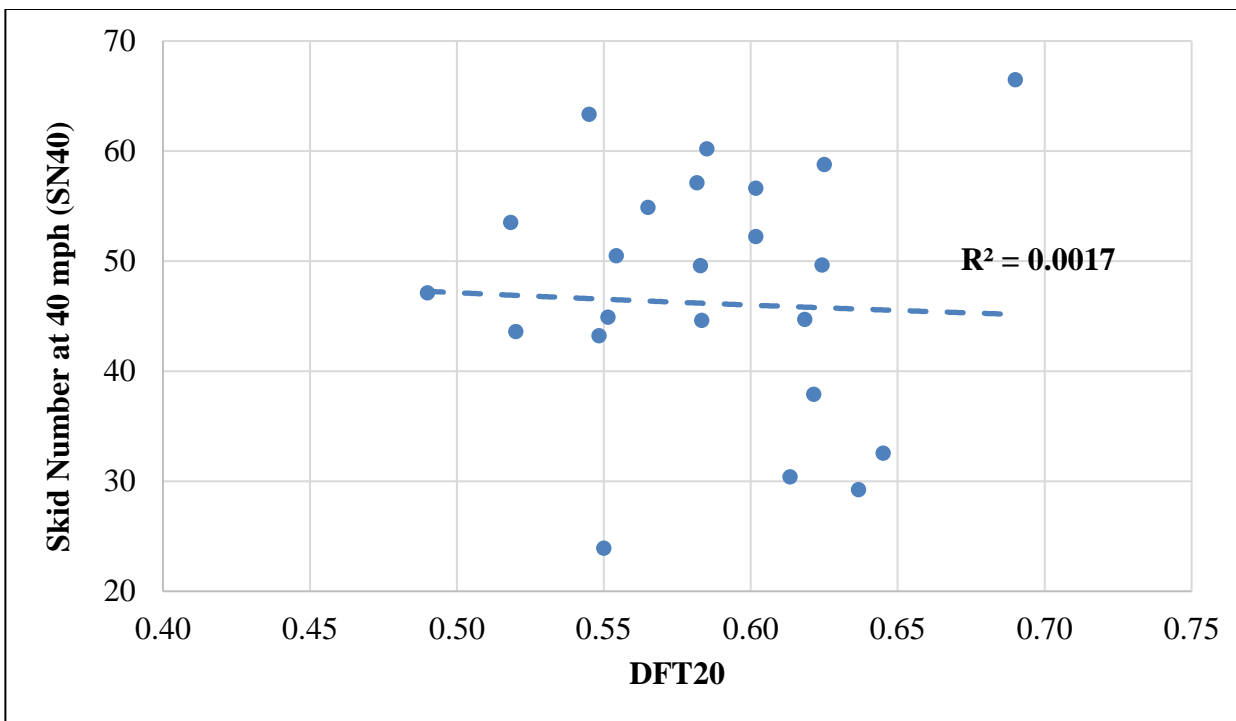


Figure D.3. Relationship between skid number at 40 mph (SN40) and DFT20

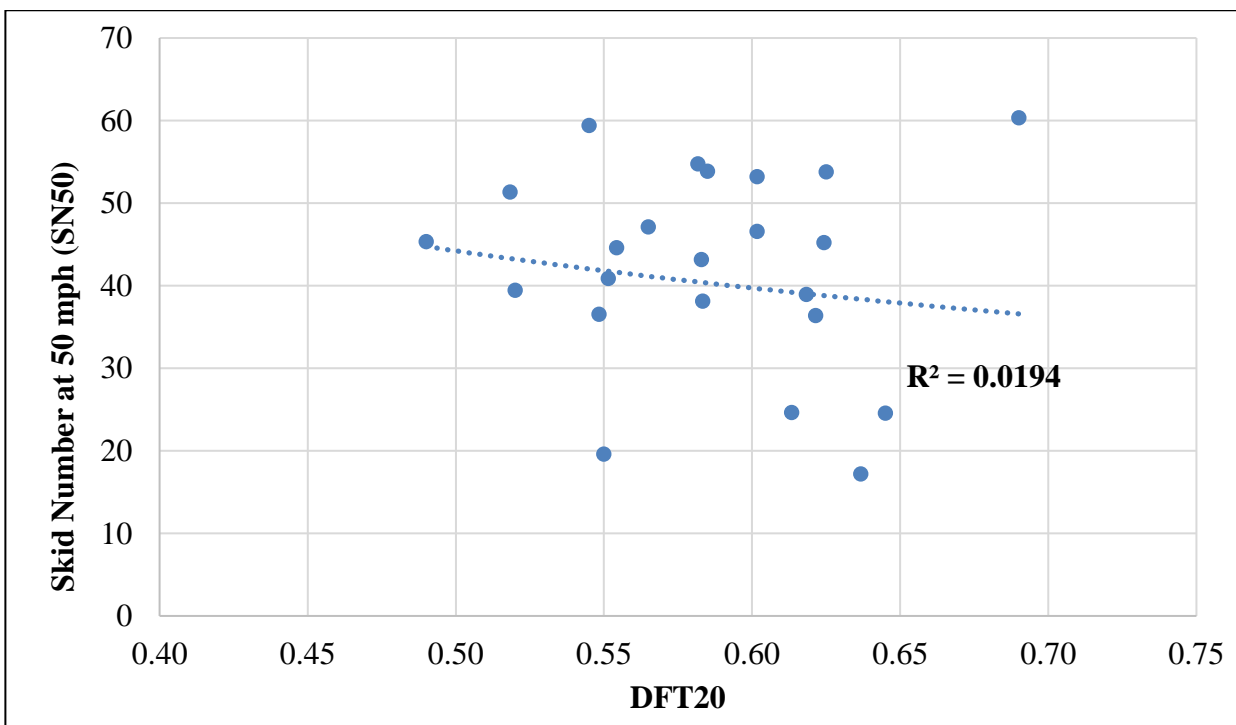


Figure D.4. Relationship between skid number at 50 mph (SN50) and DFT20

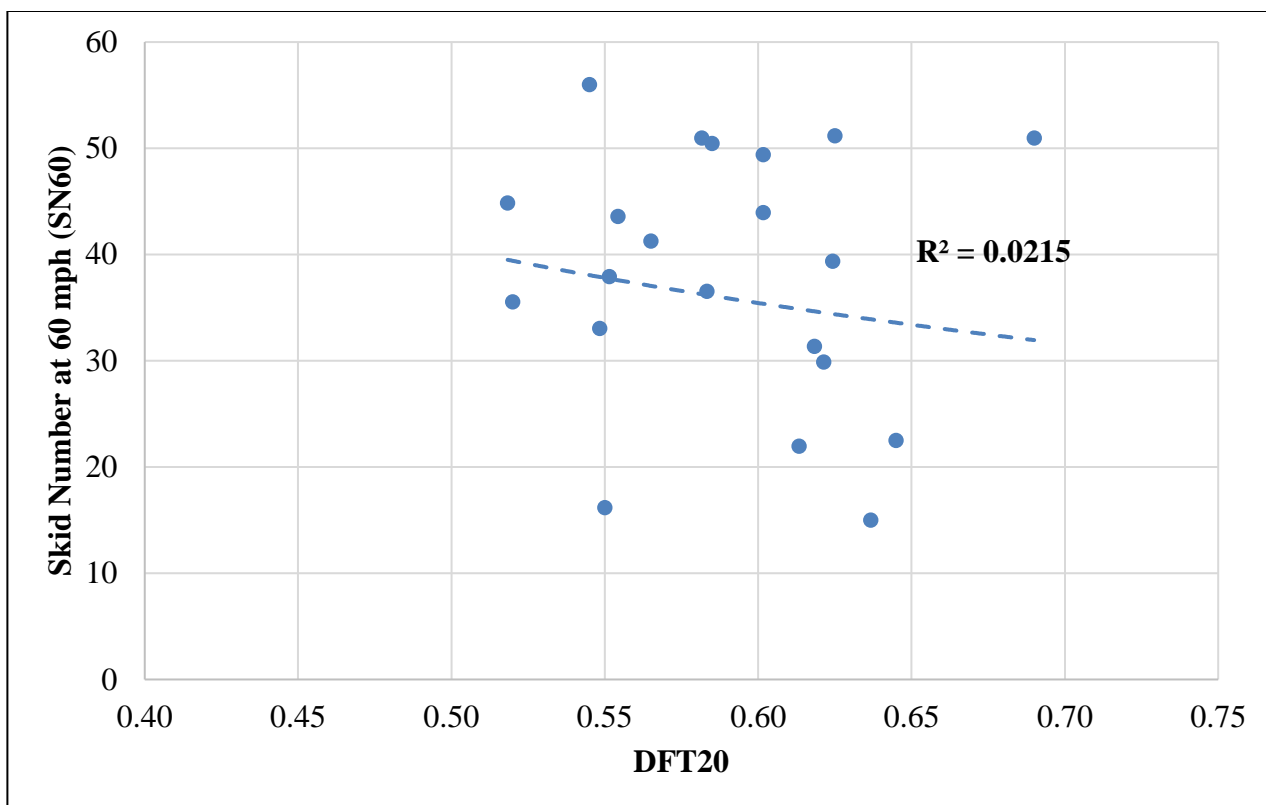


Figure D.5. Relationship between skid number at 60 mph (SN60) and DFT20

APPENDIX E SKID SOFTWARE EXAMPLES

Single Test Site Mode

1. Step 1

This is the interface of the software. The user has two options to either select Single Test Site option or Multiple Test Site option. Figure F.1 highlights the selection of “**Single Test Site**” option. The “**Clear**” command button resets the selection and allow user to make another selection. The “**Close**” command button is used to close the application.

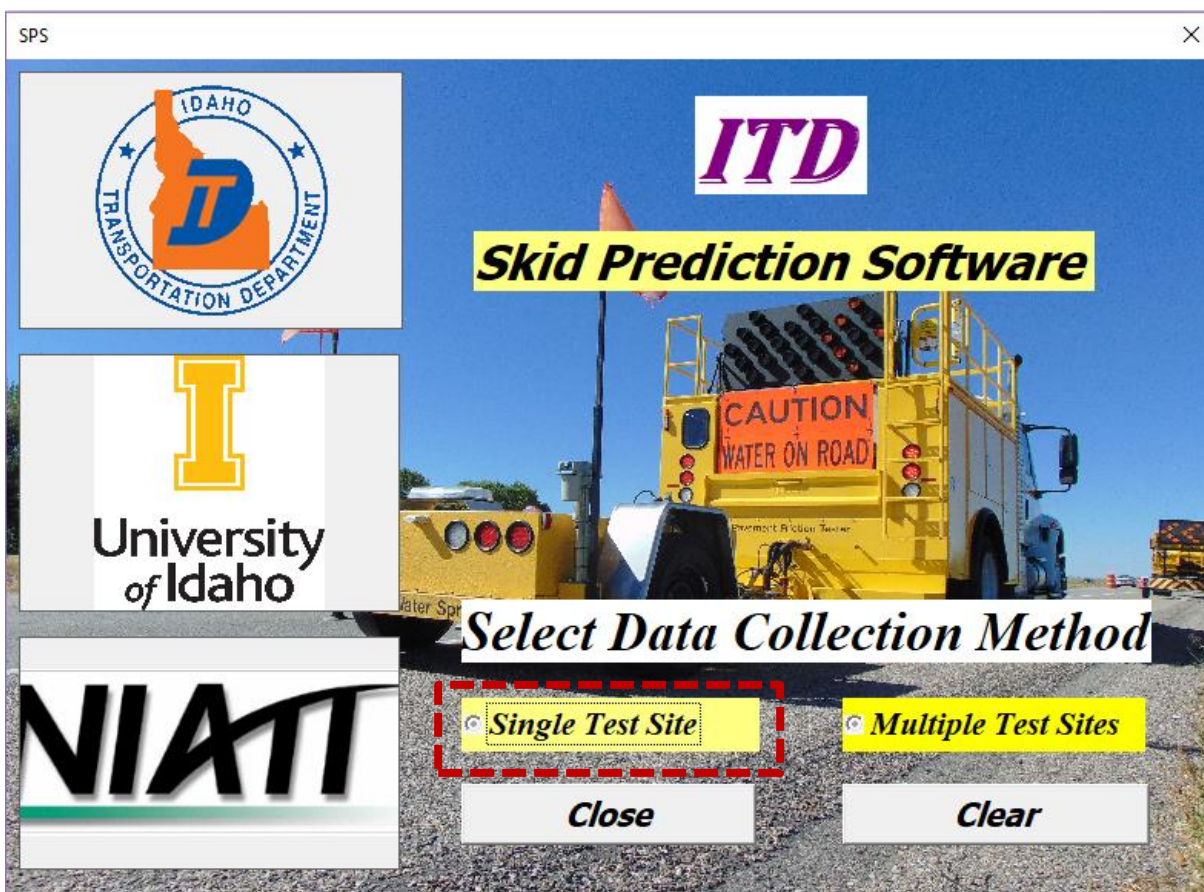


Figure F.1. “Single Test Site” Mode

2. Step 2

After the “**Single Test Site**” is selected, the interface in Figure F.2 can be used by the user to perform all steps for skid number prediction in the Single Test Site mode. First, the user need to import the skid data collected using the skid trailer by selecting the “**Browse Skid Data**” command button. This button allows the user to browse the files and select appropriate skid file.

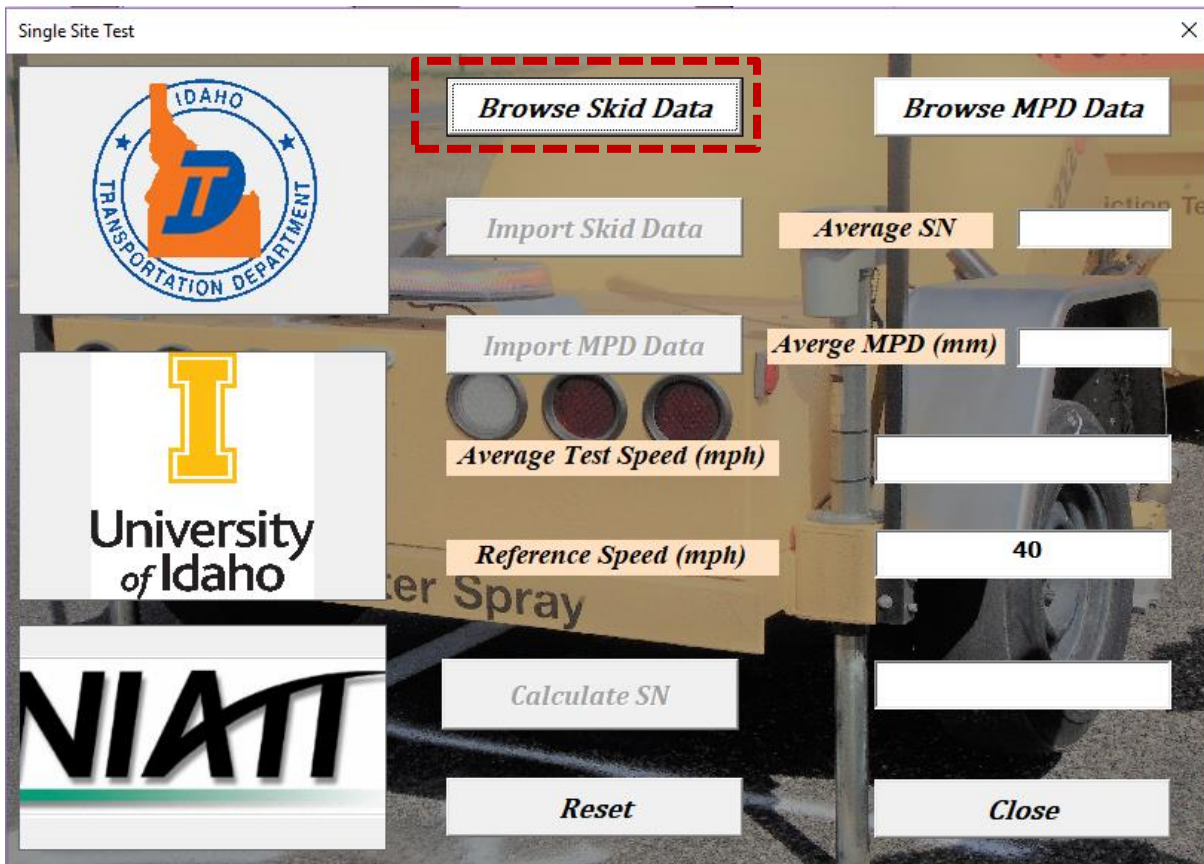


Figure F.2. Browsing Skid Data

3. Step 3

After the user selects the “**Browse Skid Data**” command button in Step 2, a dialog box (Figure F.3) opens to allow the user to locate and select the skid data files. After the user makes the selection, the user needs to click the “Open” button highlighted in red in Figure F.3 to complete the selection of the skid data.

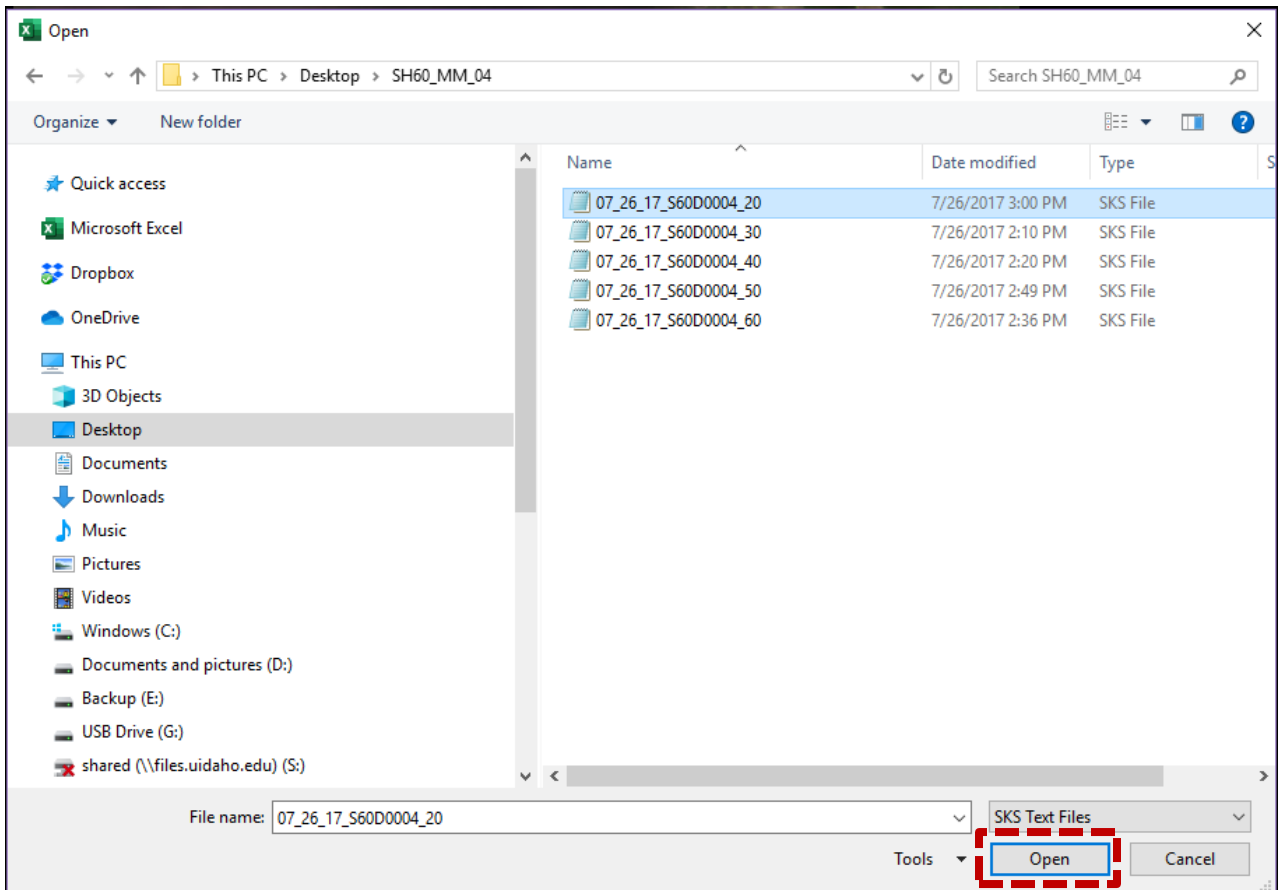


Figure F.3. Selecting Skid Data File

4. Step 4

The user needs to click the “**Browse MPD Data**” to select the MPD data. The “**Browse MPD Data**” command button is highlighted in red in Figure F.4. This button allows the user to locate and select the texture data files recorded by the laser sensor installed on the skid truck.

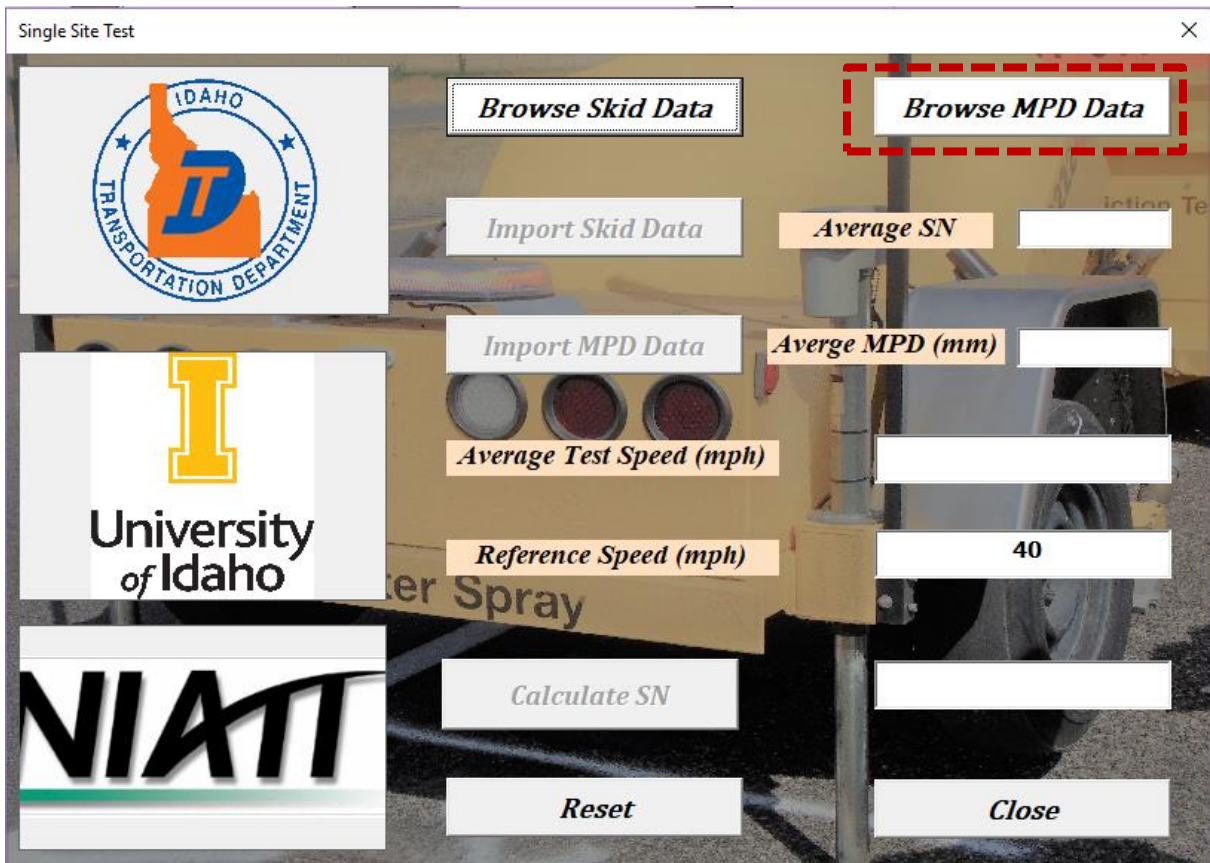


Figure F.4. Browsing MPD Data

5. Step 5

After the user selects the “**Browse MPD Data**” command button in Step 4, a dialog box (Figure F.5) opens to enable the user to locate and select the skid data files. After the user makes the selection, the user needs to click the “Open” button highlighted in red in Figure F.4 to complete the selection of the texture data. The user can select the desired MPD data file from the list of available skid data files.

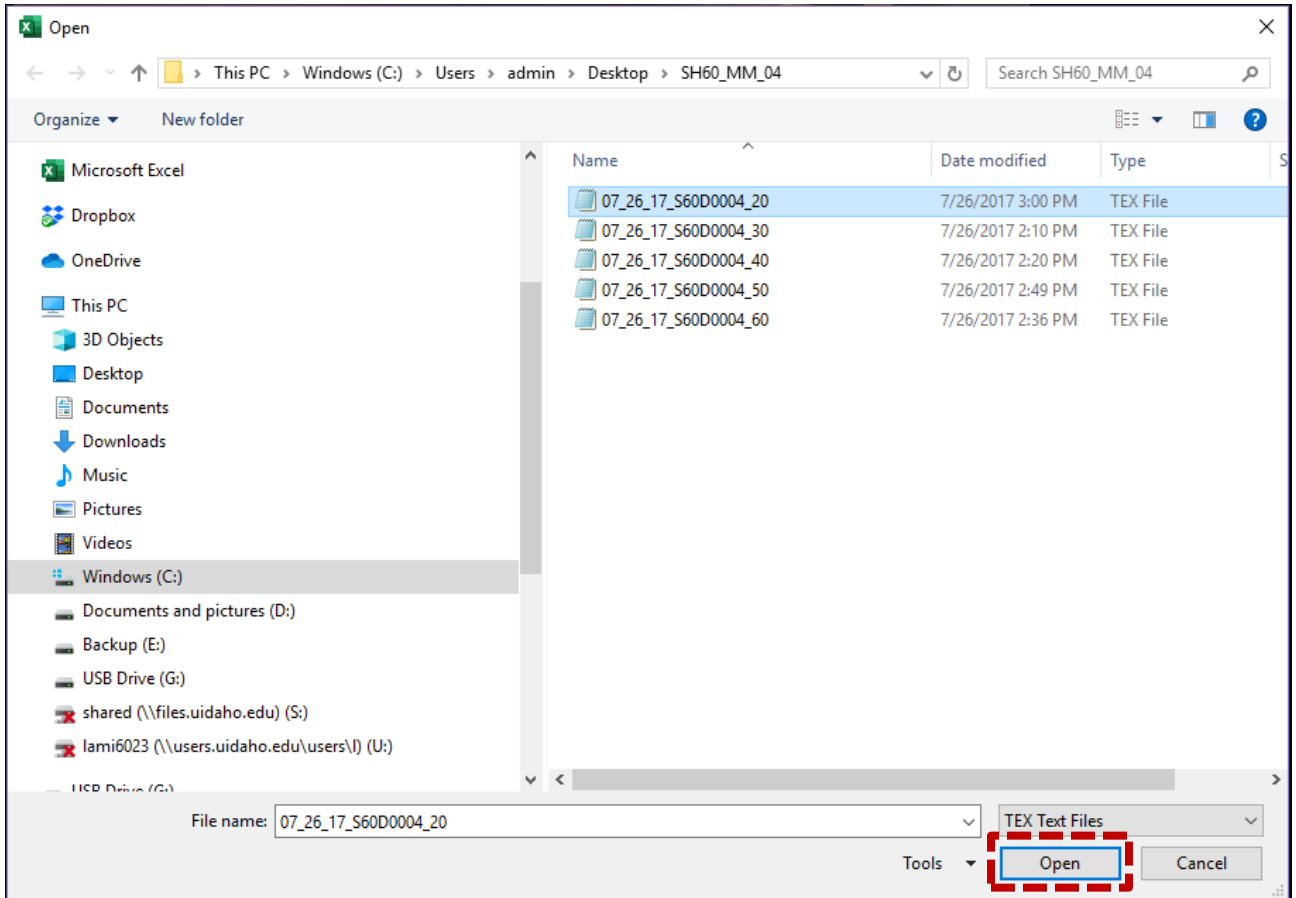


Figure F.5. Selecting MPD Data File

6. Step 6

Once the selection of skid and texture data is completed, both command buttons; “**Browse Skid Data**” and “**Browse MPD Data**”, are highlighted in green as shown in Figure F.6.

Single Site Test

Browse Skid Data **Browse MPD Data**

Import Skid Data *Average SN*

Import MPD Data *Average MPD (mm)*

Average Test Speed (mph)

Reference Speed (mph)

Calculate SN

Reset *Close*

Figure F.6. Completing Skid and Texture Data Selection

7. Step 7

After the user select the skid data file, the user needs to import the data to the software by selecting “**Import Skid Data**” command button. The average value of the uploaded skid data for the Single Site Test is calculated and reported as shown in Figure F.7.

The screenshot shows a software window titled "Single Site Test" with a close button (X) in the top right corner. The interface features three logos on the left: the Idaho Transportation Department logo, the University of Idaho logo, and the NIATT logo. On the right, there are several buttons and input fields:

- Two green buttons at the top: "Browse Skid Data" and "Browse MPD Data".
- A red dashed box highlights the "Import Skid Data" button and the "Average SN" field, which contains the value "75.09".
- Below these are the "Import MPD Data" button and the "Average MPD (mm)" field.
- The "Average Test Speed (mph)" field is empty.
- The "Reference Speed (mph)" field contains the value "40".
- At the bottom, there are four buttons: "Calculate SN", "Reset", and "Close".

Figure F.7. Importing Skid Data to the software

8. Step 8

Similar to the skid data, after the user select the texture data file, the user needs to import the data to the software by selecting “**Import MPD Data**” command button. The average value of the uploaded MPD data for the Single Site Test is calculated and reported as shown in Figure F.8. Upon importing the MPD data, the user is allowed to enter and specify the reference speed. The default value of the reference speed is set at 40 mph but the user can change this value as needed. The current practice at ITD is to measure the skid number at a reference speed of 40 mph.

Single Site Test

Average SN 75.09

Average MPD (mm) 1.23

Average Test Speed (mph) 20.11




Reference Speed (mph) 40

Figure F.8. Importing MPD Data and Specifying the Reference Speed

9. Step 9

After the user specifies the reference speed, the “**Calculate SN**” command button becomes active. The user can select this command to calculate the skid number at the reference desired speed. The calculate the skid number is displayed as shown in Figure F.9

Single Site Test

Browse Skid Data **Browse MPD Data**

Import Skid Data **Average SN** 75.09

Import MPD Data **Average MPD (mm)** 1.23

Average Test Speed (mph) 20.11

Reference Speed (mph) 40

Calculate SN **61.57**

Reset **Close**

Figure F.9. Calculation of Skid Number at the Reference Speed

10. Step 10

If the user wants to perform additional analyses, the “**Reset**” command button (Figure F.10) is used to delete all imported skid and texture data. The user needs to repeat the above steps to select new data.

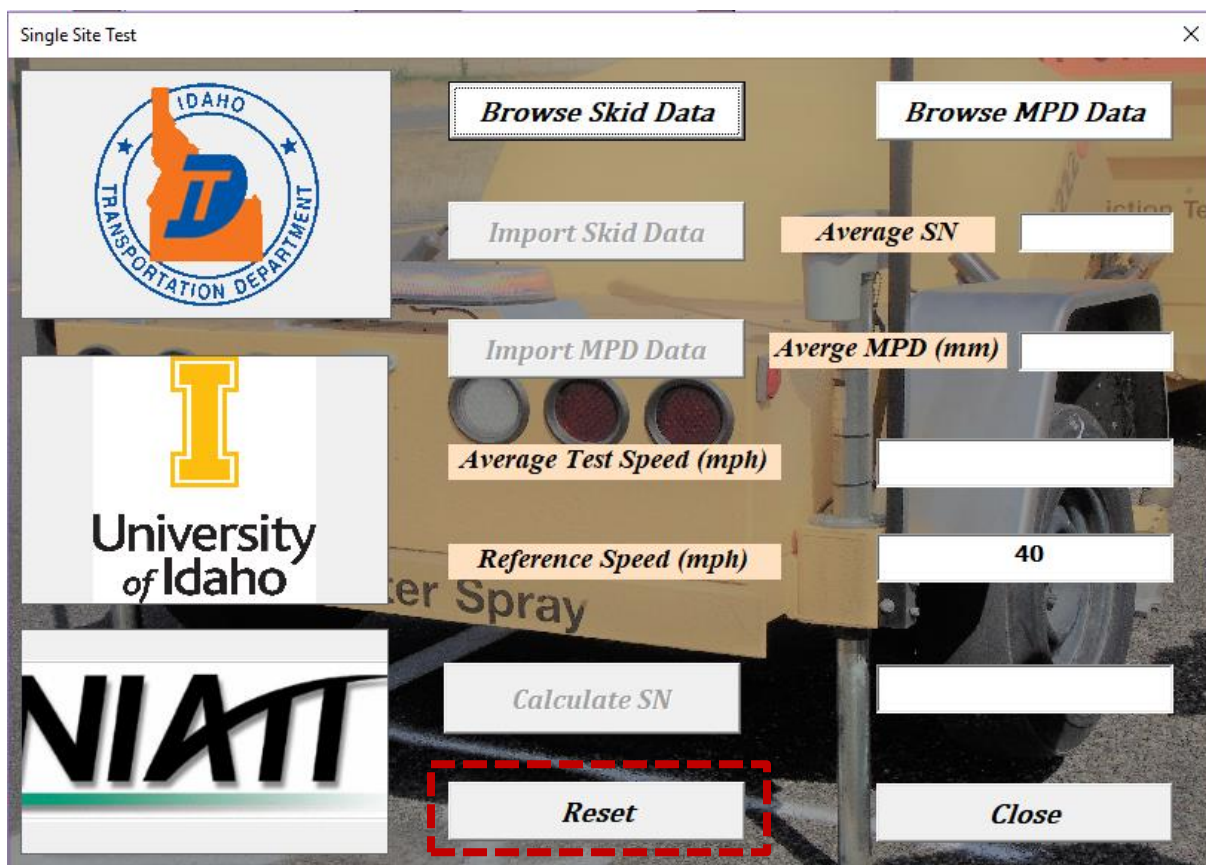


Figure F.10. Resetting the Software to Initial Conditions

11. Step 11

The user can return to the main software interface (Figure F.1) by selecting the “Close” command button as shown in Figure F.11. The user can either close the software or run the software again in different modes; Single Test Site or Multiple Test Sites.

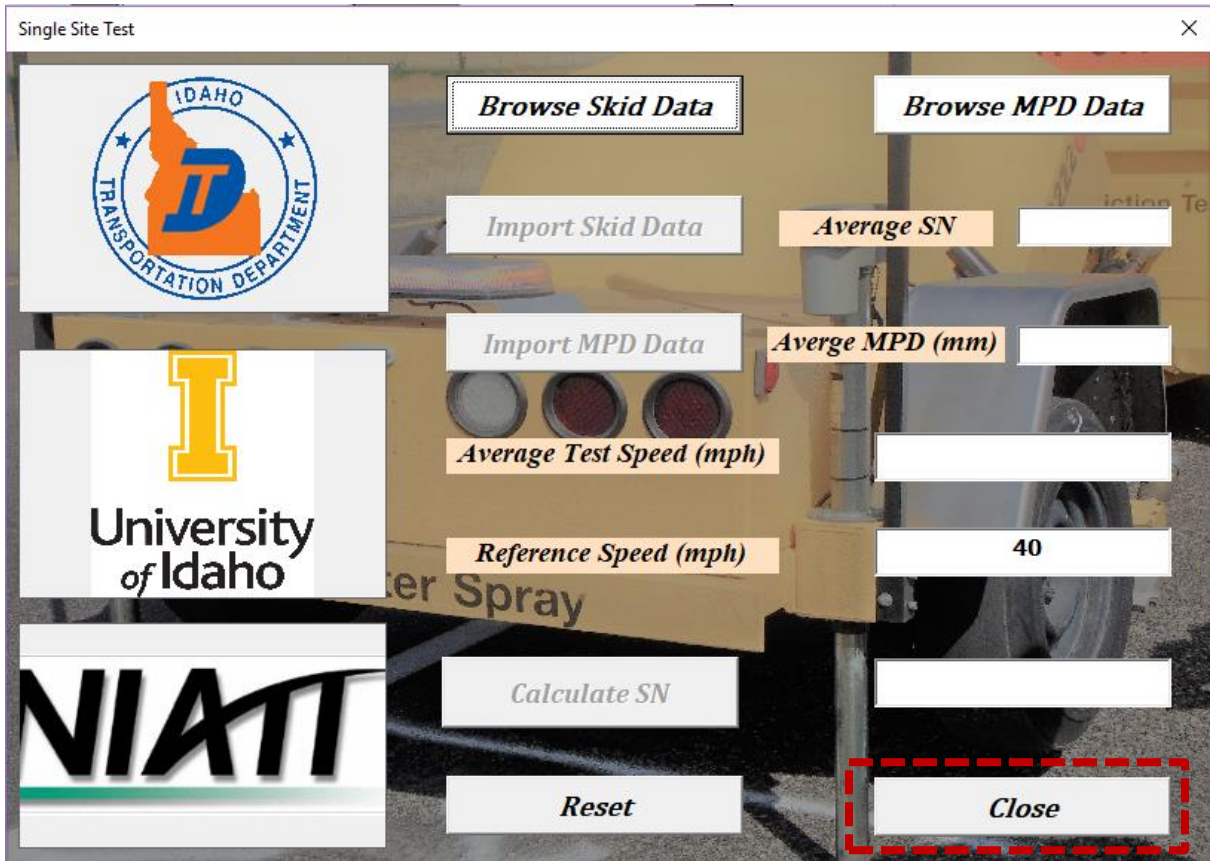


Figure F.11. Closing the Single Test Site Test Mode

Multiple Test Site Mode

1. Step 1

Figure F.12 shows the main interface of the software. The user has two options to either select Single Test Site option or Multiple Test Sites option. Figure F.1 highlights the selection of “Multiple Test Sites” option. The “Clear” command button resets the selection and allow user to make another selection. The “Close” command button is used to close the application.

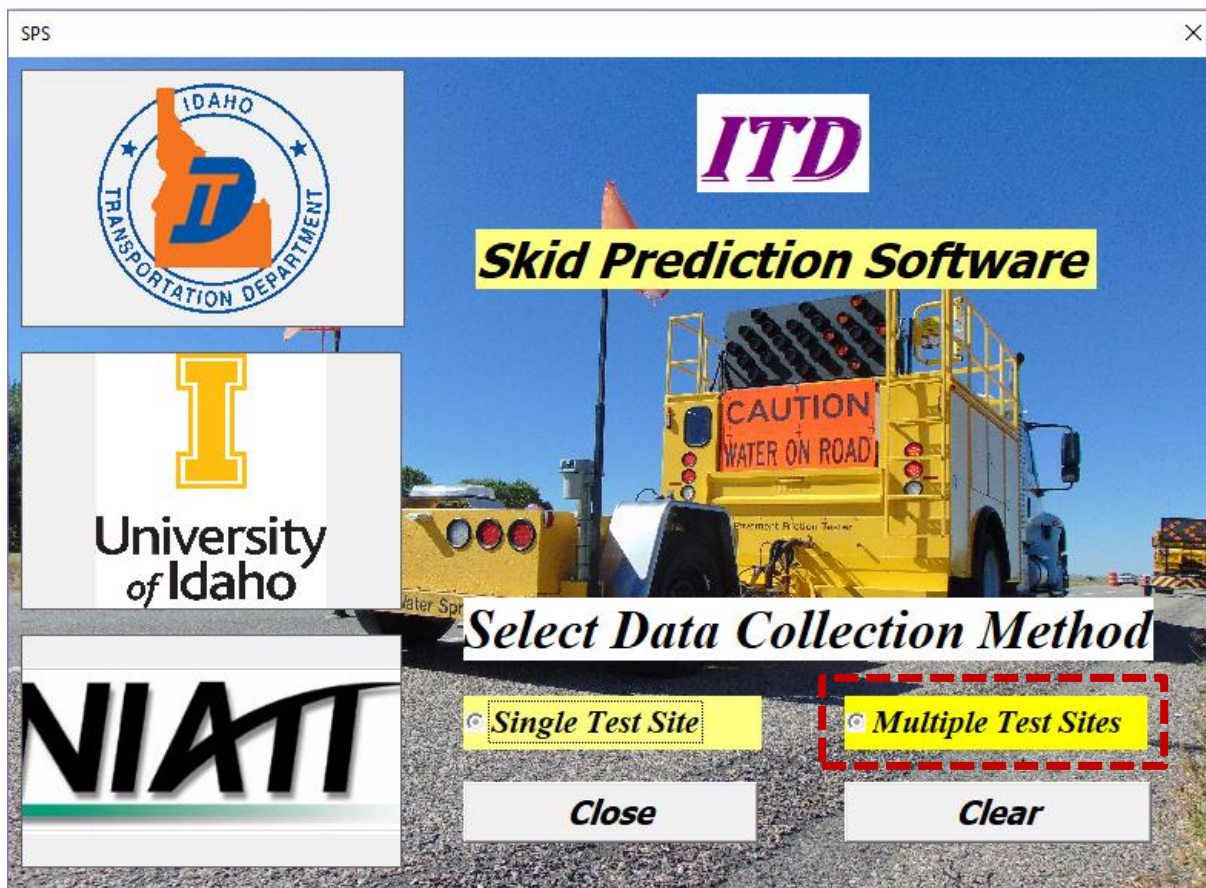


Figure F.12. “Multiple Test Site” Mode

2. Step 2

After the “**Multiple Test Sites**” mode is selected, the interface in Figure F.13 can be used by the user to perform all steps for skid number prediction under the Multiple Test Sites mode. First, the user needs to import the skid data collected using the skid trailer by selecting the “**Browse Skid Data**” command button. This button allows the user to browse the files and select appropriate skid file.

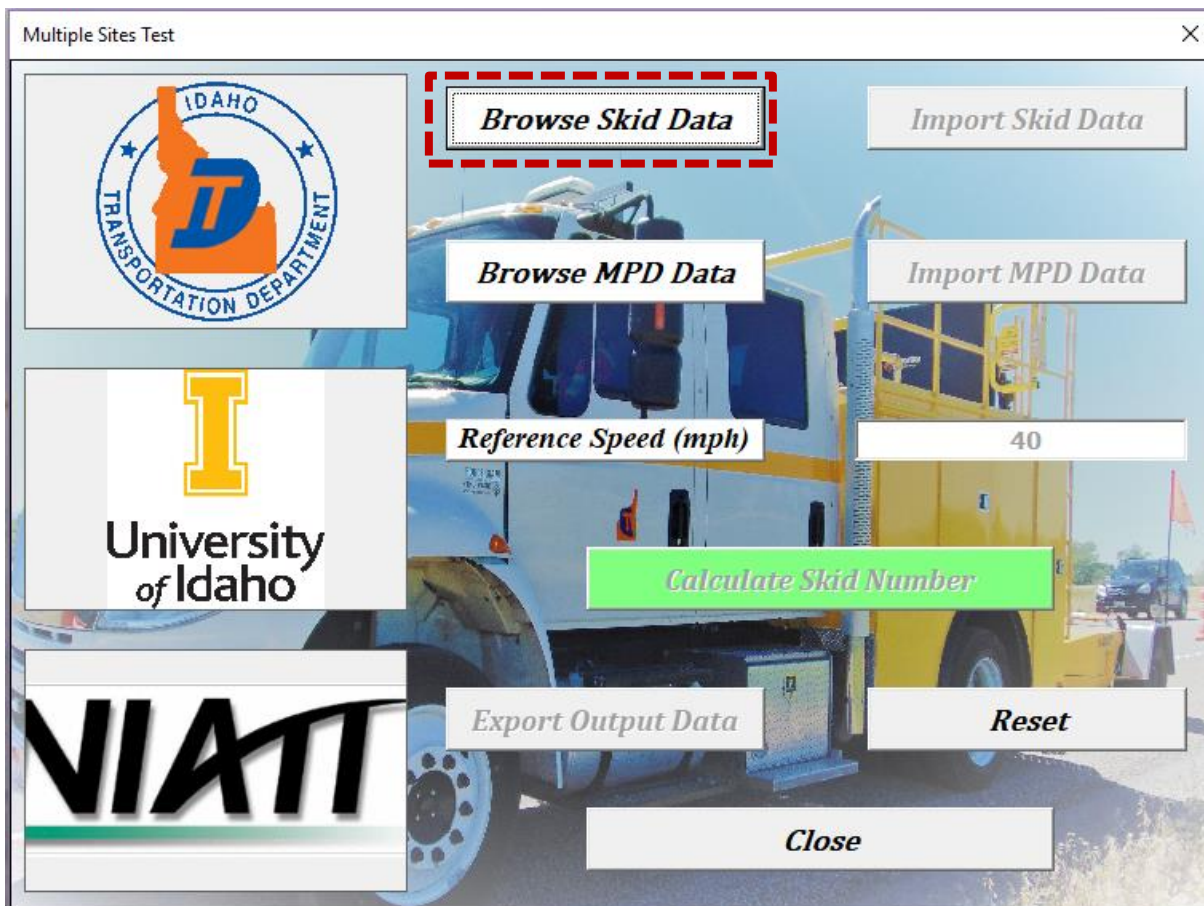


Figure F.13. Browsing Skid Data File

3. Step 3

After the user selects the “**Browse Skid Data**” command button in Step 2, a dialog box (Figure F.14) opens to allow the user to locate and select the skid data files. After the user makes the selection, the user needs to click the “Open” button highlighted in red in Figure F.14 to complete the selection of the skid data.

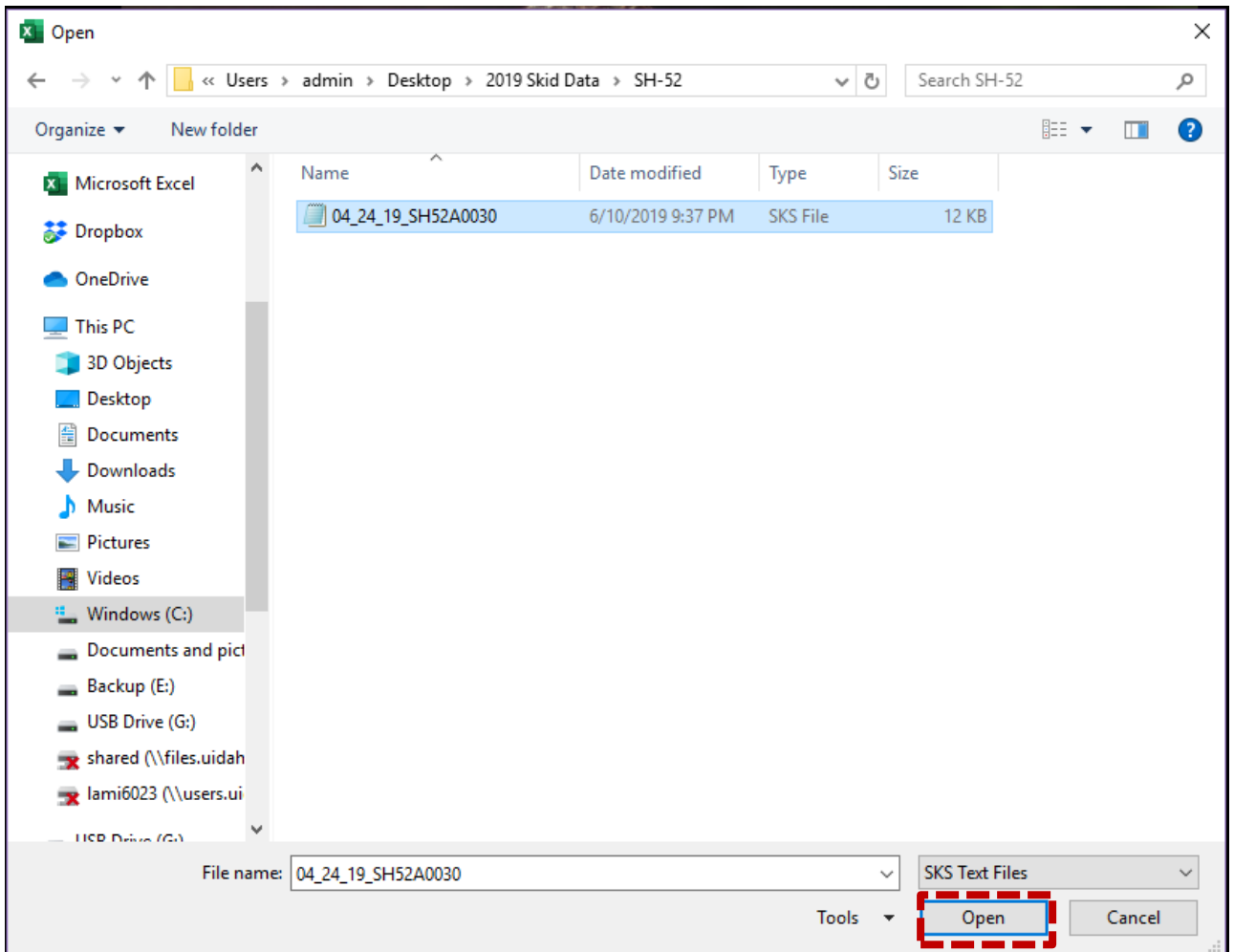


Figure F.14. Selecting Skid Data File

4. Step 4

After the selection of skid data file, the user can import the skid data into the software by selecting the “**Import Skid Data**” command button. The “**Import Skid Data**” command button is highlighted in Figure F.15. After importing the skid data, the “**Browse Skid Data**” button turns into green as shown in Figure F.15.

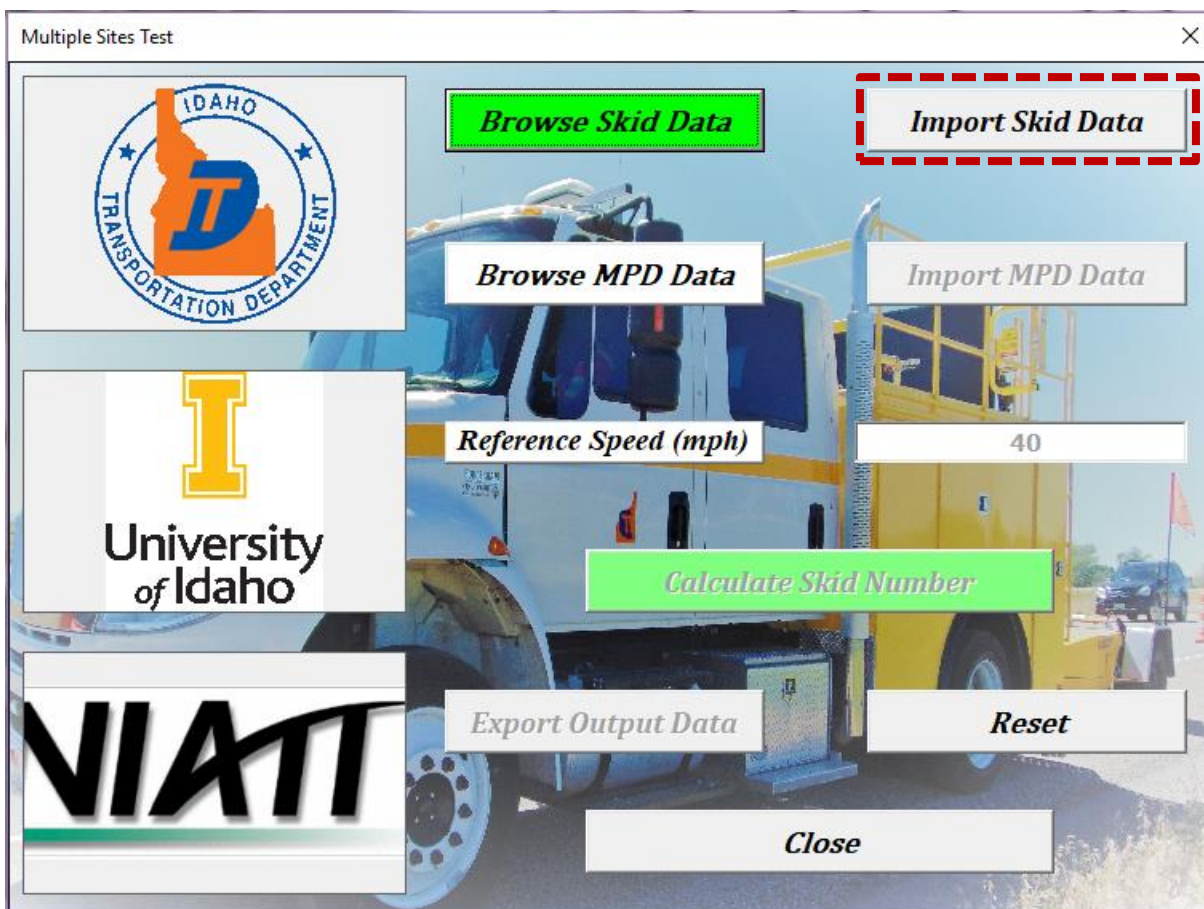


Figure F.15. Importing Skid Data

5. Step 5

The user needs to click the “**Browse MPD Data**” to select the MPD data. The “**Browse MPD Data**” command button is highlighted in red in Figure F.16. This button allows the user to locate and select the texture data files recorded by the laser sensor installed on the skid truck.

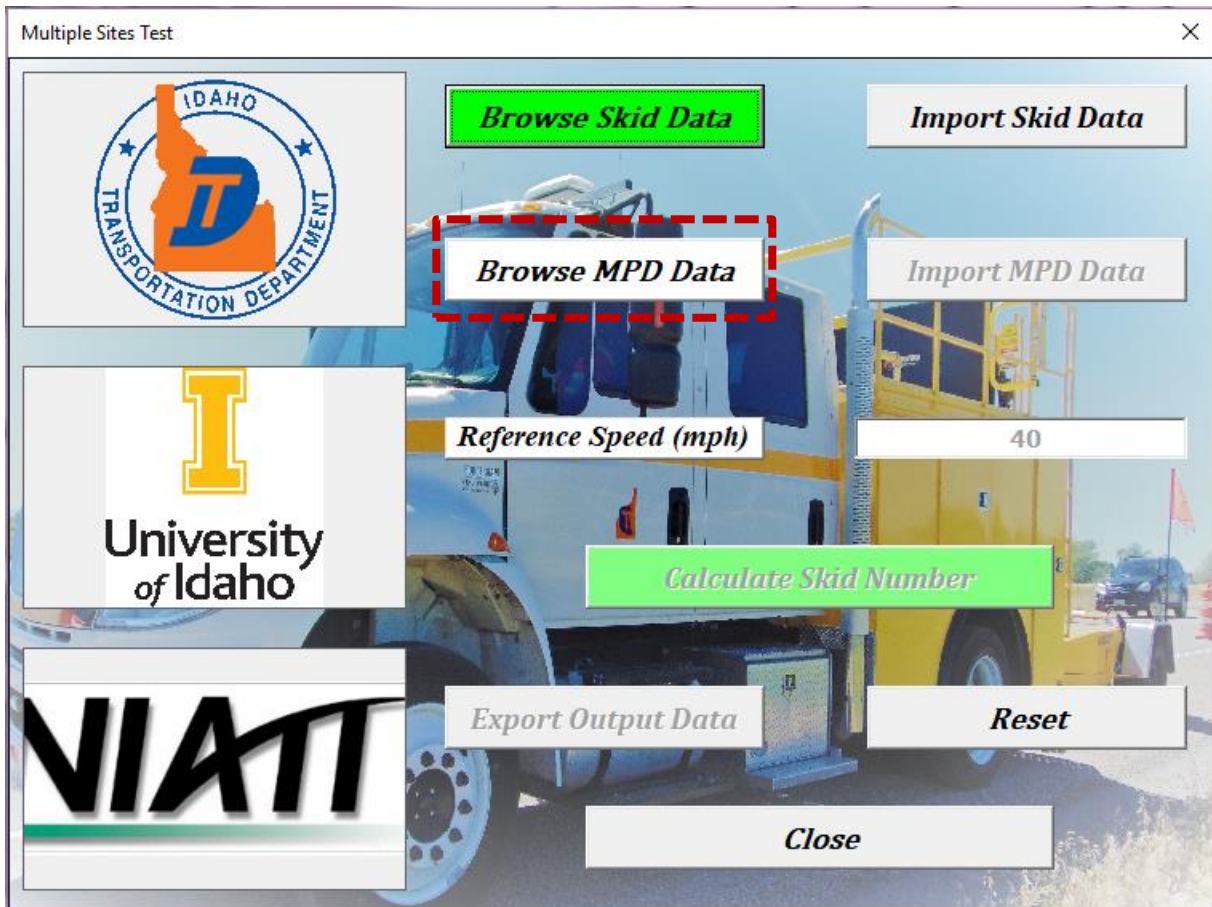


Figure F.16. Selecting the MPD Data File

6. Step 6

After the user selects the “**Browse MPD Data**” command button in Step 5, a dialog box (Figure F.17) opens to allow the user to locate and select the MPD data files. After the user makes the selection, the user needs to click the “Open” button highlighted in red in Figure F.17 to complete the selection of the MPD data.

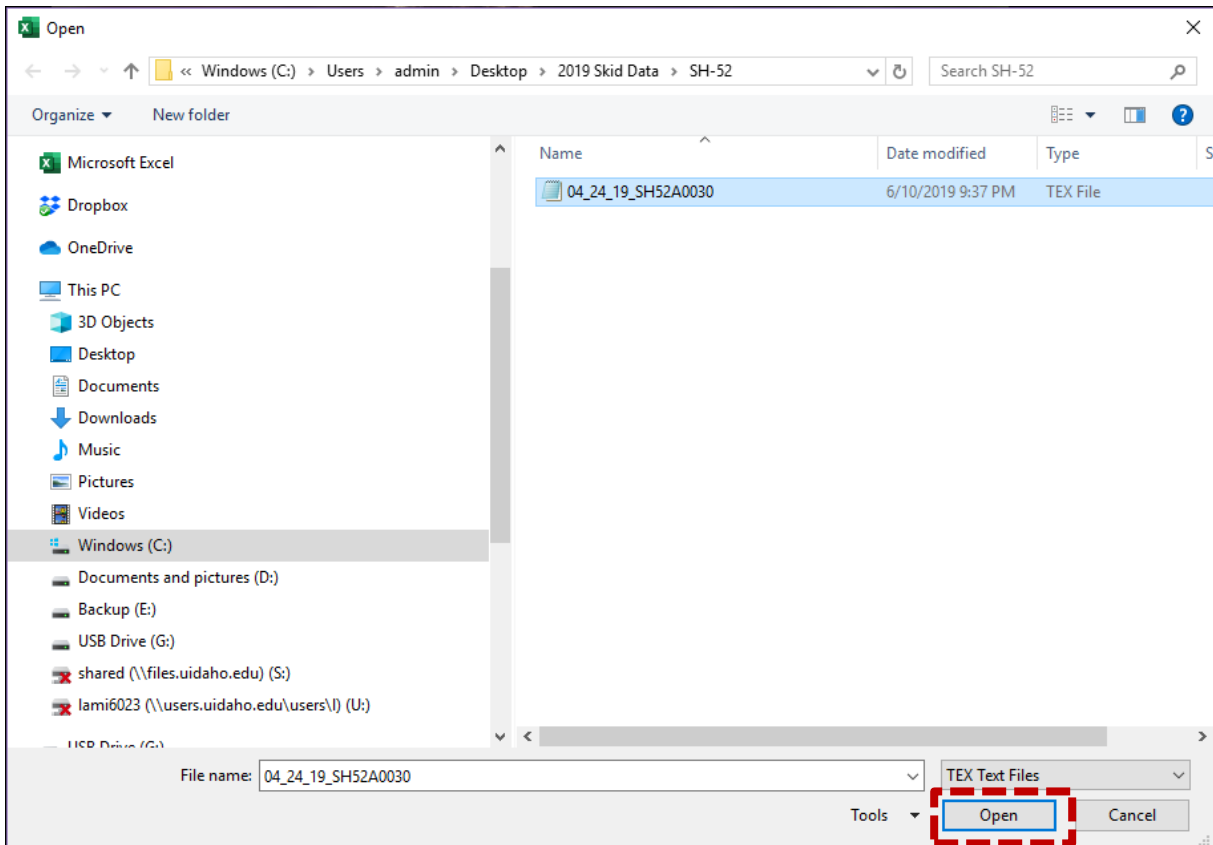


Figure F.17. Selecting the MPD Data File

7. Step 7

Similar to the skid data, after the user select the texture data file, the user needs to import the data to the software by selecting “**Import MPD Data**” command button. After importing the MPD data, the “**Browse MPD Data**” button turns into green as shown in Figure F.18. Upon importing the MPD data, the user is allowed to enter and specify the reference speed. The default value of the reference speed is set at 40 mph, but the user can change this value as needed. The current practice at ITD is to measure the skid number at a reference speed of 40 mph.

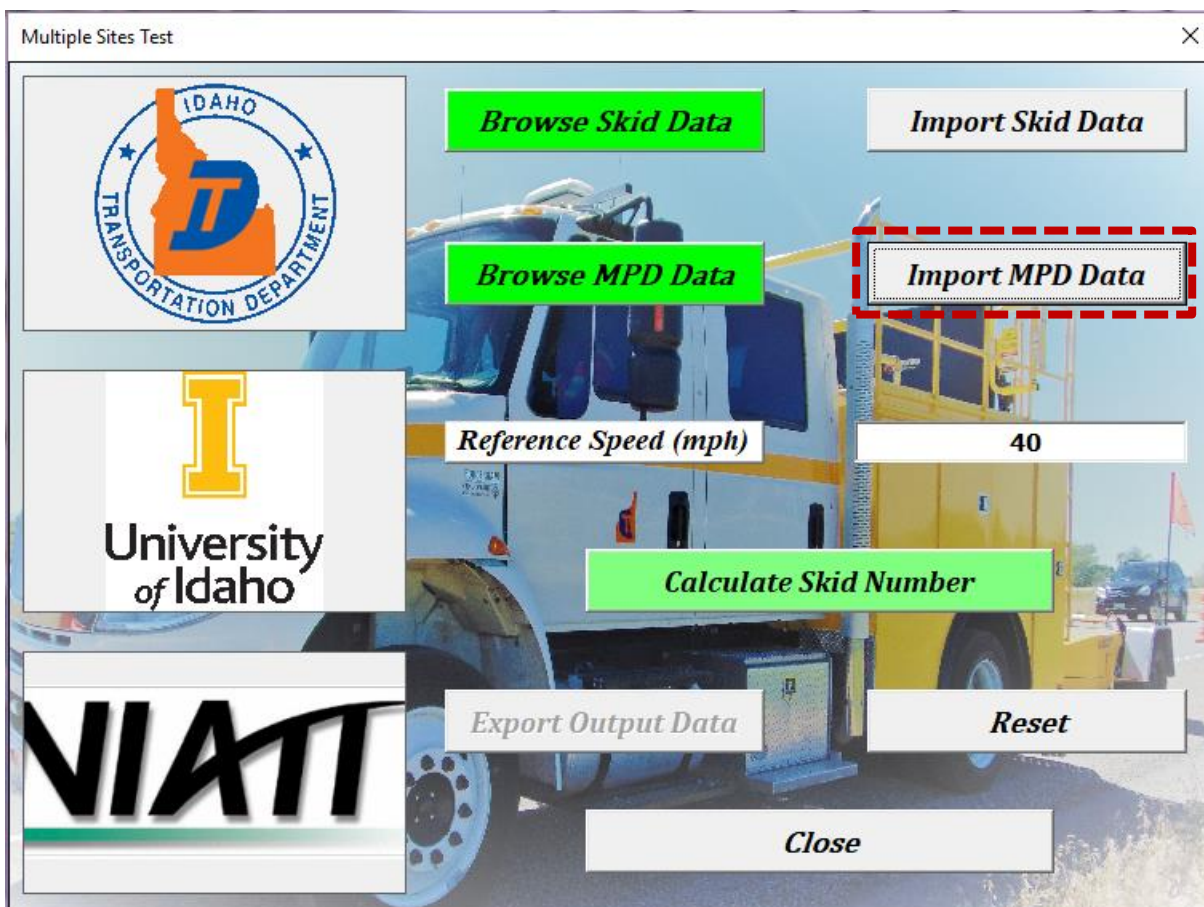


Figure F.18. Importing MPD Data

8. Step 8

After the user specifies the reference speed, the “**Calculate Skid Number**” command button becomes active. After the user specifies the reference speed, the “**Calculate Skid Number**” command button becomes active (Figure F.19). The user can select this command to calculate the skid number at the reference desired speed. The calculated skid number for various test sections can be exported to an excel sheet using “**Export Output Data**” command button. (Figure F.19).

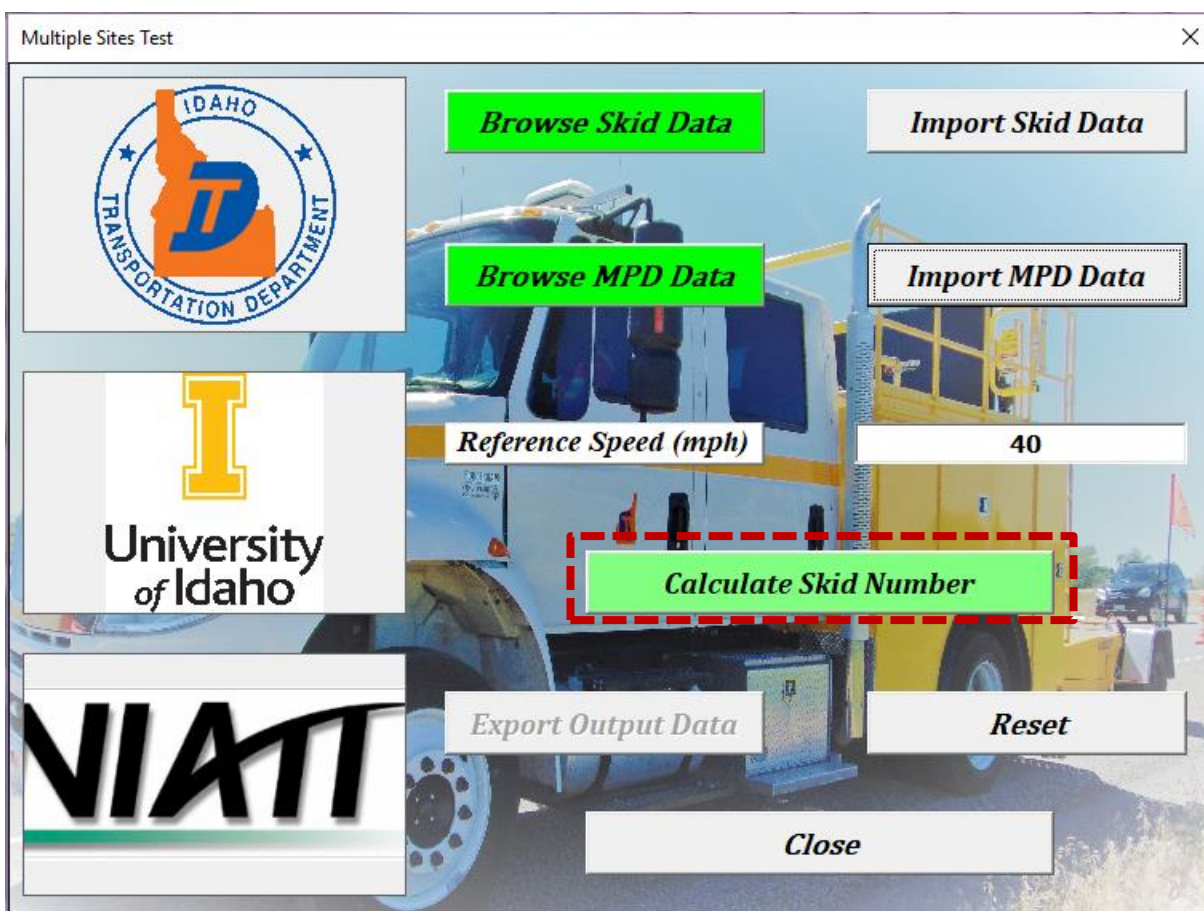


Figure F.19. Skid Number Calculation

9. Step 9

After the user selects the “**Export Output Data**” command button (Figure F.19), a dialog box is open to allow the user to save the output file as shown in Figure F.20. After the user selects the location and name for the output file, the user needs to select “**Save**” button as highlighted in red in Figure F.20.

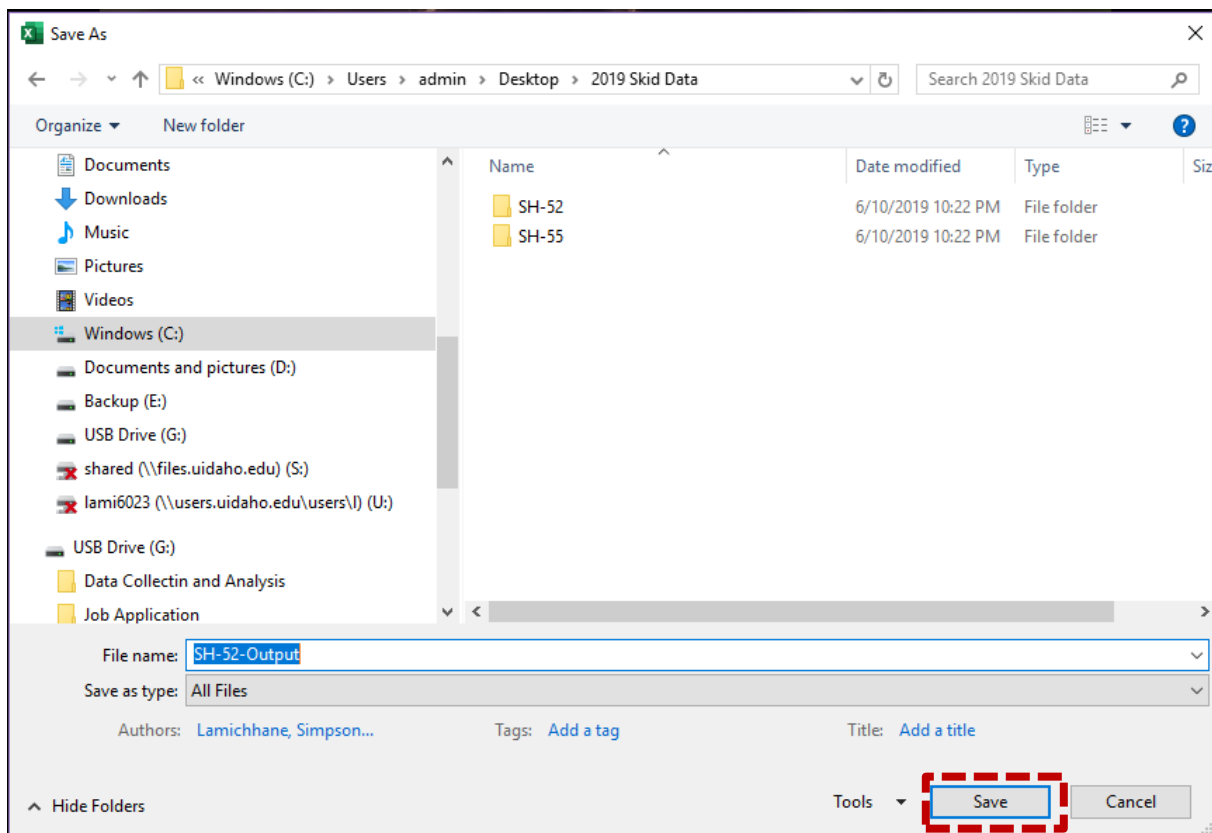


Figure F.20. Exporting and Saving the Output Data

10. Step 10

If the user wants to perform additional analyses, the “**Reset**” command button (Figure F.21) is used to delete all imported skid and texture data. The user needs to repeat the above steps to select new data.

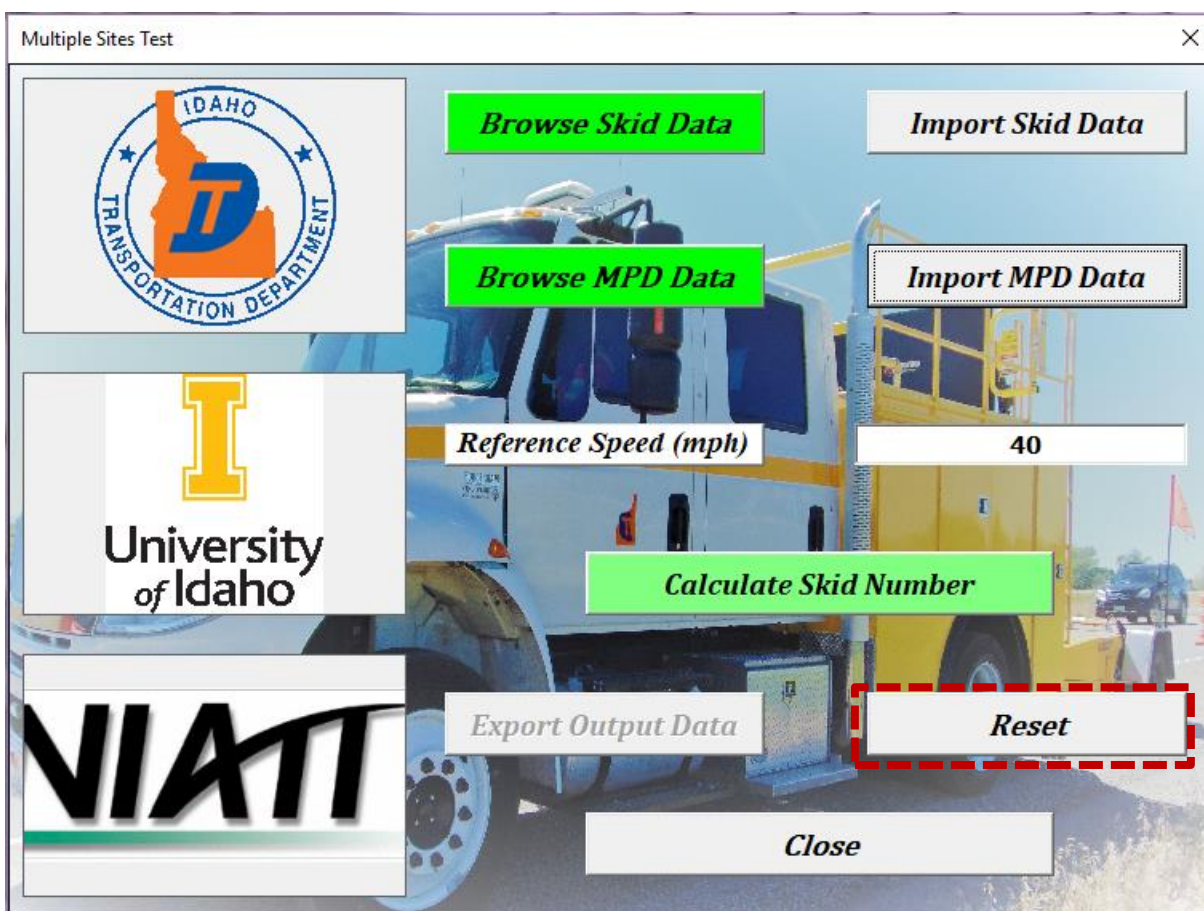


Figure F.21. Resetting the Software to Initial Conditions

11. Step 11

The user can return to the main software interface (Figure F.12) by selecting the “Close” command button as shown in Figure F.22. The user can either close the software or run the software again in different modes; Single Test Site or Multiple Test Sites.

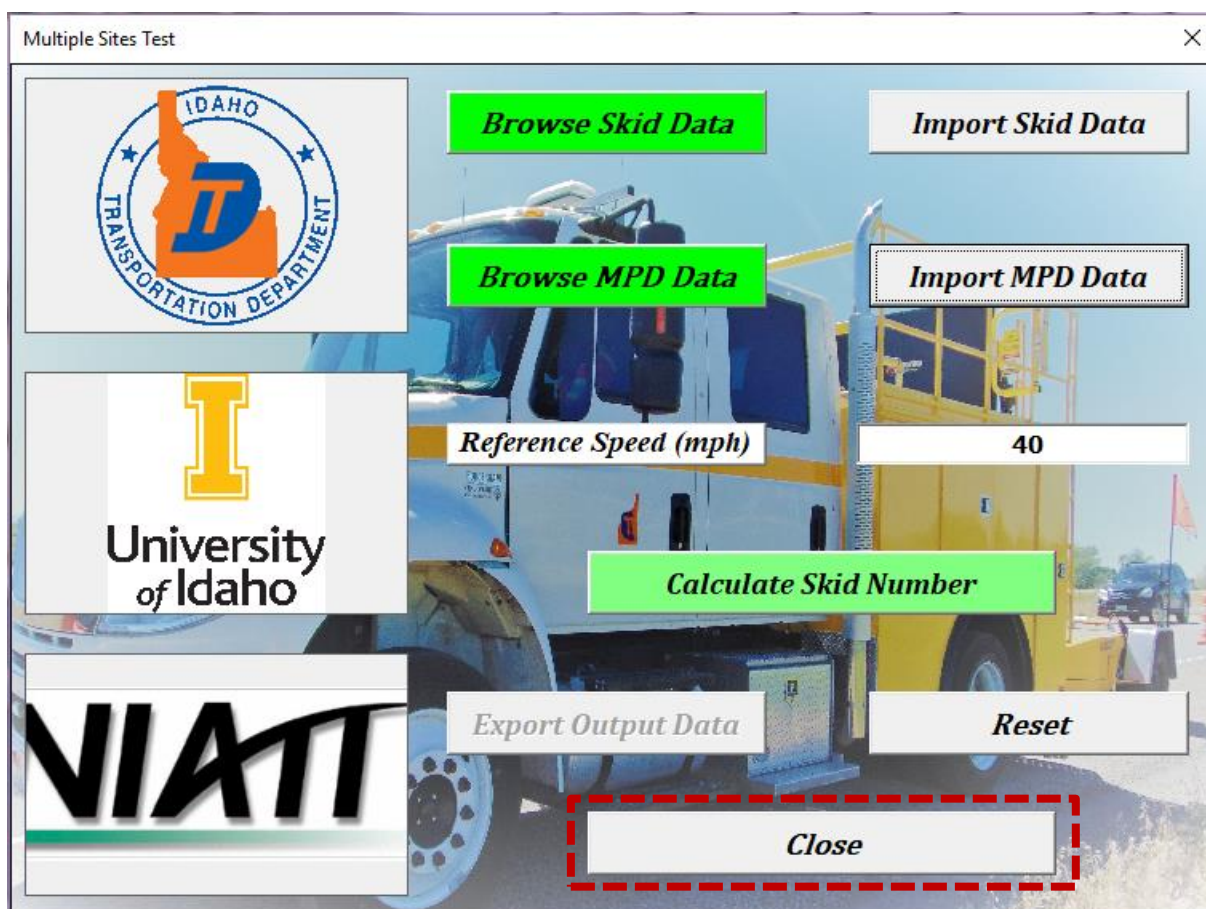



Figure F.22. Closing the Multiple Test Sites Mode

APPENDIX F COPYRIGHT PERMISSSION

1. Copyright Permission: **Figure 2.1**



Note: Copyright.com supplies permissions but not the copyrighted content itself.

1
PAYMENT
2
REVIEW
3
CONFIRMATION

Step 3: Order Confirmation

Thank you for your order! A confirmation for your order will be sent to your account email address. If you have questions about your order, you can call us 24 hrs/day, M-F at +1.855.239.3415 Toll Free, or write to us at info@copyright.com. This is not an invoice.

Confirmation Number: 11796901
Order Date: 03/07/2019

Payment Information

Simpson lamichhane
lami6023@vandals.uidaho.edu
+1 (208) 310-4523
Payment Method: n/a

If you paid by credit card, your order will be finalized and your card will be charged within 24 hours. If you choose to be invoiced, you can change or cancel your order until the invoice is generated.


Order Details

Texturing of concrete pavements

<p>Order detail ID: 71841161 Order License Id: 4543770458662 ISBN: 9780309117920 Publication Type: Book Publisher: Transportation Research Board Author/Editor: Littleton, Paul Christopher ; et al</p>	<p>Permission Status: ✔ Granted Permission type: Republish or display content Type of use: Thesis/Dissertation Requestor type: Academic institution Format: Electronic Portion: chart/graph/table/figure</p>
--	---

2. Copyright Permission: **Figure 2.2, Figure 2.5**

4/28/2019 Copyright Clearance Center



Confirmation Number: 11810765
Order Date: 04/28/2019

Customer Information

Customer: Simpson lamichhane
Account Number: 3001417108
Organization: Simpson lamichhane
Email: lami6023@vandals.uidaho.edu
Phone: +1 (208) 310-4523
Payment Method: Invoice

This is not an invoice

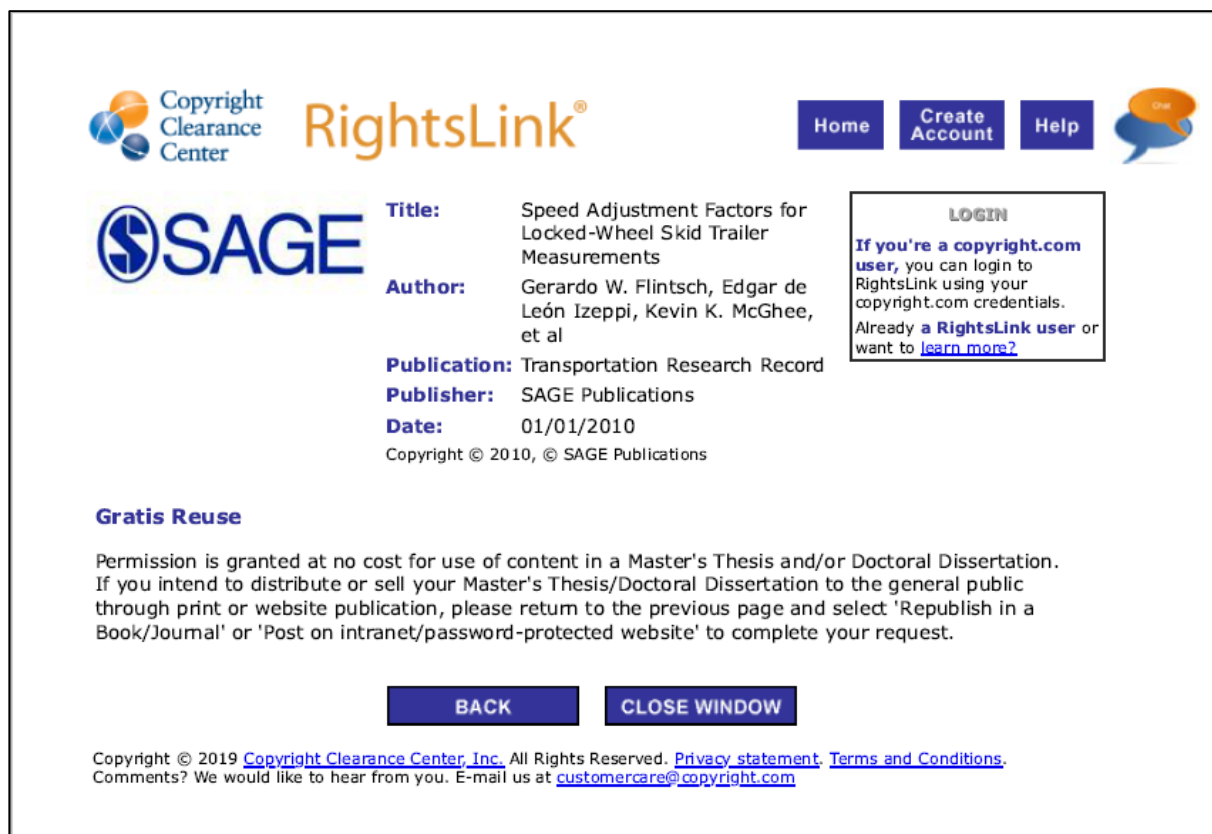
Order Details

Pavement management for airports, roads, and parking lots Billing Status:
N/A


<p>Order detail ID: 71886911 ISBN: 9780412992018 Publication Type: Book Publisher: CHAPMAN & HALL, Author/Editor: SHAHIN, MOHAMED Y.</p>	<p>Permission Status: ✔ Granted Permission type: Republish or display content Type of use: Thesis/Dissertation Order License Id: 4577851348266</p>
---	---

Requestor type	Academic institution
Format	Print, Electronic
Portion	chart/graph/table/figure
Number of charts/graphs/tables/figures	1
The requesting person/organization	Simpson Lamichhane
Title or numeric reference of the portion(s)	Chapter 6
Title of the article or chapter the portion is from	Skid Data Collection and Analysis
Editor of portion(s)	NA
Author of portion(s)	Simpson Lamichhane
Volume of serial or monograph	NA
Page range of portion	1
Publication date of portion	May 2019
Rights for	Main product
Duration of use	Life of current edition
Creation of copies for the disabled	no
With minor editing privileges	no
For distribution to	Worldwide
In the following language(s)	Original language of publication

<https://www.copyright.com/printOrder.do?id=11810765> 1/2

3. Copyright Permission: **Figure 2.4, Figure 2.10**


The screenshot shows the Copyright Clearance Center RightsLink interface. At the top left is the Copyright Clearance Center logo, and next to it is the RightsLink logo. On the top right, there are navigation buttons for 'Home', 'Create Account', and 'Help', along with a chat icon. The main content area features the SAGE logo on the left and a list of metadata on the right: Title, Author, Publication, Publisher, and Date. A 'LOGIN' box is positioned to the right of the metadata, providing instructions for users and a link to learn more. Below the metadata, there is a 'Gratis Reuse' section with a paragraph of text explaining the permission. At the bottom of the content area, there are two buttons: 'BACK' and 'CLOSE WINDOW'. A footer at the very bottom contains copyright information and contact details.

Copyright Clearance Center RightsLink[®] [Home](#) [Create Account](#) [Help](#) 

SAGE **Title:** Speed Adjustment Factors for Locked-Wheel Skid Trailer Measurements
Author: Gerardo W. Flintsch, Edgar de León Izeppi, Kevin K. McGhee, et al
Publication: Transportation Research Record
Publisher: SAGE Publications
Date: 01/01/2010
 Copyright © 2010, © SAGE Publications



LOGIN
 If you're a **copyright.com** user, you can login to RightsLink using your copyright.com credentials. Already a **RightsLink user** or want to [learn more?](#)

Gratis Reuse
 Permission is granted at no cost for use of content in a Master's Thesis and/or Doctoral Dissertation. If you intend to distribute or sell your Master's Thesis/Doctoral Dissertation to the general public through print or website publication, please return to the previous page and select 'Republish in a Book/Journal' or 'Post on intranet/password-protected website' to complete your request.

[BACK](#) [CLOSE WINDOW](#)

Copyright © 2019 [Copyright Clearance Center, Inc.](#) All Rights Reserved. [Privacy statement](#). [Terms and Conditions](#).
 Comments? We would like to hear from you. E-mail us at customercare@copyright.com

4. Copyright Permission: **Figure 2.6, Figure 2.7**

4/28/2019	Copyright Clearance Center
	
Confirmation Number: 11810844 Order Date: 04/29/2019	
Customer Information	
Customer: Simpson Lamichhane Account Number: 3001417108 Organization: Simpson Lamichhane Email: lami6023@vanda[s,uidaho,edu Phone: +1 (208) 310-4523 Payment Method: Invoice	
This is not an invoice	
Order Details	
Guide for Pavement Friction	Billing Status: N/A
Order detail ID: 71887033 ISBN: 9780309429740 Publication Type: Book Publisher: Transportation Research Board Author/Editor: National Academies of Sciences, Engineering, and Medicine	Permission Status:  Granted Permission type: Republish or display content Type of use: Thesis/Dissertation Order License Id: 4578051131458
Requestor type	Academic Institution
Format	Print, Electronic
Portion	chart/graph/table/figure
Number of charts/graphs/tables/figures	1
The requesting person/organization	Simpson Lamichhane
Title or numeric reference of the portion(s)	Chapter 3
Title of the article or chapter the portion is from	Pavement friction and highway safety
Editor of portion(s)	NA
Author of portion(s)	NA
Volume of serial or monograph	NA
Page range of portion	9-16
Publication date of portion	06/30/2019
Rights for	Main product
Duration of use	Life of current edition
Creation of copies for the disabled	no
With minor editing privileges	no
For distribution to	Worldwide
In the following language(s)	Original language of publication
https://www.copyright.com/printOrder.do?id=11810844	
1/2	

5. Copyright Permission: Figure 2.9



RightsLink®

[Home](#)
[Account Info](#)
[Help](#)




Title: Evaluation of Circular Texture Meter for Measuring Surface Texture of Pavements

Author: Brian D. Prowell, Douglas I. Hanson

Publication: Transportation Research Record

Publisher: SAGE Publications

Date: 01/01/2005

Copyright © 2005, © SAGE Publications

Logged in as:
Simpson lamichhane
Account #:
3001417108

LOGOUT

Welcome to RightsLink

SAGE Publications has partnered with Copyright Clearance Center's RightsLink service to offer a variety of options for reusing SAGE Publications content.

I would like to... ?

Important Notice Regarding Content:
This RightsLink service only provides permission for reuse. You may purchase an article through our Pay-Per-View service by selecting the "Full-Text (PDF)" link from the Journal table of contents on [SAGE Journals](#) or refer to our [Full Text Access Options](#) page for more information.

Copyright © 2019 [Copyright Clearance Center, Inc.](#) All Rights Reserved. [Privacy statement](#). [Terms and Conditions](#).
Comments? We would like to hear from you. E-mail us at customercare@copyright.com